DEVELOPMENT OF A NOVEL MOUSE MODEL FOR TRANSGESTATIONAL MALARIA INFECTION

by

CATHERINE D. MORFFY SMITH

(Under the Direction of Julie M. Moore)

ABSTRACT

Gestational malaria, a severe clinical manifestation of *Plasmodium falciparum* infection observed in pregnant women, is a major cause of severe maternal illness and neonatal mortality worldwide. I have developed a novel mouse model for transgestational malaria infection utilizing outbred Swiss Webster mice. When infected with *Plasmodium chabaudi* in early gestation, several inbred mouse strains abort their pregnancies at midgestation. However, outbred Swiss Webster mice infected with *P. chabaudi* in early gestation carry their pregnancies to term and produce live offspring. Maternal malaria infection is associated with reduced fetal viability and fetal weight at term, as well as reduced postnatal survival. This novel model allows for the exploration of the impact of maternal malaria infection on postnatal outcomes and the immunological balance between parasite clearance and pregnancy success. The composition of the gut microbiota alters this balance. We find that the composition of the gut microbiota transcends the outbred genetics of Swiss Webster mice as a determinant of infection severity. The administration of fecal microbiota transplants consisting of resistance- or susceptibility-conferring gut microbes results in the establishment of distinct microbial communities in recipient mice. Mice receiving resistance-conferring gut microbes develop lower parasite

burdens and reduced morbidity compared to mice receiving susceptibility-conferring gut microbes. In addition, fetal viability and weight at gestational term, as well as postnatal survival, are improved in infected dams possessing resistance-conferring gut microbes. To explore the immunological and placental environment at peak infection in Swiss Webster mice displaying gut microbiota-mediated susceptibility or resistance to malaria infection, mice were sacrificed at 10 days post-infection. Uterine weight was significantly reduced in infected susceptible dams compared to uninfected controls, but maternal infection severity did not significantly alter embryo viability. Although peripheral cytokine titers were not influenced by maternal infection severity, the transcriptional response of susceptible conceptuses differed subtly from the response observed in resistant conceptuses. Specifically, *Il10* was elevated in conceptuses collected from infected susceptible mice compared to infected resistant mice, perhaps indicating that susceptible mice had a more severe proinflammatory response prior to sacrifice, necessitating a greater compensatory response to reduce damaging inflammation at the maternal-fetal interface.

INDEX WORDS: gestational malaria; placental malaria; gut microbiota; mouse models; *Plasmodium chabaudi chabaudi* AS

DEVELOPMENT OF A NOVEL MOUSE MODEL FOR TRANSGESTATIONAL MALARIA INFECTION

by

CATHERINE D. MORFFY SMITH

BS, Haverford College, 2011

A Dissertation Submitted to the Graduate Faculty of The University of Georgia in Partial Fulfillment of the Requirements for the Degree

DOCTOR OF PHILOSOPHY

ATHENS, GEORGIA

2018

DEVELOPMENT OF A NOVEL MOUSE MODEL FOR TRANSGESTATIONAL MALARIA INFECTION

by

CATHERINE D. MORFFY SMITH

Major Professor:	Julie M. Moore
Committee:	David Peterson
	Lianchun Wang
	Wendy Watford

Electronic Version Approved:

Suzanne Barbour
Dean of the Graduate School
The University of Georgia
August 2018

DEDICATION

To my favorite geneticist.

ACKNOWLEDGEMENTS

First, I must thank my advisor, Dr. Julie Moore. The research described here is fairly different from the project I set out to work on when I joined the lab, and I was incredibly lucky to have a mentor who supported me in pursuing the project we stumbled across! It was a leap of faith, and I am grateful that I had an advisor who granted me the freedom to explore. Julie, thank you for providing me with such incredible opportunities to develop my skills as a scientist. I have learned a lot about how to do good research and present it well, and I owe it to your guidance. I would also like to thank my committee: Dr. Peterson, Dr. Wang, and Dr. Watford. Your support, feedback, and fascinating questions have shaped and improved my project and training. I have had the good fortune to work alongside with some wonderful labmates during my time in the Moore lab: Alicer Andrew, Tara Bracken, Caitlin Cooper, Trisha Dalapati, Sachi Shastri, Julie Range, Demba Sarr, Vivian Anderson, and Emily Martin. A huge thank you to Tara and Caitlin, who patiently taught me what I needed to know to work with mice. I am also tremendously grateful to everyone who helped me get my experiments across the finish line: Caitlin, Tara, Alicer, Trisha, Vivian, Katie Reagan, and Chris Slade. I could not have done it alone. Other friends, family, and Nick - thank you, and so much love.

TABLE OF CONTENTS

Page

LIST OF TABLES

Page

LIST OF FIGURES

Page

CHAPTER 1

INTRODUCTION & LITERATURE REVIEW

Introduction

Plasmodium falciparum infection in pregnant women causes severe maternal illness and negatively impacts fetal development. Although malaria prevention and treatment programs specifically target pregnant women, malaria in pregnancy remains a serious public health concern for two major reasons. First, antimalarial drug resistance threatens the future efficacy of the antimalarial drug combinations considered safe for use in pregnancy. Second, the pathogenesis of gestational malaria is incompletely understood, making it impossible to target host processes that may be contributing to malaria pathogenesis and poor pregnancy outcomes. The study of gestational malaria is complicated by the inaccessibility of the human placenta prior to delivery. Therefore, mouse models are important tools for the study of malaria in pregnant women because they allow for the exploration of the mechanisms linking maternal malaria infection to poor pregnancy outcomes.

My dissertation revolves around the development and characterization of a novel mouse model for malaria infection in pregnancy. The first chapter of my dissertation is a literature review that introduces the problem of malaria in pregnancy and explores the pathogenesis of gestational malaria, mouse models for malaria infection in pregnancy, and the modulation of malaria infection severity by the composition of the gut microbiota.

The second chapter of my dissertation describes the development of a novel model for pregnancy success in the context of transgestational maternal malaria infection utilizing

Plasmodium chabaudi chabaudi AS-infected outbred Swiss Webster mice. This model is novel because mice infected in early gestation carry their pregnancies to term, producing live pups that have been exposed to malaria for the duration of gestation. The current mouse models for malaria infection do not allow for the study of malaria throughout gestation because infection initiated in early pregnancy uniformly results in pregnancy loss. We believe this model is an important tool for the exploration of prolonged malaria infection on fetal and postnatal outcomes. Furthermore, we believe that outbred mice are an underutilized link between studies using inbred mouse populations and genetically diverse human populations.

The third chapter of my dissertation describes the modulation of infection severity in the Swiss Webster-*P. chabaudi chabaudi* AS model for gestational malaria by the manipulation of the gut microbiota. Not only does the composition of the gut microbiota determine malaria infection severity in a genetically diverse population of mice, microbiota-influenced maternal infection severity determines fetal and postnatal outcomes. Severe infections observed in dams with susceptibility-conferring gut microbes result in reduced fetal viability, fetal weight, and postnatal survival. Pregnancy outcomes are improved in mice with resistance-conferring gut microbes associated with the development of lower parasite burdens and reduced maternal morbidity. Susceptibility- and resistance-associated gut microbiotas are acquired from mice purchased from vendors known to differ in the composition of the gut microbiota. The murine gut microbiota has been previously identified as a major determinant of susceptibility to malaria infection; however, the ability of the gut microbiota to determine infection severity and pregnancy outcome in infected pregnant mice has not previously been explored in either inbred or outbred mice.

In the fourth chapter of my dissertation, I demonstrate that the modulation of malaria infection severity via the manipulation of the gut microbiota is a potential tool for model building and model expansion. To explore how maternal infection severity modulated by the gut microbiota influences the peripheral and placental environment, I assess peripheral inflammation, placental parasite burdens, the transcriptional response of conceptuses, and embryo viability at midgestation or peak infection in *P. chabaudi chabaudi* AS-infected mice possessing resistance- and susceptibility-conferring gut microbes. We believe this is an important early demonstration of the utility of a mouse model where infection severity and outcomes are 'tunable' via the manipulation of the gut microbiota.

The second, third, and fourth chapters of this document describe my work on novel research projects and are presented in the style of manuscripts. Figures are included at the end of each of these chapters, and figure legends are located on the page preceding the figure. In the fifth chapter of my dissertation, I revisit the conclusions of the second, third, and fourth chapters, address outstanding questions posed by my work, and briefly discuss future studies and potential new avenues of research.

Literature Review

The global burden of malaria infection

Malaria, a preventable and treatable infection, remains a major cause of morbidity and mortality worldwide. In 2016, an estimated 216 million people were infected with malaria, resulting in 445,000 deaths [1]. *Plasmodium* species, the etiological agents of malaria, are mosquito-vectored protozoan parasites capable of infecting a wide range of vertebrates. Individual *Plasmodium* species are highly host-specific, and generally restricted to a single intermediate vertebrate host species. *Plasmodium falciparum*, *Plasmodium vivax*, *Plasmodium*

malariae, and *Plasmodium ovale* cause malaria in humans, though zoonotic malaria infections do occasionally occur. *P. falciparum* causes the most severe human infections and is responsible for the vast majority of the deaths attributed to malaria. In 2016, *P. falciparum* infections in Africa were responsible for roughly 90% of the 216 million malaria cases and 445,000 deaths observed globally [1].

The global burden of malaria infection is not distributed evenly geographically or demographically. The WHO African region accounts for the vast majority of malaria cases and deaths globally, and a large share of these infections are reported in sub-Saharan Africa. Eighty percent of malaria infections reported globally are detected in 15 countries, 14 of which are in sub-Saharan Africa [1]. Alarmingly, improved malaria surveillance in Africa suggests that the burden of *P. falciparum* malaria is significantly greater than the current estimates [1]. Children and pregnant women are especially vulnerable to *P. falciparum* infection. Children under the age of 5 absorb approximately two thirds of malaria cases [1], largely because they have not developed the protective antimalarial immune responses observed in malaria-experienced adults [2]. Pregnant women are also considered especially vulnerable to malaria infection because they can develop placental malaria (PM). PM causes a variety of poor birth outcomes, including low birth weight resulting from intrauterine growth restriction or premature delivery, abortion, and stillbirth [3-8]. In the early 2000s, an estimated 125 million pregnant women were considered at risk for developing malaria infection and more than 300,000 infant deaths were attributable to malaria infection during pregnancy in Sub-Saharan Africa annually [5, 9, 10]. New models indicate that this number has dropped precipitously in the last decade. In 2015, an estimated 9.5 million pregnant women would have been exposed to malaria infection resulting in 750,000 low birthweight deliveries in the absence of malaria control programs targeting pregnant women [11,

12]. The treatment of pregnant women with antimalarial drugs is estimated to have prevented 128,000 underweight births [11, 12]. However, the estimated fatality rate of malaria-associated low birthweight is 37.5% [10], so PM remains a significant cause of preventable infant death worldwide.

The child health impacts of maternal malaria infection are not restricted to poor birth outcomes. Infants born to women with PM are more likely to be infected with malaria [13, 14] and develop extremely high parasite burdens [15] in early life. Furthermore, the impact of maternal malaria infection on infants is not homogenous. For example, Cameroonian infants born to women with lower placental parasite burdens have a greater risk of acquiring a *P. falciparum* infection and a shorter average time to infection than infants born to women with higher placental parasite burdens [16]. Most women in the lower placental parasitemia group were multigravidae, suggesting that the gravidity-dependent reduction in infection severity observed in multigravid women does not necessarily protect their children against the detrimental impact of *in utero* exposure to PM [16]. Finally, PM has been proposed as a contributor to neurodevelopmental disorders in children exposed to malaria infection *in utero* [17, 18]. Ongoing efforts to prevent and treat malaria in pregnant women are critical for reducing the life-altering impacts of PM on young children.

The life cycle of *Plasmodium* parasites

All *Plasmodium* species possess a complex life cycle spanning the mosquito and vertebrate host. Like other *Plasmodium* species, *P. falciparum* is transmitted by the bite of the female *Anopheles* mosquito, which must blood feed to produce eggs. When an infected female takes a blood meal, sporozoites are injected into the human host with the mosquito's saliva. There is believed to be a direct relationship between feeding time and the number of sporozoites

transmitted [19]. A fraction of the deposited sporozoites enter the blood stream and travel to the liver, where they enter hepatocytes and replicate asexually, resulting in the release of a large number of merozoites into the blood stream. Merozoites invade erythrocytes and become immature mononucleated trophozoites. Trophozoites mature into schizonts and produce merozoites that are released into the blood with the rupture of the infected cell. The rupture of parasitized erythrocytes also releases parasitic products, including hemozoin, the immunogenic malarial pigment produced by the parasite as a byproduct of hemoglobin consumption, into circulation. Blood-stage malaria infection is the only phase of malaria infection associated with the development of clinical illness in the infected vertebrate host. In *P. falciparum* infection, blood-stage parasites tend to be synchronized. As a result, human malaria infection is associated with a periodic fever coordinated with the synchronous rupture of schizonts throughout the body [20]. This occurs at approximately 48 hour intervals [20]. In addition to fever, uncomplicated malaria infection is accompanied by non-specific symptoms such as headache and vomiting.

Blood stage infection of the human host will also yield gametocytes, which reproduce sexually within the mosquito midgut. Following erythrocyte invasion, merozoites can alternatively differentiate into gametocytes. When ingested by the *Anopheles* mosquito, male microgametocytes and female macrogametocytes sexually reproduce, producing zygotes. The zygote migrates through the mosquito midgut wall and matures into an oocyst. After a period of time, the oocyst bursts and the released sporozoites travel to the salivary glands of the mosquito. The extrinsic incubation period, or the amount of time between parasite ingestion and transmission, is generally two to three weeks, though this varies as a function of environmental temperature [21].

Variation and sequestration: mechanisms of immune invasion

P. falciparum utilizes two major strategies to avoid the host immune system: antigenic variation and sequestration in peripheral tissues. Both of these immune evasion strategies depend on parasite proteins displayed at the surface of the infected erythrocyte. Intraerythrocytic malaria parasites express a number of proteins that modify the plasma membrane of the host cell. In *P. falciparum*, the protein *P. falciparum* erythrocyte membrane protein 1 (PfEMP1), encoded by the *var* family of genes, functions both as a variant antigen and as a receptor for binding to host endothelium [22, 23]. A single *P. falciparum* genome may possess as many as 60 unique *var* genes, but parasite isolates from different geographic regions rarely share *var* genes, so the global repertoire of *var* genes is vast [24]. The transcription of *var* genes is controlled epigenetically, and transcripts for a single *var* gene are expressed by mature intraerythrocytic parasites [25, 26]. By expressing a single version of the variant protein at a time, the parasite can evade recognition and clearance by the host adaptive immune response [23]. The regulation of *var* gene expression switching is complex. Experiments utilizing cultured blood-stage *P. falciparum* and mathematical modeling suggest that a single, highly conserved family member, *var2csa*, may serve as a 'sink node' in the *var* gene expression network [27]. Essentially, *var2csa* may be expressed transiently between other *var* family members or *var2csa* expression may represent a default expression pattern [27].

Adults residing in malaria-endemic regions develop a wide array of antibodies that bind to specific PfEMP1 variants [28], as well as antibodies against conserved epitopes [29]. These antibodies confer protection against malaria infection by opsonizing infected red blood cells (iRBCs) [30] and blocking the binding of iRBCs to the endothelium [29, 31-33]. Impeding the binding of infected erythrocytes to vascular beds in the periphery is a critical component of the

antimalarial immune response because PfEMP1 contributes to malaria pathogenesis by mediating the binding of iRBCs to the host endothelium [22, 34]. This allows the parasite to avoid circulating through the spleen, where iRBCs would be destroyed by splenic macrophages [22, 34]. Variant surface proteins encoded by *var* genes confer the ability to bind to different host receptors. Therefore, PfEMP1 enables tissue-specific sequestration, which is responsible for many of the organ-specific syndromes associated with *P. falciparum* infection [22].

In pregnant women, PM is caused by the accumulation of iRBCs within the intervillous spaces of the placenta, triggering a robust local immune response that results in inflammation, hyperplasia, and fibrin deposition [35, 36]. The sequestration of iRBCs within the maternal blood spaces of the placenta is mediated by the binding of PfEMP1 to the syncytiotrophoblast [37-39], the fetally derived layer of cells that comes into contact with maternal blood in the placenta. Unlike the vascular beds throughout the rest of the body, the syncytiotrophoblast is considered a modified epithelium, not an endothelium. Specifically, *P. falciparum*-infected erythrocytes in the maternal blood bind to a glycosaminoglycan, chondroitin sulfate A (CSA), expressed by the syncytiotrophoblast [39]. This binding is mediated by the expression of the VAR2CSA variant of PfEMP1 [37, 38]. Therefore, *var2csa* serves important functions in both *var* gene expression switching and pathogenesis in a subset of hosts. The ability to bind CSA is unique to and frequently shared by parasites isolated from infected placentae [40-42]. In fact, parasites isolated from infected non-pregnant individuals tend to have a higher affinity for other molecules, such as CD36, a cell surface protein that is expressed by the endothelium but only expressed at very low levels by syncytiotrophoblast [41, 43]. Other molecules, including hyaluronic acid and intercellular adhesion molecule 1 (ICAM-1), are believed to contribute to the binding of infected erythrocytes [44-47]. Despite the contribution of PfEMP1 variants specific to other

syncytiotrophoblast surface molecules, the ability of infected erythrocytes to bind CSA remains the most important driver of PM [40].

In endemic regions, many people exposed to malaria since childhood do not develop clinically evident malaria infections as adults. However, pregnant women can be infected by VAR2CSA-expressing malaria parasites to which they do not have pre-existing immunity, allowing the parasites to sequester in the placenta and cause severe chronic infections [6, 33, 48]. For this reason, PM is most frequently observed in primigravid women and the severity of infection generally decreases with gravidity as women develop antibodies specific to the PfEMP1 variants associated with placental sequestration [32, 33, 40, 48-50].

The pathogenesis of placental malaria

PM is exclusively associated with *P. falciparum* infection because *P. falciparum* is the only human malaria capable of placental sequestration. Therefore, this discussion of the pathogenesis of PM will focus exclusively on the infection of pregnant women with *P. falciparum*. However, it is important to acknowledge that maternal infection with either *P. falciparum* or *P. vivax* during pregnancy may be associated with low birth weight [6].

The histopathological features of PM are best described at gestational term, following the expulsion of the placenta at delivery. The sequestration of iRBCs within the intervillous spaces and the deposition of hemozoin results in the development of intervillositis, or the massive accumulation of maternal immune cells within the intervillous spaces of the placenta [36, 51-56]. Intervillositis is observed less frequently in women that are not actively infected with malaria at the time of delivery [36, 52, 54-56]. In the absence of an active infection, defined by the absence of parasites within the placenta, hemozoin embedded in fibrin is associated with past infection [36, 51, 52, 54, 56]. As a result of parasite sequestration and the subsequent inflammatory

response, basal membrane thickening, fibrinoid necrosis, syncytial knots, and fibrin deposition are frequently observed in women who develop PM during their pregnancies [35, 36, 50, 56]. Despite the noxious stimuli associated with PM, syncytiotrophoblast apoptosis is not considered a feature of PM pathogenesis [35, 57]. However, syncytiotrophoblast necrosis has been observed in PM and experimental mouse models for malaria during pregnancy [35, 36, 58, 59]. As a result of these pathologies, which interfere with normal placental function and processes, placental malaria infection is associated with low birth weight, infant mortality, and stillbirth [3, 5, 6, 8]. Fortunately, effective malaria treatment reduces the incidence of PM and increases birth weights of infants born in malaria endemic regions although drug availability and resistance pose serious challenges [4, 7, 11].

A number of immunological and cellular mechanisms contribute to the development of PM-associated poor birth outcomes. Inflammation, coagulation, and oxidative stress are major contributors to PM pathogenesis, and the interrelatedness of these responses contributes to the amplification of placental damage and dysfunction in PM. The immune response to PM involves both the innate and adaptive arms of the maternal immune system. This discussion will focus primarily on maternal inflammatory cells, specifically monocytes, macrophages, and dendritic cells (DCs), as these cell types are present at high densities in the malaria-infected placenta. Additionally, this discussion will focus on iRBCs and hemozoin, both of which may be present in great abundance in the parasitized placenta.

Intervillositis is considered a major feature of PM and is significantly associated with low infant birthweight and preterm delivery [52, 53]. Intervillositis due to PM is associated with elevated cytokine titers in the placental plasma. These cytokines both reflect the existence of intervillositis and attract additional maternal leukocytes to the placenta. The association between

PM and placental cytokines has been observed in a number of studies. In placental plasma collected from Cameroonian women, elevated levels of IFN-γ, TNF-α, and IL-10 were found in plasma collected from malaria-infected placentae compared to uninfected placentae [55]. The expression of IL-10, an anti-inflammatory cytokine, suggests a compensatory mechanism seeking to reduce detrimental inflammation at the maternal-fetal interface [55]. Consistent with this, elevated levels of IL-1β, IL-8, TNF-α, and IL-10 were observed in placental plasma collected from primigravid Malian women with PM at the time of delivery [60]. Similarly, levels of TNF, IL-6, and IL-10 were elevated in the placental plasma of Kenyan women with PM at delivery [56]. Macrophage migration inhibitory factor (MIF), a cytokine associated with macrophage activation, was also found to be significantly more abundant in the placental plasma of Kenyan women with PM [61]. Furthermore, in a cohort of women residing in Malawi, MIP-1α, MIP-1β and IL-8 were elevated in the placental plasma of women with PM [62]. However, once parity and HIV status were accounted for, only MIP-1α and IL-8 were significantly elevated in the placental plasma of women with PM [62]. Both of these chemokines were associated with placental monocyte density, suggesting that they contribute to monocyte recruitment in PM [62]. Similar results were produced in a study examining the levels of MIP-1α and MIP-1β in the placental plasma of Kenyan women [63]. MIP-1β was elevated in the placental plasma of women with PM, regardless of HIV status, while MIP-1α was only elevated in women with high-density parasite burdens [63]. Notably, elevated placental cytokine titers and associated poor birth outcomes may not be dependent on active PM infection at delivery. In Kenyan women residing in a holoendemic region, primigravid women who delivered low birth weight infants displayed significantly greater concentrations of placental TNF-α and IFN-γ whether or not the placenta was actively infected at the time of delivery [31]. Systemic

inflammation may also be associated with poor birth outcomes. In Malian women with PM, the elevation of proinflammatory cytokines in peripheral blood predicted poor birth outcomes, including preterm birth and pregnancy loss [60], but no correlation was observed in a cohort of Kenyan women [31].

The *ex vivo* culture of intervillous immune cells suggests that these mononuclear cells are activated during PM. Intervillous leukocytes (14% monocytes/macrophages) collected from placentae of Cameroonian women with PM at the time of delivery produce significantly more TNF-α, IL-10, IP-10, MCP-1, MIP-1α, and MIP-1β in culture, and the higher titers of these cytokines and chemokines were associated with greater intervillous infiltration of monocytes and macrophages [55]. The activation of intervillous mononuclear cells may contribute to the protection of multigravid women against PM. Placental blood mononuclear cells collected from multigravid women without PM at delivery produce more IFN-γ, TNF-α, and IL-10 in culture than placental blood mononuclear cells from uninfected primigravid and secundigravid women or multigravid women with PM, suggesting that the overproduction of these cytokines may protect multigravid women against PM [64]. Within this study population, intervillous mononuclear cells collected from PM-infected primigravid and secundigravid women produce significantly more TNF-α than cells collected from gravidity-matched uninfected women, indicating that proinflammatory cytokines are also produced by intervillous mononuclear cells in response to PM [64]. The precise secretory phenotype of cultured intervillous mononuclear cells is informed by the placental environment at the time of delivery. Broadly speaking, intervillous mononuclear cells collected from HIV^- women with moderate- to high-density *P. falciparum* parasite burdens produce more IFN-γ, TNF-α, and IL-10 in culture than cells collected from women with lower density infections [65]. Hemozoin load has the opposite impact on cytokine

production. In general, greater hemozoin accumulation is associated with reduced IFN-γ, TNF-α, and IL-10 production in culture by intervillous mononuclear cells collected from HIV^- women with PM at delivery [65]. Altogether, these data demonstrate that PM alters the activation status and secretory phenotype of intervillous mononuclear cells, partially explaining the high levels of proinflammatory cytokines in placental plasma during infection.

In the malaria-infected placenta, both maternal and fetal cells contribute to the accumulation of maternal immune cells within the placenta. Hemozoin and iRBCs are two major markers of malaria infection that elicit responses from both maternal immune cells and the fetal syncytiotrophoblast. The reported effects of hemozoin on immune cells, specifically monocytes, are diverse. Monocytes can respond to hemozoin prior to phagocytosing the molecule. When exposed to natural hemozoin produced by plasma-cultured parasites *in vitro*, primary human monocytes react rapidly, producing TNF-α and MIP-1 within 3 hours [66]. The ability of monocytes that have ingested hemozoin to produce cytokines is more controversial. Cultured CD14+ peripheral blood mononuclear cells (PBMCs) treated in culture with a relatively high dose (10μg/mL) of either synthetic or natural hemozoin in conjunction with IFN-γ and lipopolysaccharide (LPS) for 24 hours produce significantly more IL-10 and TNF-α than cells treated with IFN-γ and LPS alone [67]. Similarly, murine bone marrow-derived macrophages (BMDMs) exposed to synthetic hemozoin produce low levels of TNF-α, IL-6 and MIP-1α unless primed with LPS [68]. LPS-primed BMDMs produce relatively high levels of IL-1β and IL-18 [68]. Taken together, these data suggest that maternal phagocytes that have ingested hemozoin may produce large amounts of cytokines and chemokines, especially in the context of appropriate co-stimulation. However, other studies suggest that the phagocytosis of hemozoin reduces cytokine production. PBMCs cultured with hemozoin for at least 48 hours produce less

prostaglandin E_2 (PE_2) when stimulated with LPS and IFN-γ [69]. Consistent with this, monocyte-derived DCs are hyporesponsive following natural hemozoin phagocytosis in culture. Following the phagocytosis of hemozoin, primary human monocyte-derived DCs fail to differentiate or mature normally in culture after several days of exposure, an effect that is attributed to the induction of peroxisome proliferator-activated receptor-γ (PPAR-γ), a receptor that binds 15(*S*)-hydroxyeicosatetraenoic acid (15(*S*)-HETE), a lipid peroxidation product produced by hemozoin-mediated heme-catalyzed lipoperoxidation [70, 71]. The mechanisms underlying these contradictory results are incompletely understood, although the quantity of internalized hemozoin may modulate cytokine production. Cultured intervillous mononuclear cells collected from women with PM at delivery containing a moderate amount of hemozoin phagocytosed *in vivo* produce more TNF-α and IL-10 than cells without hemozoin when cultured in medium alone for 48 hours [72]. In contrast, cultured intervillous mononuclear cells containing a large quantity of hemozoin produce significantly less TNF-α, IL-10, and PE_2 when maintained under the same culture conditions [72]. This dose-dependent phenotype is consistent with the theory that the ingestion of hemozoin is toxic to phagocytes (reviewed in ref. [73]). Hemozoin toxicity may be due to the release of iron from ingested hemozoin. Trophozoite-iRBCs and hemozoin phagocytosed by monocytes render monocytes unable to repeat phagocytosis or undergo oxidative burst, an effect that is partly due to the release of labile iron from the hemozoin crystal in the conditions of the phagolysosome [74]. Alternatively, hydroxy fatty acids produced by hemozoin-mediated lipoperoxidation, such as 15(*S*)-HETE, may contribute to the toxification of phagocytic cells [75]. Taken together, these data indicate that the impact of hemozoin on maternal immune cells likely varies as a function of cell type, exposure

time, co-stimulatory conditions, hemozoin density, hemozoin preparation, and a variety of other factors.

In addition to hemozoin, maternal immune cells encounter iRBCs within the parasitized placenta. Like hemozoin, the presence of iRBCs within the placenta may promote intervillositis in PM. Monocyte/macrophage phagocytosis of iRBCs is a major component of the innate immune response to malaria infection. The phagocytosis of iRBCs can occur via opsonic or nonopsonic mechanisms. Nonopsonic phagocytosis is an especially important mechanism for parasite clearance in the nonimmune host. Cultured CD36-expressing monocytes collected from healthy donors phagocytose nonopsonized infected erythrocytes via a CD36-dependent mechanism [76]. Although this is not associated with the secretion of the proinflammatory cytokine TNF-α, CD36+ monocytes do retain the ability to produce TNF-α in response to parasitic products released during schizont rupture via a PPAR-γ dependent mechanism [76, 77]. Primary human monocytes also efficiently phagocytose *P. falciparum*-iRBCs opsonized with nonimmune serum, an effect that can be partially attributed to complement and anti-phosphatidylserine antibodies, though the extent to which this influences monocyte cytokine secretion is unknown [78]. Opsonization with immune serum also promotes iRBC phagocytosis. IFN-γ-primed human monocyte-derived macrophages exposed to iRBCs opsonized with immune serum phagocytose iRBCs and produce IL-1β, TNF-α, and IL-6 [30]. In contrast to the results reported above, no significant iRBC phagocytosis was observed in the absence of opsonization in this study [30]. Parasite proteins may also influence cytokine production by maternal phagocytes. Primary human monocytes exposed to red blood cells infected with lab strain CS2 *P. falciparum* parasites, which exclusively express the VAR2CSA variant of the PfEMP1 protein, produce significantly less IL-1β, IL-6, IL-10, MCP-1, MIP-1α, MIP-1β, and TNF than human monocytes

exposed to transgenic CS2 parasites (CS2-SBP1-KO) deficient in skeletal binding protein 1 (SBP1), which is required for the transportation of PfEMP1 to the erythrocyte surface [79]. These data indicate PfEMP1 is immunomodulatory and may inhibit the inflammatory immune response to iRBCs. Ultimately, the extent to which iRBCs promote the production of proinflammatory cytokines by maternal inflammatory cells in PM is unclear. Monocyte responses to iRBCs, like monocytes responses to hemozoin, likely depend on a number of factors including antibody opsonization, co-stimulation, and the expression of parasite proteins on the iRBC surface. Ultimately, maternal immune cells encountering iRBCs and hemozoin in the placenta likely contribute to PM-associated intervillositis by producing cytokines and chemokines, but the mechanisms by which this occurs have not been fully defined.

Fetal responses also contribute to the recruitment of maternal monocytes to the parasitized placenta. *P. falciparum*-iRBCs selected for binding to cultured syncytiotrophoblast bind CSA on the syncytiotrophoblast surface and trigger intracellular signaling, namely tyrosine phosphorylation [80]. Intracellular signaling within iRBC-exposed primary syncytiotrophoblast results in the secretion of elevated levels of MIF and MIP-1α compared to untreated syncytiotrophoblast or syncytiotrophoblast exposed to uninfected erythrocytes [81]. The elevated secretion of these cytokines, as well as the potential secretion of other cytokines, was associated with increased migration of primary human PBMCs in a transwell assay [81]. Consistent with this, the syncytiotrophoblast of infected placentae displays widespread high intensity cytoplasmic staining for MIF compared to uninfected placentae [82]. Although a statistically significant difference between infected and uninfected placentae was not detected, these results suggest that the production of MIF by syncytiotrophoblast observed *in vitro* is physiologically relevant in PM [82]. The syncytiotrophoblast also responds to hemozoin. Cultured primary

human syncytiotrophoblast exposed to hemozoin produces elevated levels of CXCL8, CCL3, CCL4, and TNF-α, and promotes the migration of PBMCs in a transwell assay [83]. In addition, cultured fetal villous tissue collected from women with PM at the time of delivery secretes larger amounts of IFN-γ than villous tissue collected from uninfected women [55]. Taken together, these data indicate that the syncytiotrophoblast produces molecular signals that contribute to the development of intervillositis in PM.

In addition to massive inflammatory infiltration, the deposition of large fibrin clots is frequently observed in malaria-infected placentae [35, 56, 84]. Coagulation is increasingly appreciated as an immunological strategy for the physical containment of pathogens, but coagulation in the placenta can constrict or occlude maternal blood spaces, severely disrupting normal blood flow [84]. Macrophages within the intervillous spaces of the placenta express high levels of tissue factor, the initiator of the extrinsic coagulation cascade [84]. The relatively large quantity of monocyte-borne tissue factor in the malaria-infected placenta relative to the uninfected placenta is a major driver of clot formation in PM [84]. The potential contribution of fetal tissue factor expressed on the syncytiotrophoblast has not been determined.

The success of anticoagulant therapy in a mouse model for malaria in pregnancy, wherein the treatment of *Plasmodium chabaudi chabaudi* AS-infected pregnant C57BL/6 (B6) mice with low molecular weight heparin improves fetal viability at midgestation, demonstrates that hypercoagulation is a major contributor to malaria-associated poor birth outcomes and a potential therapeutic target [56]. However, the use of anticoagulant drugs as adjunctive therapeutics for PM has not been extensively explored due to concerns about severe bleeding, although the risk of bleeding in pregnant women treated with low-molecular-weight heparins is believed to be quite low [85].

The inflammatory immune response is also closely associated with oxidative stress. The production of reactive oxygen and nitrogen species is an important antimicrobial mechanism of the innate immune response. While these molecules are critical for the destruction of pathogens, damage to the surrounding host tissue is a frequent byproduct of this response. Elevated oxidative stress has been observed in both pregnant women infected with *P. falciparum* and in mouse models for malaria in pregnancy. In Cameroonian women with PM, the levels of the lipid peroxidation product malondialdehyde (MDA) are significantly elevated in placental tissue [86]. Furthermore, a significant positive correlation was detected between MDA level and parasitemia, suggesting that *P. falciparum* infection drives placental oxidative stress in a parasite burden-dependent manner [86]. Nitric oxide and the antioxidant enzymes superoxide dismutase (SOD), catalase (CAT), and glutathione peroxidase (GSH) are also considered biomarkers of oxidative stress. Nitric oxide, which can react with free radicals to produce reactive nitrogen species, is depleted in the context of oxidative stress. Conversely, the expression and activity of antioxidant enzymes is often elevated during the oxidative stress response. However, significant differences in nitric oxide bioavailability and antioxidant enzyme activity were not detected between malaria-infected and uninfected placentae [86]. Intriguingly, SOD and CAT were negatively associated with maternal inflammatory infiltration, indicating that a robust antioxidant response might protect against placental inflammation in PM [86].

Mouse models for malaria infection in pregnancy recapitulate the oxidative stress observed in human PM and suggest that oxidative stress may contribute to placental dysfunction in PM. In BALB/c mice infected with *Plasmodium berghei* NK65 on gestational day (GD) 10±2, elevated oxidative stress is observed in the placentae of infected pregnant dams compared to uninfected dams at 4 and 6 days post-infection (dpi) [87]. In addition, CAT activity was reduced

in the placentae of infected dams at these timepoints, indicating that the antioxidant responses within the placenta are dysregulated by infection [87]. Although pregnancy loss was not observed at or prior to 6 dpi, increased oxidative stress in the placentae of infected dams was associated with a significant increase in the proportion of apoptotic nuclei in the placenta [87]. The placentae of pregnant B6 mice infected with *P. chabaudi chabaudi* AS in early gestation, GD 0, display significant lipid peroxidation at peak infection (GD 10), the time of abortion in infected pregnant mice [88]. Embryo viability was negatively correlated with lipid peroxidation [88], suggesting that placental oxidative stress contributes to pregnancy loss in malaria-infected pregnant mice.

The origin of oxidative stress in the malaria-infected placenta is incompletely understood. Maternal immune cells likely contribute to lipid peroxidation in the placenta. For example, monocyte oxidative burst, characterized by the production of reactive oxygen species, is observed within minutes of contact with natural hemozoin [66]. Consistent with the pre-phagocytic activation of oxidative burst, murine monocytes and human PBMCs that have phagocytosed hemozoin also contribute to the production of nitric oxide-derived reactive nitrogen species. Following exposure to either synthetic or natural hemozoin and IFN-γ for 24 hours, a murine monocyte cell line displayed a dramatic increase in nitric oxide generation compared to cells treated exclusively with IFN-γ [89]. Importantly, treatment with either hemozoin preparation alone did not result in significant nitric oxide production [89]. Similarly, the production of reactive nitrogen species and the expression of nitric oxide synthase type 2 are elevated in PBMCs exposed to hemozoin, IFN- γ, and LPS for 48 hours compared to PBMCs exposed to IFN-γ and LPS alone [90].

The phagocytosis of hemozoin itself may contribute to lipid peroxidation. Free iron released by hemozoin in the phagolysosome may mediate lipid peroxidation via a nonenzymatic reaction [75]. As a result, hemozoin is associated with esterified monohydroxy derivates, the end products of polyenoic fatty acid peroxidation. Intriguingly, these peroxidation products reduce the ability of human peripheral monocytes to perform normal oxidative burst when stimulated with phorbol 12-myristate 13-acetate (PMA) [75], in addition to impairing cytokine secretion as previously discussed [70, 71, 75]. Furthermore, the direct interaction of free hemozoin with primary human syncytiotrophoblast in culture also results in oxidative stress in the absence of leukocytes (D. Sarr, *in preparation*). Therefore, syncytiotrophoblast may experience endogenous oxidative stress by an unknown mechanism due to hemozoin exposure. The extent to which the syncytiotrophoblast produces radical species in response to exposure to malaria infection and the mechanisms by which this might occur have not been extensively explored.

Due to the extensive oxidative stress observed in PM, as well as the association of oxidative stress with placental pathology and poor birth outcomes in PM, antioxidant therapy has been pursued as a potential therapy for PM. In malaria-infected pregnant mice, treatment with the antioxidant 4-hydroxy-TEMPO (TEMPOL), a superoxide dismutase mimetic, reduces oxidative stress in the spleen but oxidative stress in the placenta is modestly and inconsistently reduced [88]. There are two obvious potential explanations for this effect. First, TEMPOL may be ineffective in placental tissues [88]. Second, the bioavailability of TEMPOL in the placenta may be poor [88]. Nanotechnology may allow for the circumvention of the latter issue. Theoretically, targeted nanoparticles capable of binding to CSA on the syncytiotrophoblast surface would allow for the delivery of antioxidant drugs directly to the placenta, perhaps improving drug efficacy and bioavailability [91].

The pathways associated with inflammation, coagulation, and oxidative stress are closely linked. In PM, these relationships enable the formation of positive feedback cycles that promote pathogenesis and ultimately result in poor birth outcomes. The multifaceted role of maternal monocytes as promoters of inflammation, coagulation, and oxidative stress in the parasitized placenta exemplifies this pattern in PM. Host fibrinogen, the uncleaved precursor to fibrin, stably binds to natural hemozoin produced by cultured blood stage *P. falciparum* [66]. Fibrinogen-bound natural hemozoin activates human monocytes resulting in oxidative burst, TNF release, and MCP-1 release prior to monocyte phagocytosis of the hemozoin-fibrinogen molecule [66]. In PM, hemozoin produced within the placenta binds fibrinogen within the maternal plasma. Maternal immune cells encountering hemozoin-bound fibrinogen likely respond by producing TNF and MCP-1, which attracts additional immune cells to the placenta [66]. Recruited monocytes might bear a large amount of tissue factor on their surfaces, promoting additional coagulation within the placenta [84]. In addition, these newly attracted monocytes could encounter fibrinogen-bound hemozoin in the placenta and produce additional reactive oxygen species that would cause oxidative damage to the placenta, as well as cytokines that would promote further inflammatory infiltration [66]. Therefore, the associations between inflammation, coagulation, and oxidative stress may magnify placental pathology and placental dysfunction in PM.

Mechanisms of pregnancy compromise in PM

The placental mechanisms underpinning the poor birth outcomes associated with PM are only beginning to be elucidated. In pregnancies disrupted by maternal *P. falciparum* infection, the function of the placenta is disrupted at the organ and cellular level.

As an organ, the placenta exists to facilitate exchange between maternal and fetal circulatory systems. Normal blood flow through the placenta is required to fulfill this function and supply the fetus with adequate oxygen and nutrients. As a result, the disruption of placental circulation impairs placental function and may compromise the pregnancy. In a study conducted in Kenya, Doppler ultrasound scans indicated that uteroplacental blood flow was disrupted at 32-35 weeks of gestation in women infected with malaria. Abnormal uteroplacental blood flow was associated with low birth weight, preterm delivery, and neonatal death, indicating that the disruption of placental circulation due to PM is associated with poor birth outcomes [92].

Appropriate placental function is also absolutely dependent on the cellular function of the syncytiotrophoblast because all nutrient, waste, and gas exchange between the mother and the fetus occurs through this tissue. The disruption of the cellular function of the syncytiotrophoblast can have devastating impacts on the growth and development of the fetus. Connections between PM-mediated syncytiotrophoblast dysfunction and fetal growth restriction have only recently been identified. Amino acid transport is disrupted in parasitized human placentas displaying intervillositis [93]. The disruption of amino acid transport in PM is attributed to impaired mechanistic target of rapamycin (mTOR) signaling due to the proinflammatory placental environment associated with intervillositis [94]. mTOR, a master regulator, is involved in signaling pathways associated with sensing nutrients, oxygen, and other environmental and intracellular cues. As a result of aberrant mTOR signaling, PM is also associated with abnormal syncytiotrophoblast autophagy. The negative inhibition of autophagy by mTOR is lifted when mTOR signaling is impaired by PM [95]. As a result, PM with intervillositis is also associated with increased autophagosome formation [95]. However, these autophagosomes fail to fuse normally with lysosomes and accumulate within the syncytiotrophoblast [95]. A negative

relationship is observed between the accumulation of autophagosomes and the activity of amino acid transport System A [93].

Intervillositis in parasitized placentae may also contribute to low birth weight by disrupting normal glucose transport across the syncytiotrophoblast. The transplacental transportation of glucose may be impaired in women with PM, impeding fetal growth. Glucose transporter isoform 1 (GLUT1) is critical for transporting glucose across the microvillous and basal plasma membranes of the syncytiotrophoblast. GLUT1 is more abundant on the maternal-facing microvillous membrane than on the fetal-facing basal membrane of the syncytiotrophoblast [96]. Therefore, the flow of glucose to the fetus is controlled by the expression of GLUT1 in the basal plasma membrane [96]. The expression of GLUT1 in the basal plasma membrane is significantly reduced in placental biopsy specimens collected from women with PM and intervillositis at the time of delivery [97]. PM alone is not associated with a reduction in the expression of GLUT1 in the basal plasma membrane, suggesting that the maternal inflammatory response, not malaria infection itself, disrupts GLUT1 expression [97]. Consistent with this, GLUT1 expression in the basal plasma membrane is negatively correlated with monocyte density in the placenta [97]. The abnormal reduction of GLUT1 expression by the syncytiotrophoblast in women with PM and intervillositis may be attributable to the disruption of the insulin-like growth factor (IGF) axis. Experiments utilizing cultured primary human syncytiotrophoblasts and placental explants, as well as a human choriocarcinoma cell line, demonstrate that exposure to IGF-1 increases the expression of GLUT1 on the basal plasma membrane of the syncytiotrophoblast and increases the basal membrane transport of glucose [96]. In a population of malaria-exposed women, IGF-1 levels were significantly reduced in the maternal and cord plasma of women with PM and intervillositis at the time of delivery [98].

Again, a negative relationship is observed between the concentration of IGF-1 and monocyte density in the placenta [98]. These data suggest that PM-associated intervillositis reduces fetal growth by reducing the plasma concentration of IGF-1, thereby reducing the expression of GLUT1 on the basal plasma membrane of the syncytiotrophoblast and limiting the transportation of glucose into the fetal circulation. Consistent with this, concentrations of IGF-1 and GLUT1 are positively correlated with birth weight [97, 98]. In sum, these data indicate that inflammation due to PM-associated intervillositis alters normal nutrient transport across the syncytiotrophoblast resulting in restricted fetal growth.

Oxidative stress may contribute to placental dysfunction in PM by inducing premature placental senescence. Placental senescence, or placental ageing, is a normal phenomenon observed over the course of gestation. Syncytiotrophoblast senescence can be induced *in vitro* by subjecting placental explants to oxidative stress [99]. Furthermore, placental samples collected from women with preeclampsia, a placental pathology associated with abnormal placentation, display inappropriate placental ageing [99]. This is significant, because placentae impacted by PM and preeclampsia share many features, including oxidative stress [100]. Therefore, it is possible that premature placental senescence, caused by PM-associated oxidative stress, contributes to intrauterine growth restriction, preterm birth, and other poor birth outcomes observed in *P. falciparum*-infected pregnant women.

Mouse models have also contributed to our understanding of the mechanisms driving PM-associated poor birth outcomes. Specifically, studies using mice demonstrate that inflammation contributes to pregnancy loss during maternal malaria infection. The proinflammatory cytokine TNF is associated with pregnancy loss in malaria-infected mice in mid- and late gestation. In B6 mice infected with *P. chabaudi chabaudi* AS on GD 0, the

ablation of endogenous TNF prevents the placental destruction normally observed at GD 12, as well as fetal loss [101]. TNF also contributes to fetal loss in CBA/H dams infected with *Plasmodium vinckei* on GD 12 [102]. *P. vinckei* infection induces fetal expulsion on GD 17, an event that is associated with elevated levels of peripheral TNF [102]. The administration of small doses of exogenous TNF accelerates pregnancy loss in infected, but not uninfected, dams at GD 16 [102]. Taken together, these data suggest that inflammation drives fetal or embryo demise and expulsion in mouse models for gestational malaria. Although inflammation has not been conclusively identified as the cause of preterm birth in human pregnancies, the significant association between intervillositis and preterm delivery in human women infected with *P. falciparum* suggests that inflammation may contribute to premature delivery due to PM [52, 53]. Ultimately, further studies using animal models for malaria infection in pregnancy or primary human tissue are required to fully dissect the causes of PM-associated poor birth outcomes.

Mouse models for malaria infection in pregnancy

Mouse models for malaria infection in pregnancy are tractable and inexpensive tools for the study of the placenta during maternal malaria infection. These models are extremely important for exploring the impact of maternal malaria infection on the function of the placenta because human placentae are rarely available for study prior to delivery at term. The human placenta and the murine placenta serve the same function, though they differ structurally. In the context of maternal malaria infection, it is important to note that the trophoblast, the layer of fetally-derived tissue that comes into contact with maternal blood, is a single layer in the late gestation human placenta and three layers in the murine placenta [103]. Despite this, the murine and human trophoblasts are considered analogous structures, both acting as the feto-maternal interface [103].

The direct comparison of specific murine models for malaria in pregnancy is complicated by the use of different mouse strains or stocks, the use of different parasite species or strains, the use of different modes of infection initiation, and variable infectious dose. However, the range of outcomes observed in these models allows for the recreation of different aspects of infection. Most mouse models utilize the murine malaria species *Plasmodium berghei* and *Plasmodium chabaudi* to study malaria infection in a pregnant host.

In pregnant mice, infection with the highly virulent murine malaria species *P. berghei* results in the development of placental pathologies associated with human PM, including the accumulation of iRBCs in the maternal blood spaces, hemozoin deposition, maternal mononuclear infiltrate, fibrinoid necrosis, and placental hyperplasia [59, 104, 105]. When infected with *P. berghei* ANKA between GD 11 and GD 13, pregnant BALB/c mice display the intervillous accumulation of iRBCs, maternal inflammatory infiltrate, and the constriction of the placental vasculature [59]. Intrauterine growth restriction and reduced fetal viability are observed as a result. However, the assessment of postnatal outcomes in this model is complicated by maternal death between 5 and 10 dpi [59]. Similar histopathological features and pregnancy outcomes are observed following infection with another *P. berghei* strain, *P. berghei* NK65. When BALB/c or ICR dams are infected with *P. berghei* NK65 between GD 12 and GD 16, dams experience poor birth outcomes including the birth of underweight pups, premature labor, and stillbirth [104, 106]. When the infection of ICR dams is initiated at GD 14, the accumulation of iRBCs, maternal inflammatory infiltrate, and trophoblastic hyperplasia are observed at gestational term (5 dpi) [104]. Dams infected with *P. berghei* NK65 at GD 7 or earlier experience fetal resorption and abortion prior to death [104, 105]. As with *P. berghei* ANKA, the assessment of postnatal outcomes is complicated in models utilizing *P. berghei* NK65 because

maternal mortality is observed in all infected dams [104, 106]. Infection with a third strain of *P. berghei* yields similarly lethal results. When infected with *P. berghei* NICD on GD 6, pregnant outbred Swiss albino mice die prior to reaching gestational term at approximately 7 dpi [105]. When infection is initiated on GD 13, approximately half of Swiss albino dams produce live pups at term, although the pups are significantly underweight compared to pups produced by uninfected controls [105]. Of the infected dams that do not produce live pups at term, 20% display fetal resorption at term and 30% die prior to delivery [105].

In general, pregnant mice infected with *P. berghei* display a greater susceptibility to infection than virgin controls as indicated by the accelerated development of parasitemia [59, 104, 106]. Intriguingly, Swiss albino dams infected on GD 13 do not develop parasite burdens more rapidly than virgin control animals, while Swiss albino dams infected on GD 6 do display an accelerated development of parasitemia [105]. The mechanism underlying this discrepancy is not understood.

P. berghei-based mouse models for malaria infection in pregnancy have a number of strengths. These models recreate many of the characteristic features of placental pathology, including intervillositis, which is considered a major characteristic of human PM [36, 51-55]. In addition, *P. berghei*-infected mice can recreate many of the pregnancy outcomes associated with maternal malaria infection. Dams abort their pregnancies when infection is initiated in early gestation [104, 105], but when infection is initiated later in gestation, dams experience preterm birth, stillbirth, or deliver underweight pups [59, 104, 105]. However, the use of *P. berghei*-based mouse models is limited for the following reasons. First, the lethality and rapid progression of *P. berghei* make it difficult to study maternal malaria infection throughout gestation. Understanding persistent malaria infection is important, as many malaria-infected

pregnant women develop chronic infections as a result of placental parasite sequestration. Second, *P. berghei* infection is generally lethal in naïve mice, regardless of pregnancy status. Although malaria infections cause a significant number of deaths globally, *P. falciparum* infection is not uniformly fatal. Therefore, the severity of *P. berghei* infection is relatively extreme compared to human malaria infection. Third, it is not possible to study maternal malaria infection using *P. berghei* in early gestation, as infections initiated prior to GD 7 generally result in implantation failure due to the rapid progression of infection [106]. Finally, although it is possible to produce malaria-exposed pups using a *P. berghei* model for maternal malaria infection, the maternal morbidity observed as a result of infection necessitates fostering the pups if their survival is required for subsequent assessment of postnatal outcomes [18, 59]. Neonatal fostering is a well-established husbandry technique, but it is logistically complicated and labor intensive.

P. chabaudi is less virulent than *P. berghei*, although mortality in some strains of mice is significant [57, 107, 108]. The reduced virulence of *P. chabaudi* compared to *P. berghei* allows for the exploration of malaria infection in early pregnancy [109]. When B6 and A/J mice are infected with *P. chabaudi chabaudi* AS on GD 0, both B6 and A/J mice abort their pregnancies by midgestation, or GD 12 [57, 109, 110]. B6 dams subsequently recover from infection but mortality is observed in A/J dams [57]. When B6 dams are infected with *P. chabaudi chabaudi* AS on GD 6, GD 8, or GD 10, dams undergo pre-term delivery on GD 15, GD 16, and GD 17, respectively. Regardless of the day of delivery, all pups are stillborn. It is important to note that the initiation of preterm labor is accelerated the later in gestation infection is initiated (CA Cooper, *in preparation*). As naïve B6 dams infected with *P. chabaudi chabaudi* AS do not produce live pups even when infection is initiated as late as GD 10, infection with *P. chabaudi*

chabaudi AS has not been used to generate malaria-experienced progeny (CA Cooper, *in preparation*).

As observed in *P. berghei*-infected mice, the development of peak parasitemia in *P. chabaudi*-infected mice is accelerated in pregnant mice compared to nonpregnant mice [109]. The accumulation of iRBCs in the placenta is associated with pregnancy loss in B6 mice infected with *P. chabaudi chabaudi* AS in both early [109] and midgestation (CA Cooper, *in preparation*). In B6 mice infected on GD 0, abortion at midgestation is also associated with the development of a proinflammatory, pro-coagulant placental environment, similar to that observed in human PM [56, 101, 109, 110]. In addition, the placentae of infected pregnant mice exhibit histological features associated with PM, including fibrin deposition and hemozoin accumulation, as well as widespread damage to placental structures [101, 111]. Notably, *P. chabaudi chabaudi* AS-infected B6 mice do not demonstrate maternal inflammatory infiltrate, though maternal inflammatory infiltrate is observed in the placentae of *P. chabaudi chabaudi* AS-infected A/J mice at the time of abortion [57, 109].

Although *P. chabaudi chabaudi* AS-based models of malaria infection in pregnancy have been criticized because maternal inflammatory infiltrate is absent, these models have two major strengths. First, the reduced virulence of *P. chabaudi chabaudi* AS compared to *P. berghei* allows for the exploration of maternal malaria in early gestation [57, 88, 101, 109-111]. In *P. berghei*-based models, infection progresses so rapidly that mice lose their pregnancies and die within several days of infection [59, 104, 106]. Second, *P. chabaudi chabaudi* AS-infected B6 dams lose their pregnancies but survive infection [57, 88, 101, 109-111], better modeling the trajectory of infection observed in *P. falciparum*-infected women [112]. Therefore, mouse

models utilizing *P. chabaudi chabaudi* AS are an important companion to *P. berghei*-based mouse models for malaria infection in pregnancy.

The exact mechanisms underlying pregnancy loss in both *P. berghei*- and *P. chabaudi chabaudi* AS-infected pregnant mice have not been fully dissected. However, inflammation has been identified as a major driver of pregnancy loss in mouse models utilizing both parasite species. In *P. berghei*-infected pregnant mice, the genetic ablation of toll-like receptor 4 (TRL4) reduces inflammation and placental pathology in infected pregnant mice, improving fetal outcomes [113]. In addition, the proinflammatory cytokine TNF-α is a significant driver of pregnancy loss in *P. chabaudi chabaudi* AS-infected pregnant mice [101]. Pregnancy in B6 mice can be rescued by treating mice with a TNF-α-ablating antibody, suggesting that TNF-α contributes directly to pregnancy loss [101, 111]. Hypercoagulation and oxidative stress are also associated with pregnancy loss in *P. chabaudi chabaudi* AS-infected mice [56, 88]. Ultimately, a complex constellation of mechanisms, including inflammation, coagulation, and oxidative stress, result in pregnancy loss in malaria-infected dams.

All of the models described above utilize malaria-naïve mice. In contrast, many of the women who develop PM live in malaria-endemic regions and have been repeatedly exposed to malaria infection throughout their lives. Unlike humans, mice cannot be reinfected with the same strain of *Plasmodium* because they develop sterilizing immunity. However, the use of non-naïve or semi-immune mice has been posed as a potential model for the enhanced susceptibility observed in pregnant women who are otherwise considered resistant to clinical malaria infection.

Malaria-exposed mice can experience recrudescence during pregnancy following the clearance of infection by drug treatment. In nonpregnant inbred C3H/StZ and outbred Swiss mice immunized by the injection of *P. berghei* K173 prior to drug treatment, immunization

protects against death due to infectious challenge although parasites persist for months post-challenge in both groups of mice [114]. The prolonged persistence of parasites in these animals has been leveraged to explore waning immunity to malaria infection during pregnancy. Approximately 40-50% inbred C3H/StZ, inbred B10LP, and outbred Swiss mice infected with *P. berghei* K173 prior to antimalarial treatment develop recrudescent malaria infections during pregnancy [115]. Although these infections are only fatal in a subset of dams, recovery is not observed prior to parturition, suggesting that pregnancy impairs the antimalarial immune response in immunized animals [115]. Recrudescence during pregnancy is not restricted to mice infected with *P. berghei* species. Infection of B6 mice with *P. chabaudi chabaudi* CB sporozoites also yields a modest recrudescence in late pregnancy when female mice are mated 35 days after the initial infection [116]. Taken together, these studies demonstrate that pregnancy can trigger the recrudescence of a persistent parasite population that is not clinically evident in a nonpregnant host. Consistent with this, women with sub-microscopic *P. falciparum* infections prior to conception are more likely to develop clinically evident malaria infections in the first trimester, representing the outgrowth of persistent parasites in a pregnant host environment [117].

Subsequent experiments using *P. berghei* K173-immunized C3H/StZ, BALB/c, and Swiss mice demonstrate that immunity during pregnancy increases with gravidity [118]. When drug treatment is used during the initial pregnancy to prevent recrudescence, re-mated mice are less likely to develop detectable parasitemia during a second pregnancy [118]. As this effect is not observed in animals who received a curative dose of chloroquine prior to their first pregnancy, these data suggest that the presence of a small number of parasites throughout pregnancy protects against recrudescence in a subsequent pregnancy [118]. This is consistent

with the effect observed in pregnant women – women must be infected during pregnancy and develop an immune response against placental-binding parasites to be protected from infection during subsequent pregnancies.

Malaria-experienced dams can also be generated by heterologous infection with different *Plasmodium* strains or substrains. When inoculated with *P. chabaudi chabaudi* AS sporozoites, B6 mice clear detectable parasites by 16 dpi [116]. When infection with *P. chabaudi chabaudi* CB is initiated 45 days after the initiation of the initial infection, nonpregnant mice develop very low parasite burdens that do not exceed 5% peripheral parasitemia at peak infection [116]. In contrast, pregnant mice infected with *P. chabaudi chabaudi* CB 45 days after the initial infection and on GD 10 can develop peripheral parasitemia of approximately 20% [116]. Heterologous infection, especially high intensity heterologous infection, is associated with increased production of proinflammatory cytokines, including IL-6, IL-12, MCP-1, and TNF-α, as well as IL-10 [116]. A significant proportion of the dams that develop high parasite burdens during pregnancy produce stillborn pups or neonates that die within the first day of life [116]. Furthermore, weight gain in the surviving progeny of heterologously infected dams is reduced compared to the progeny of uninfected dams prior to and following weaning [116]. This recently developed model has yet to be used extensively for the study of gestational malaria, but it represents an important tool for the study of malaria pathogenesis in a partially immune pregnant host.

The use of outbred mice to study malaria infection may serve as an important link between inbred mouse populations and genetically diverse human populations. The innate genetic characteristics of each inbred mouse strain are a major determinant of susceptibility to murine malaria infection [108, 119]. Outbred mice may allow for the exploration of malaria

pathogenesis in a genetically diverse population that is inexpensive to maintain and relatively easy to manipulate. However, outbred mice have not been used extensively to study malaria infections in recent years, which may be due to the emphasis by funding agencies and animal use committees on reducing animal numbers and concerns about genetic quality control.

Outbred mice were once frequently used for the study of murine malaria infection. Early studies using pregnant outbred ICR and Swiss albino mice infected with *P. berghei* yielded results similar to those observed in *P. berghei*-infected pregnant inbred animals [59, 104, 106]. Swiss Webster mice are perhaps the most accessible outbred mouse stock available commercially today. Most albino Swiss mouse stocks are interrelated, but Swiss Webster stocks have a unique pedigree (reviewed in ref. [120]). Specifically, Swiss Webster mice are derived from Swiss mice that were imported to the US by a researcher prior to being shared with a colleague bearing the surname Webster (reviewed in ref. [120]). To our knowledge, outbred Swiss Webster mice have not been used to study murine malaria in pregnancy, although nonpregnant Swiss Webster mice have been used to study both *P. berghei* and *P. chabaudi* infection [114, 115, 118]. As in B6 mice, *P. berghei* infection is fatal in Swiss Webster mice [121]. In addition, roughly 63% of *P. berghei*-infected Swiss Webster mice develop the symptoms of experimental cerebral malaria and display the histopathological features associated with experimental cerebral malaria in inbred mouse strains [121]. Similarly, Swiss Webster mice infected with a highly virulent strain of *P. chabaudi* develop a peripheral parasitemia that approaches 80% at peak infection [122]. Taken together, these studies indicate that Swiss Webster mice are not inherently resistant to murine malaria infection.

Modulation of malaria infection severity by the gut microbiota

Although the influence of the gut microbiota has been extensively explored in other murine infection models, the study of the gut microbiota's impact on susceptibility to malaria infection has only recently begun. The existing studies in the field demonstrate that the gut microbiota can both modulate susceptibility to malaria transmission and influence blood-stage malaria infection severity. There are three major mechanisms by which gut microbes can influence malaria infection. First, an immune response to gut microbes could also incidentally target parasite epitopes. Second, the gut microbes or their metabolites could shape nonspecific systemic immune responses. Third, microbial metabolites could promote accelerated or reduced parasite development and/or replication in the host.

Enteric microbes and *Plasmodium* species share at least one epitope that can drive an antibody-based immune response capable of targeting both organisms. The immune response against a surface glycan expressed by some gut bacteria also targets *Plasmodium* sporozoites, which bear the same glycan on their surface [123]. Specifically, antibodies against microbial Galα1-3Galβ1-4GLcNAc-R (α-gal) can cross-react with *Plasmodium* α-gal on the surface of *P. falciparum*, *P. berghei*, and *P. yoelli* sporozoites [123]. The experimental assessment of the protective capacity of cross-reactive anti-α-gal antibodies was performed in transgenic mice deficient in α-gal because wild type mice, unlike humans, express α-gal [123]. When colonized with α-gal expressing *Escherichia coli* O86:B7, mice are protected against infection with *P. berghei* ANKA sporozoites [123]. Anti-α-gal antibodies may be an important component of the adaptive immune response against *P. falciparum* sporozoites in humans [123]. Malaria-exposed adults residing in Mali have significantly higher levels of anti-α-gal IgG and IgM than unexposed adults or malaria-exposed children under the age of two [123]. Furthermore, children

that did not acquire malaria during the transmission season had significantly higher anti-α-gal IgM concentrations, but neither a relationship between anti-α-gal antibody titers prior to the transmission season and the risk of *P. falciparum* infection nor a relationship between antibody titers prior to the transmission season and the risk of febrile malaria was observed [123]. A similar pattern between anti-α-gal antibodies and malaria exposure was observed in the Indian state of Odisha (formerly Orissa) [124]. Greater anti-α-gal antibody titers were observed in uninfected and *P. falciparum*-infected adults living in a malaria-endemic region than in malaria naïve controls [124]. Intriguingly, a significant difference in antibody titers is not observed between malaria naïve donors and *P. falciparum*-exposed donors with cerebral malaria, perhaps suggesting that lower antibody titers are associated with reduced protection against severe, complicated malaria infection [124]. In conclusion, immune responses against gut microbes may also contribute to the destruction of *Plasmodium* parasites.

Different communities of gut microbes appear to alter susceptibility to malaria infection via nonspecific modulation of systemic immune responses. This effect is pronounced in experimental mice sourced from different vendors. Mice sourced from the Jackson Laboratory (JAX) or Taconic are relatively resistant to murine malaria infection, while mice sourced from National Cancer Institute Mouse Repository (NCI) or Harlan are relatively susceptible [125]. This effect is observed across inbred mouse strains and *Plasmodium* species and can be attributed to vendor-dependent differences in the composition of the gut microbiota [125]. Specifically, resistant mice sourced from JAX and Taconic possess a greater abundance of bacteria belonging to the Clostridiaceae, Erysipelotrichaceae, Lactobacillaceae, and Peptostreptococcaceae families [125]. Mice sourced from JAX also possess a larger proportion of Bifidobacteriaceae [125]. In contrast, mice purchased from NCI and Harlan possess a larger

abundance of Bacteroidaceae, Prevotellaceae, and Sutterellaceae family members [125]. In resistant mice sourced from JAX and Taconic, the expansion of T follicular helper cells, CD4+/CD49d^{hi} T cells, and germinal center B cells in the spleen is accelerated [125]. Consistent with this cellular response, the production of IgG isotype antibodies specific to parasitic epitopes is accelerated in resistant mice [125]. The mechanisms by which the microbial communities associated with JAX and Taconic influence the adaptive immune response to another pathogen have yet to be defined. Follow up studies demonstrate that resistance- and susceptibility-conferring gut microbes display different transcriptional and metabolic profiles, so this effect could be due to the direct interaction of the gut microbiota with the host immune system or the indirect interaction of microbial metabolites with the host immune system [126].

Finally, microbial metabolites have the potential to modulate malaria infection severity by either altering the host immune response or by modulating parasitic growth. Different microbial community members can produce different metabolites, so different gut microbiotas are associated with different metabolite pools in the gut and systemically. In the context of experimental murine malaria infections, mice displaying vendor-dependent variation in *P. yoelli* infection severity also exhibit different microbe-associated metabolic profiles in the cecal lumen [126]. Absorbed metabolites in the peripheral plasma were not measured but may reflect the metabolite pool within the gut. Various microbial metabolites have diverse and far-reaching impacts on immune cells throughout the body (reviewed in ref. [127]), so a greater abundance of some members of the gut microbiota could enhance the immune response to malaria infection indirectly via the production of metabolites. Alternatively, specific microbial metabolites could promote the accelerated growth of blood-stage malaria parasites or, conversely, impair the growth of blood-stage parasites. No specific metabolites serving either of the above functions has

been identified in the context of human or murine malaria infection. However, it is theoretically possible the microbial metabolites play an important role in determining malaria infection severity by acting on either the host immune system or the parasite itself.

The studies above pose the tantalizing possibility that the gut microbiota may modulate the susceptibility of humans to malaria. Furthermore, these studies suggest that manipulation of the gut microbiota may reduce infection severity or prevent malaria transmission in human populations. Of course, the study of the gut microbiota in human populations is complicated by human diversity. Unlike experimental mice, humans have diverse diets, lifestyles, and environmental exposures. At this time, a single study has sought to explore the relationship between the composition of the gut microbiota and malaria infection. In a Malian population, two main gut microbiota community types were identified [128]. The first community type, characterized by a greater relative abundance of Bifidobacterium and Streptococcus species, was more commonly found in children that were less likely to have detectable *P. falciparum* infections than children with a gut microbiota characterized by a greater relative abundance of Ruminococcaceae and Lachnospiraceae species [128]. No significant relationship between taxonomic profile and the likelihood of developing febrile malaria infection was observed [128]. Taken together, these data suggest that some microbial communities may protect against malaria infection but that neither taxonomic profile reduces malaria infection severity, perhaps indicating that some microbial communities protect against infection, either via immunomodulation or by stimulating the production of antibodies capable of cross-reacting with *Plasmodium* antigens [128]. Future studies may dissect the interactions between malaria transmission or infection severity and the composition of the gut microbiota, perhaps allowing for the development of probiotic-based adjunctive therapies for malaria.

Thus far, the discussion of the relationship between the gut microbiota and malaria infection has been unilateral, focusing on the impact of the gut microbiota on malaria infection. In the context of PM, it is important to acknowledge that both malaria infection and pregnancy can alter the gut microbiota as well. In both B6 and BALB/c mice, *P. berghei* ANKA infection is associated with intestinal pathology and the dysbiosis of the gut microbiota. Both intestinal pathology and dysbiosis are more profound in B6 mice, which are considered more susceptible to *P. berghei* ANKA infection [129]. Although the precise cause of this intestinal dysbiosis was not determined, dysbiosis in BALB/c mice with little to no intestinal pathology suggests that malaria infection or the immune response to malaria infection, not malaria-associated intestinal pathology, disrupts the gut microbiota [129]. Consistent with this, B6 mice infected with *P. yoelli* also display dysbiosis during infection, which recedes as the infection is cleared [130]. These data suggest that, at least in a murine host, *Plasmodium* infection can alter the composition of the gut microbiota. Although malaria-induced dysbiosis is transient, it can have significant functional consequences. For example, *P. yoelli*-infected B6 mice display reduced colonization resistance to non-typhoidal *Salmonella enterica* serotype Typhimurium [130]. Collectively, these studies demonstrate that the gut microbes and malaria parasites sharing a host have a complex reciprocal relationship.

Additionally, the composition of the gut microbiota shifts as a result of both human and murine pregnancy. In human women, the composition of the gut microbiota changes over the course of gestation. When gut microbes collected from women in their first and third trimesters of pregnancy are transferred to germ-free Swiss Webster mice, mice receiving third trimester microbes develop greater inflammation, excess weight gain, and insulin insensitivity compared to mice that receive first trimester microbes [131]. The alteration of the gut microbiota in

pregnancy is one of a suite of metabolic changes responsible for promoting the hyperglycemic state required to continuously nourish the developing fetus throughout gestation [131]. Compared to the human gestational period, murine gestation is extremely brief. Despite this, the maternal gut microbiota shifts during murine pregnancy, with significant changes in the composition of the gut microbiota detectable as early as GD 0.5 [132]. The extent to which these changes alter nutrient availability and absorption or modulate maternal metabolism has yet to be determined. In a mouse model for gestational malaria, it is likely that both pregnancy and infection transiently alter the gut microbiota but the ability of these changes to influence malaria infection severity and pregnancy outcome in these models has not been explored.

Conclusions

The complex pathogenesis of malaria infection in a pregnant host remains incompletely understood, necessitating the ongoing use of animal models. The development of new models for studying gestational malaria is critical, as most mouse models only partially recreate human malaria infection in pregnancy. Furthermore, the ability of the gut microbiota to determine murine malaria infection severity has only recently been identified. Thus, the study of the mechanisms linking bacteria within the gut lumen to susceptibility to malaria, a hematogenous infection, has only just begun.

The research described here seeks to develop new tools for the study of malaria infection in a pregnant host. Briefly, I describe the development of a novel model for pregnancy maintenance using *P. chabaudi chabaudi* AS-infected outbred Swiss Webster mice and demonstrate that infection severity and pregnancy outcome in this model are determined by the composition of the gut microbiota. Finally, I demonstrate that modulation of infection severity

via the manipulation of the gut microbiota is a valuable tool for understanding the maternal-fetal relationship in the context of variable maternal infection severity.

CHAPTER 2

A NOVEL MURINE MODEL FOR ASSESSING FETAL AND BIRTH OUTCOMES FOLLOWING TRANSGESTATIONAL MATERNAL MALARIA INFECTION[1]

[1] Morffy Smith, CD, CA Cooper, JM Moore. To be submitted to *Scientific Reports.*

Abstract

Plasmodium falciparum infection in pregnant women is a major cause of pregnancy loss, neonatal mortality, and severe maternal illness globally. We have developed a novel mouse model for pregnancy maintenance during maternal malaria infection utilizing outbred Swiss Webster mice, which allows for the exploration of infection in a model system that better reflects the genetic diversity of the human population. When infected with *Plasmodium chabaudi chabaudi* AS in early gestation, several inbred mouse strains abort their pregnancies at midgestation. However, outbred Swiss Webster mice infected with *P. chabaudi chabaudi* AS in early gestation carry their pregnancies to term, despite developing high peripheral parasite burdens and severe malarial anemia. Maternal malaria infection is associated with reduced fetal weight and viability at term, as well as a reduction in pup number at weaning. However, no significant difference in postnatal weight gain prior to weaning is detected between the progeny of infected and uninfected dams. Taken together, these data indicate that infection negatively impacts fetal development and postnatal survival, but surviving pups develop normally. This model allows for the exploration of malaria infection throughout pregnancy, modeling the chronic infections observed in pregnant women prior to the birth of an underweight infant. We anticipate that this model will allow for the exploration of the balance between the maternal antimalarial response and pregnancy success. This model also enables the straightforward production of mice exposed to malaria *in utero*, a critical tool for understanding the postnatal repercussions of maternal malaria infection. Finally, the use of outbred Swiss Webster mice may allow for the identification of universally relevant mechanisms associated with the antimalarial response in pregnancy or malaria-related pregnancy compromise.

Introduction

Gestational malaria, or *Plasmodium falciparum* infection in pregnant women, results in severe maternal illness and an array of poor pregnancy outcomes, including low birth weight [3-8]. In the absence of malaria control programs targeting pregnant women, an estimated 9.5 million pregnant women would have been exposed to malaria in 2015 and 750,000 low birthweight babies would have been born as a result [11, 12]. Intermittent preventative treatment in pregnancy protected an estimated 128,000 infants from this outcome [11, 12]; however, gestational malaria is still a significant cause of infant death because the mortality rate of malaria-associated low birth weight is estimated to be 37.5% [10]. In addition to an increased risk of death, children born to women infected with malaria during their pregnancies can face an increased risk of developing neurodevelopmental disorders [17] and clinical malaria in early life [13-15]. Therefore, preventing and treating *P. falciparum* infections in pregnant women remains an urgent public health challenge because the negative impact of maternal malaria infection on child health and development extends beyond the perinatal period.

The poor birth outcomes associated with gestational malaria are a result of placental dysfunction. In the malaria-infected placenta a number of pathologies are observed, such as the accumulation of malaria-infected red blood cells (iRBCs) [39], intervillositis [52, 53], fibrin deposition [35, 36, 50], syncytial knotting [35, 36, 133], and villous tissue necrosis [36]. These pathological features are associated with the disruption of a number of placental processes and functions, including placental perfusion [92], amino acid transport [93, 94], glucose transport [97, 98], and autophagy [95], which limit the placenta's ability to support the developing fetus.

Mouse models for malaria infection in pregnancy allow for the interrogation of these mechanisms in an inexpensive, genetically tractable model system. Different mouse models best

recapitulate different features of gestational malaria. Infection with *Plasmodium berghei* ANKA or *P. berghei* NK65 recreate the placental accumulation of iRBCs and maternal inflammatory infiltrate observed in gestational malaria [59]. When initiated in early gestation, infection results in abortion and embryo resorption [104, 106]. Infection initiated in mid- to late-gestation causes preterm delivery, low birthweight, and stillbirth [104, 106]. Despite the diversity of possible pregnancy outcomes, *P. berghei*-based models are limited by the extreme virulence and rapid progression of *P. berghei* infection. As a result, *P. berghei*-based models cannot be used to study prolonged infection over the course of gestation. In addition, *P. berghei* infection uniformly results in maternal death, an infrequent outcome of malaria infection in pregnant women [112].

In contrast, infection with *Plasmodium chabaudi chabaudi* AS is not lethal in C57BL/6 (B6) mice. The infection of B6 mice on GD 0 results in midgestational pregnancy loss associated with the accumulation of iRBCs in the placenta and the disruption of placental architecture [56, 57, 101, 109-111]. Infection of B6 mice with *P. chabaudi chabaudi* AS at GD 6, GD 8, or GD 10 results in the preterm delivery of stillborn fetuses on GD 15, GD 16, or GD 17, respectively (CA Cooper, *in preparation*). *P. chabaudi chabaudi* AS infection better models the trajectory of human infection in pregnancy, as dams develop severe maternal illness but survive.

While pregnancy loss is observed in a small subset of malaria-infected pregnant women, women residing in malaria-endemic regions often develop chronic infections but carry their pregnancies to term [112]. The current mouse models for gestational malaria are limited in scope because they do not model persistent infection over the course of gestation culminating in a live birth. To overcome this limitation, we have developed a novel model for pregnancy maintenance during maternal malaria infection utilizing outbred Swiss Webster mice. We anticipate that this

model will serve as an important tool for studying fetal and postnatal outcomes following maternal malaria infection initiated in early gestation. Swiss Webster dams infected with *P. chabaudi chabaudi* AS on GD 0 deliver live pups at gestational term despite developing high parasite burdens and severe anemia. Maternal infection results in reduced fetal weight and viability at term, and infected dams have fewer pups at weaning. However, maternal infection does not impact weight gain in surviving pups between birth and weaning. This novel model will allow for the exploration of the complex host-parasite interactions that cause significant maternal morbidity but allow for fetal survival. In addition, this model enables the straightforward production of progeny exposed to malaria infection and the subsequent immune response *in utero*, allowing for the exploration of prenatal exposure to malaria on postnatal development, which is critical because gestational malaria remains a leading cause of preventable infant death [9].

Materials & Methods

Mice

Seven- to ten-week-old female Swiss Webster mice and eight- to ten-week-old male Swiss Webster mice (Clr:CFW) were purchased from the National Cancer Institute Mouse Repository (Frederick, MD). Mice were maintained under specific-pathogen-free conditions, in *Helicobacter* species and norovirus-free rooms, at the University of Georgia (UGA) Coverdell Vivarium, a barrier facility. Husbandry and experiments were performed in accordance with guidelines and regulations set forth by the UGA Institutional Animal Care and Use Committee. All animals were supplied food (PicoLab Mouse Diet 20 5053; St. Louis, MO) and water ad libitum. Mice were adjusted to a 14-hour light/10-hour dark cycle and housed in conditions of 65-75°F and 40-60% humidity.

Parasites and infection monitoring

The following reagent was obtained through BEI Resources Repository, NIAID, NIH: *Plasmodium chabaudi chabaudi*, Strain AS, MRA-741, contributed by David Walliker. Parasites were maintained as frozen stock in accordance with supplier guidelines and amplified in A/J mice for the purposes of infecting experimental Swiss Webster mice.

Peripheral parasitemia was estimated by flow cytometry using a method adapted from Jimenez-Diaz et al. [134]. Blood samples were collected by tail-clip [135], diluted 1:50 in isotonic saline, and stained within 4 hours of collection with 2.5μM SYTO® 16 Green Florescent Nucleic Acid Stain (ThermoFisher Scientific; Waltham, MA). Samples were incubated at room temperature in the dark for 20 minutes, diluted 1:9 in isotonic saline, and analyzed using a CyAn ADP Flow Cytometer (Beckman Coulter; Brea, CA) within 4.5 hours of collection. Thirty thousand cells were analyzed per mouse, and iRBCs were identified by size and fluorescence intensity. A stained sample of uninfected blood was analyzed alongside infected blood samples on each day of measurement to serve as an internal control. Parasitemia is reported as the percentage of iRBCs in the total number of counted red blood cells.

Experimental design

Eight- to ten-week-old female Swiss Webster mice were paired with sexually mature Swiss Webster males. Each morning, female mice were examined for the presence of a vaginal plug, indicating successful mating. The day a vaginal plug was observed was considered gestational day zero (GD 0). Successfully mated female mice were distributed randomly into infected (Mal+) and uninfected (Mal-) cohorts. Age-matched mice that had not been mated were infected as virgin controls. Body weight and hematocrit were measured immediately prior to infection. Gravid and virgin Mal+ mice were infected intravenously with 10^3 *P. chabaudi*

chabaudi AS-iRBCs in 200µl 1x phosphate-buffered saline (PBS) per 20 grams of body weight. Gravid Mal- control mice were intravenously injected with 200µl 1x PBS per 20 grams of body weight to control for stress and handling. At the time of infection or mock infection, all experimental animals, regardless of pregnancy status, were transitioned to a higher fat chow (PicoLab Mouse Diet 20 5058; St. Louis, MO) better suited to the nutritional needs of a pregnant or lactating mouse. Following the measurement of weight and hematocrit immediately prior to infection (GD 0 and Experimental Day 0, ED 0), mice were left undisturbed until GD/ED 6 to maximize blastocyst implantation (GD 4.5) and pregnancy success. Beginning at GD/ED 6, body weight, hematocrit, and parasitemia were measured daily until GD/ED 18 to assess the development of infection and pregnancy progress. Mated female mice displaying a 10% or greater increase in body weight between GD 0 and GD 8 were considered gravid.

Mice were anesthetized with 2.5% Tribromoethanol prior to sacrifice at gestational term, GD/ED 18. Fetal number and viability were determined in gravid mice. Fetal viability was determined by the assessment of reactive movement in response to prodding with blunt-tipped forceps. Viable pups and their placentae were individually weighed.

In an alternative study design, gravid Mal+ and Mal- mice were allowed to proceed to spontaneous delivery of the litter. Dams were single housed beginning at GD 17 and cages were checked at least twice daily for pups beginning at GD 18. Pups were not counted until 4 days of age because maternal distress within the first few days of life can result in the rejection of the litter. At four days of age, pups were uniquely identified by footpad tattooing with nontoxic carbon pigment ink (Super Black Speedball India Ink; Statesville, NC) [136, 137]. Individual pups were weighed at four days of age and every three days thereafter until weaning at 22 days

of age. Pups that did not survive to 13 days of age were excluded from analysis. Pup sex was visually determined at weaning.

Statistics

Descriptive statistical analyses were performed using GraphPad Prism 7 (GraphPad Software; La Jolla, California). All raw clinical data are presented as mean ± SEM. Error bars are not depicted if the error bars are shorter than the height of the symbol. The area under the curve (AUC) of percent starting weight, hematocrit, and parasitemia was calculated for each mouse between GD 0 and GD 18 and is presented as a scatter plot with a bar representing the mean. AUC data of parasitemia between gravid Mal+ and virgin Mal+ cohorts were compared using a two-tailed Student's *t* test. AUC data of percent starting weight and hematocrit were analyzed by one-way analysis of variance (ANOVA) followed by Bonferroni's multiple comparison test between gravid Mal- and gravid Mal+ cohorts and gravid Mal+ and virgin Mal+ cohorts. The number of total and viable fetuses produced by Mal+ and Mal- dams were compared using a two-tailed Student's *t* test. Fetal and placental weights, pooled by dam infection status, are presented as box and whisker plots with whiskers extending from the 10^{th} to the 90^{th} percentile for visualization only. Outliers are depicted as individual data points. Gestational duration of Mal+ and Mal- dams is presented as a Kaplan-Meier curve and groups were compared using the Mantel-Cox test. Viability data and sex data were compared by two-tailed Fisher exact test. The starting weights of mated mice assigned to Mal+ and Mal- cohorts were compared using a two-tailed Student's *t* test. P values ≤ 0.05 were considered statistically significant.

Mixed linear models analysis (SAS 9.4) was used to estimate differences in term fetal and placental weights and postnatal pup growth as a function of dam infection. In both cases, the

interrelatedness of pups born to the same dam was controlled with a random term for the dam. Best fit for the former model was obtained with inclusion of infection status (binary variable), dam starting weight (continuous variable) and number of viable pups in each dam (continuous variable). The latter model assessed trends over time for changes in pup growth; repeated measures in the pups were accommodated with a repeat command and the relatedness of pups born to the same dam was accounted for with a random term for the dam. Model fitting revealed that only dam weight at initiation of the experiment, number of pups at weaning, and age at weight measurement, with associated interaction terms with the latter, influenced trends in weight gain. Pup sex and maternal infection status were not significant in initial models but are depicted in the figure for illustration purposes.

Results

Swiss Webster mice maintain pregnancies to term despite developing high parasite burdens and severe malarial anemia

Swiss Webster mice are highly susceptible to *P. chabaudi chabaudi* AS. Following infection with *P. chabaudi chabaudi* AS on GD/ED 0, parasitemia was estimated daily by flow cytometry for each Mal+ mouse between GD/ED 6 and GD/ED 18. Both virgin and gravid Swiss Webster mice developed high peripheral parasite burdens, with most animals achieving peak infection on GD/ED 9 or GD/ED 10 (Fig. 2.1a). There is no statistically significant difference in parasite burden between virgin Mal+ and gravid Mal+ mice over the course of infection (Fig. 2.1d). The development of peak parasitemia is not accelerated in gravid animals compared to virgin controls (Fig. 2.1a) as reported in other mouse models [57, 59, 101, 104, 109, 111]. No fatalities were observed as a result of infection.

Malarial anemia, a major cause of morbidity and mortality in malaria-infected humans and rodents, is an important indicator of infection severity. Hematocrit was measured daily between GD/ED 6 and GD/ED 18 to track the development of malarial anemia. Infection-related anemia was the most severe in the one to two days following the development of peak parasitemia, GD/ED 10 and GD/ED 11 (Fig. 2.1b). A subtle reduction in hematocrit was observed in gravid Mal- mice over the course of gestation due to the increase in blood volume observed in pregnant animals (Fig. 2.1b). As expected, infection in gravid mice was associated with a statistically significant reduction in hematocrit over the course of gestation (Fig. 2.1e). In addition, pregnancy was associated with a significant reduction in hematocrit among Mal+ animals. Gravid Mal+ mice developed a more severe anemia than virgin Mal+ mice over the course of infection, likely reflecting the cumulative impact of malaria-associated anemia and pregnancy-related hemodilution (Fig. 2.1e).

Unlike *P. chabaudi chabaudi* AS-infected B6 or A/J mice [57, 88, 101, 109-111], Swiss Webster mice infected on GD 0 do not uniformly abort their pregnancies at midgestation. In mated female mice, pregnancy was indicated by an increase in body weight of at least 10% by GD 8 (Fig. 2.2). Six of 29 Mal+ females that met this cut-off did not produce viable fetuses at term, indicative of spontaneous pregnancy loss. Such pregnancy loss was not observed in any gravid Mal- mice. As pregnancy loss was observed in fewer than one quarter of gravid Mal+ animals, aborting mice were excluded from analysis. However, it is notable that aborting Mal+ mice do not develop more severe infections than gravid Mal+ mice that remain pregnant. Parasitemia and hematocrit are indistinguishable between gravid Mal+ mice that carry their pregnancies to term and gravid Mal+ mice that spontaneously abort, although weight gain in aborting gravid Mal+ mice is reduced over the course of the experiment (Fig. 2.3).

Between GD/ED 9 and GD/ED 11, non-aborting gravid Mal+ mice displayed a stasis in weight gain compared to gravid Mal- controls, which gain weight steadily over the course of gestation (Fig. 2.1c). However, from GD/ED 11 onward, gravid Mal+ and gravid Mal- mice gained weight at approximately the same rate (Fig. 2.1c), indicating that gravid Mal+ mice remain pregnant and that their fetuses continue to grow as parasite burdens descend (Fig. 2.1a). Despite this recovery, infection significantly reduced overall weight gain in gravid mice between GD/ED 0 and GD/ED 18, although significant pregnancy-associated weight gain was observed in Mal+ gravid mice compared to Mal+ virgin controls (Fig. 2.1f).

Malaria-infected Swiss Webster mice produce viable fetuses at term

To determine litter size, fetal viability, fetal weight, and placental weight prior to parturition, dams were sacrificed at gestational term (GD 18) and uteri were removed for assessment. Fetuses and placentae were dissected away from the uterus and weighed, and fetal viability was determined by reactive movement. When the typical total and viable litter sizes were compared for Mal+ and Mal- dams, infection was not associated with a reduction in the mean number of total fetuses nor the mean number of viable fetuses produced by Mal+ dams relative to Mal- dams (Fig. 2.4a). However, in pooled populations of progeny, maternal infection was associated with a tendency towards reduced fetal viability. A cohort of 11 Mal- dams produced 123 fetuses, 105 of which were viable (85%). In contrast, a cohort of 13 Mal+ dams produced 142 fetuses, 108 of which were viable (76%), indicating that infection may reduce fetal viability on a population level ($P = 0.064$, two-tailed Fisher exact test).

When fetal and placental weights are pooled by maternal infection status, infection appears to be associated with a reduction in fetal weight on a population level (Fig. 2.4b). No notable change in placental weight was detected as a result of infection (Fig. 2.4c). However,

fetal and placental weights vary both within and between dams (Fig. 2.5). To determine the impact of maternal malaria infection throughout gestation on fetal and placental growth while controlling for the lack of independence of pups born to the same dam, fetal and placental weights were analyzed by mixed linear models. In our cohorts of Mal- and Mal+ dams, infection status, starting dam weight, and the number of viable fetuses within a litter account for 46% of the variance in fetal weight between dams ($P < 0.0001$). If dam weight and the number of viable pups is held constant, infection significantly influences fetus weight and is associated with a 0.21g reduction in fetal weight on average ($P = 0.0002$). It is important to note that the variance in body weight observed in Swiss Webster dams randomized to Mal+ or Mal- cohorts was evenly distributed across infection groups at GD/ED 0 (Fig. 2.6). Placental weight was not significantly influenced by any of the variables included in the analysis.

Malaria-infected dams produce fewer live pups at weaning, but maternal infection does not impact pre-weaning pup growth

To determine the impact of malaria infection on postnatal outcomes, gravid Mal- and Mal+ mice were allowed to proceed to delivery. All gravid Mal- mice ($n = 7$) spontaneously delivered their litters on GD 19, while gravid Mal+ animals ($n = 11$) delivered their litters between GD 18 and GD 21 (Fig. 2.7). However, this apparent extension in time to delivery did not reach statistical significance ($P = 0.1188$, Mantel-Cox test). Of the 11 gravid Mal+ mice, 2 delivered live pups that did not survive to four days of age. These two litters were delivered on GD 18 and GD 19. Pup number and exact time of death was not determined for these litters, as human disruption of the nest was strenuously avoided in the first 4 days of life to prevent the rejection of the litter.

Malaria infection was associated with a statistically significant reduction in pup number at weaning. Mal- dams (n = 7) had a mean of 12 ± 2 pups (± SD) at weaning, while Mal+ dams (n = 11) had a mean of 5 ± 4 pups at weaning (P = 0.0005, Mann-Whitney test). The reduction in gravid Mal+ progeny observed at weaning likely occurs between birth and four days of age because infection was not associated with a significant reduction in the average number of viable fetuses produced by Mal+ dams at GD 18 (Fig. 2.4a). Furthermore, the loss of pups between 4 and 22 days of age was a rare event, with only a single pup produced by a Mal+ dam perishing during this period. Intriguingly, our cohort of Mal+ dams produced significantly more male progeny (33/51, 65%) than our cohort of Mal- dams (39/86, 45%) when pups were pooled by dam infection status (P = 0.032, two-tailed Fisher's exact test).

Individual pup growth was tracked between birth and weaning to assess the impact of infection on postnatal growth and development. Starting at 4 days of age, each pup was weighed every three days until weaning at 22 days of age (Fig. 2.8). In general, a negative relationship between litter size and the average weight of pups in a litter was detected (Fig. 2.9). Trends in pup growth were analyzed by linear mixed models. No significant relationship between maternal infection status and pup growth trends was detected. Consistent with the observed negative influence of large litter size on pup growth, the model revealed that number of pups in the litter at weaning (P = 0.0001) significantly influenced the pup growth trajectory. Weight of the dam also exerted an effect that varied over time (interaction term, P = 0.0215). Pup sex did not impact weight change over time.

Discussion

Infants exposed to malaria infection *in utero* face an elevated risk of death due to fetal growth restriction, preterm delivery, and low birth weight [3-9]. These poor birth outcomes are

attributed to placental dysfunction stemming from the damage sustained by the placenta during malaria infection. At delivery, the accumulation of iRBCs and maternal immune cells [35, 36, 50], hypercoagulation [56, 84], syncytial knotting and rupture [35, 36, 133], and villous tissue necrosis [35, 36, 50, 133] are observed in parasitized placentae, suggesting that placental damage due to gestational malaria is profound even when the pregnancy culminates in a live birth.

Placental dysfunction due to gestational malaria is incompletely understood. Animal models for gestational malaria are vital to understanding how maternal malaria infection impedes fetal development. The most widely used mouse models for malaria in pregnancy entail the infection of a naïve mouse resulting in abortion, preterm delivery, or stillbirth [56, 57, 59, 101, 104, 106, 109-111]. As the impact of exposure to maternal malaria infection *in utero* on child development is one of the primary public health concerns associated with gestational malaria, the inability of these models to produce live progeny is a major limitation. The existing models for generating malaria-experienced pups utilize infection with *Plasmodium berghei* or heterologous *P. chabaudi* infection. When *P. berghei* is used, dams must be infected late in pregnancy to allow the fetuses to reach gestational term prior to pregnancy loss or maternal death [18, 59]. Progeny exposed to *P. berghei* during gestation must be fostered due to maternal mortality [18, 59]. Heterologous infection with nonlethal *P. chabaudi* strains has also been used to produce malaria-experienced progeny. When dams are infected with *P. chabaudi chabaudi* CB prior to pregnancy, then infected with *P. chabaudi chabaudi* AS on GD 10, they proceed to term and deliver live pups following the development of significant parasite burdens [116]. However, this model requires monitoring infected dams throughout two infections, resulting in a protracted experimental timeline [116]. In both of the models described above, significant parasitemias are observed only in the last third of the pregnancy, not throughout gestation [18, 59, 116]. We

speculate that the duration and timing of malaria exposure may result in different postnatal outcomes, and we believe that a longer period of fetal exposure to malaria infection better models the chronic infections observed in pregnant women residing in malaria-endemic areas.

Here, we describe a novel model for gestational malaria utilizing outbred Swiss Webster mice, which do not suffer pregnancy loss when infection is initiated on GD 0. Mouse models of malaria infection rely heavily on inbred mice, although different strains can vary dramatically in the response to a given infection as a result of their innate immunological biases [108, 119]. Thus, restricting studies of malaria to inbred mice limits the ability of scientists to accurately model aspects of the outbred human immune response to a given infection. Outbred mice have not been extensively used for the study of malaria or other infectious diseases for a number of reasons. First, the genetic variability of outbred mouse stocks has not been rigorously explored (reviewed in ref. [120]), leading to concerns about genetic quality control. Second, the inherent diversity of an outbred mouse stock can yield a more diverse range of outcomes, necessitating the use of larger cohorts of animals and increasing experimental costs. Finally, outbred mice are not appropriate for the study of some genetically determined traits, as phenotypic variability may reflect genetic diversity, not experimental treatment. Nonetheless, outbred mice by their very nature should faithfully represent the breadth of disease responses within genetically diverse populations. It follows that responses shared by many of the members of the population may be illuminating, because they may represent universally relevant mechanisms. This was a major appeal of utilizing Swiss Webster mice for the model described here. Moreover, Swiss Webster mice allow us to model the infection outcome observed most frequently in women suffering from gestational malaria: chronic infection throughout gestation, concluding in the delivery of a live infant that is underweight for gestational age. We believe that this novel model represents an

important tool for the study of the antimalarial responses of a pregnant host and the assessment of fetal outcomes in a persistently infected dam, as well as a strategy for the production of malaria-experienced pups for the study of immunological and developmental sequelae of gestational malaria. It is important to note that the Swiss Webster mice used in this model, unlike women living in malaria-endemic regions, have no previous exposure to malaria infection.

Following infection with *P. chabaudi chabaudi* AS on GD/ED 0, gravid Swiss Webster mice develop high parasite burdens and severe malarial anemia. A stasis in pregnancy-associated weight gain is also observed around the time of peak infection. The mechanisms by which gravid Mal+ Swiss Webster mice remain pregnant despite developing parasite burdens exceeding those observed in *P. chabaudi chabaudi* AS-infected B6 mice [57, 101, 109-111] remain to be explored. Mal+ dams ultimately recover and produce live progeny, but fetal weight at term and postnatal survival are reduced in the progeny of Mal+ dams compared to the progeny of Mal- controls. The reduction in fetal weight at term of gravid Mal+ progeny suggests that intrauterine fetal growth restriction contributes to this reduction in gestational weight gain observed in gravid Mal+ mice. However, the potential contribution of anorexia, malaria-related metabolic disruption, or other maternal behaviors and physiological processes cannot be excluded.

The average number of viable fetuses produced by Swiss Webster dams at GD 18 is not reduced by *P. chabaudi* infection. However, the average number of pups present at weaning is significantly reduced in the litters of Mal+ dams. We speculate that the majority of pup deaths occur between birth and 4 days of age, because pup deaths between 4 and 22 days of age are rare. There are two likely explanations for the contraction in Mal+ litter size between GD 18 and 4 days of age. First, fetal viability at GD 18, as determined by reactive movement, may be a poor predictor of postnatal survival. Second, Mal+ dams may be more likely to cannibalize their

young or fail to care for them appropriately in the first hours of life. We speculate that fetal growth restriction observed in GD/ED 18 fetuses produced by Mal+ dams results in the birth of underweight pups, and that low birth weight is associated with an elevated risk of neonatal death. However, it is also possible that maternal malaria infection results in other developmental delays in malaria-exposed fetuses resulting in an increased risk of death due to inadequate prenatal development.

These results are consistent with the patterns of mortality observed in low birth weight human infants. Low birth weight is associated with a significantly higher risk of infant death, regardless of etiology. In the early 2000s, low birth weight was estimated to account for 60-80% of neonatal deaths, although low birth weight was only observed in approximately 14% of births globally [138]. The highest rates of neonatal mortality were observed in Sub-Saharan Africa [138], perhaps partially reflecting the burden of *P. falciparum* infection in the region. Maternal malaria infection is a major cause of low birth weight, and therefore, a major cause of infant death in malaria-endemic regions [4-6, 8]. Notably, a large proportion of these deaths occur within the neonatal period, or the first month of life [6, 8]. Therefore, the novel mouse model described here may recapitulate this outcome of gestational malaria infection.

Despite the attrition in pup number observed in the litters of Mal+ dams prior to 4 days of age, the surviving progeny gain weight normally between birth and weaning. The number of pups in the litter at weaning and the starting weight of the dam significantly influence the trajectory of pup growth, but neither maternal infection status nor pup sex has a significant impact. This is inconsistent with the previously described model for heterologous *P. chabaudi* infection during gestation, where heterologous infection during pregnancy was associated with reduced pre- and post-weaning weights in progeny [116]. Similarly, infection with *P. berghei*

ANKA in midgestation reduces pre-weaning growth in the progeny of Mal+ BALB/c dams [59]. A number of factors could explain these discrepancies. First, infection in the models described above were initiated on GD 10 and GD 13, respectively, whereas infection is initiated on GD 0 in the novel model described here. The timing of infection initiation and peak parasite burden may contribute to postnatal growth phenotypes. Alternatively, these differences may be attributable to innate differences between inbred BALB/c or B6 mice and outbred Swiss Webster mice or to innate differences between *P. chabaudi chabaudi* AS and *P. chabaudi chabaudi* CB or *P. berghei* ANKA. Notably, infection with *P. berghei* ANKA was associated with increased pup mortality between 2 and 21 days of age, although the timing of pup deaths was not described. In contrast, heterologous infection with *P. chabaudi* during pregnancy was not associated with increased pup mortality between birth and weaning. The variable pup survival outcomes observed in these models may again reflect differences in experimental design, or they may reflect inherent differences between parasite species and mouse strains or stocks.

The underlying mechanisms that allow gravid Swiss Webster mice infected with *P. chabaudi chabaudi* AS in early gestation to carry pregnancies to term remain to be explored. We anticipate that future studies will allow for the elucidation of antimalarial host mechanisms compatible with pregnancy success and those that contribute to fetal loss during maternal infection. In addition, future studies probing the causes of neonatal death in malaria-exposed progeny may enhance our understanding of the impact of maternal malaria infection on infant survival. In the context of human infections, we believe that the study of outbred mouse models is important, as commonly observed responses may be universal phenomena, not artifacts observed throughout a murine population as a result of inbreeding. These future mechanistic studies, as well as the further characterization of the impact of transgestational maternal malaria

infection on fetal and postnatal outcomes, demonstrate the power of this model to enhance our understanding of placental dysfunction during gestational malaria.

Acknowledgements

We thank Julie Nelson at the Flow Cytometry Facility of the Center for Tropical and Emerging Global Diseases for flow cytometry services and technical assistance. Research reported in this manuscript was supported by the National Institute of Allergy and Infectious Diseases and the Eunice Kennedy Shriver National Institute of Child Health and Human Development of the National Institutes of Health under award numbers T32AI060546 (to CDMS), and R01HD46860 and R21AI111242 (to JMM). The content is solely the responsibility of the authors and does not necessarily represent official views of the Eunice Kennedy Shriver National Institute of Child Health and Human Development, the National Institute of Allergy and Infectious Diseases, or the National Institutes of Health.

Figure 2.1. Parasitemia, hematocrit, and weight change in *P. chabaudi chabaudi* AS-infected Swiss Webster mice.

a) Parasitemia in virgin and gravid Mal+ mice was estimated by flow cytometry and is presented as the percentage of iRBCs in the peripheral blood.
b) Percent hematocrit was measured throughout infection in virgin and gravid Mal+ mice and gravid Mal- controls.
c) Weight change in virgin and gravid Mal+ mice and gravid Mal- mice is presented as the percentage of body weight relative to 0 days post-infection or post-mock infection.
d) Area under the curve (AUC) was calculated for the parasitemia curve of each individual mouse. A statistically significant difference in parasite burdens is not detected between virgin and gravid Mal+ mice (Student's *t* test, $P = 0.9355$).
e) AUC was calculated for the hematocrit curve of each individual mouse. Statistically significant differences in hematocrit are observed between virgin and gravid Mal+ mice ($P < 0.001$) and between gravid Mal- and Mal+ mice ($P < 0.001$; one-way ANOVA with Bonferroni multiple group comparisons).
f) AUC was calculated for the weight change curve of each individual mouse. Statistically significant differences in weight change are observed between gravid Mal+ and Mal- mice ($P < 0.01$), as well as virgin and gravid Mal+ mice ($P < 0.001$; one-way ANOVA with Bonferroni multiple group comparisons).

Virgin Mal+ $n = 11$; Gravid Mal+ $n = 23$; Gravid Mal- $n = 18$; *** $P \leq 0.001$; ** $P \leq 0.01$; ns $P > 0.05$.

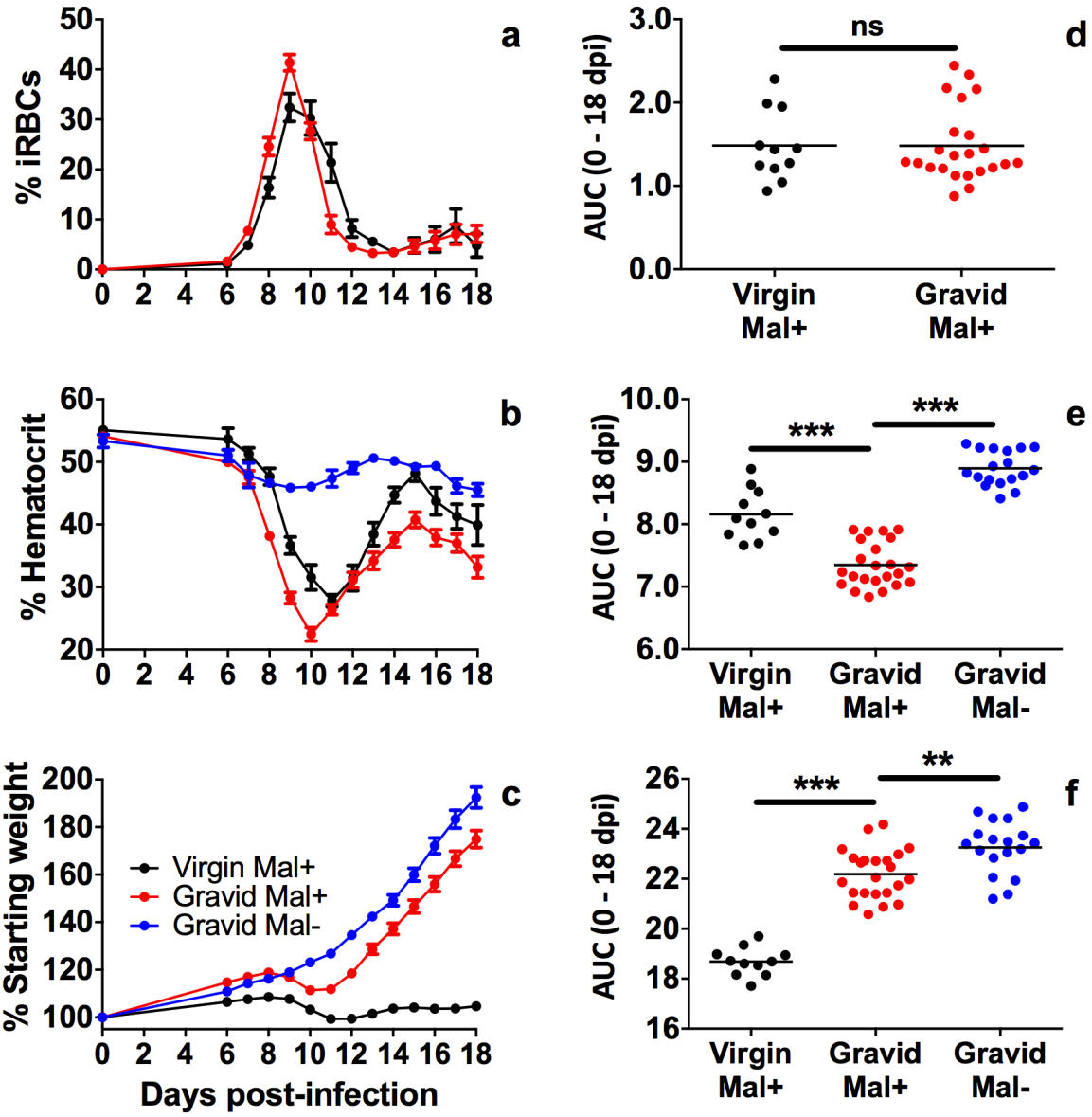
a
% iRBCs
50
40
30
20
10
0
0 2 4 6 8 10 12 14 16 18
b
% Hematocrit
60
50
40
30
20
0 2 4 6 8 10 12 14 16 18
c
% Starting weight
200
180
160
140
120
100
Virgin Mal+
Gravid Mal+
Gravid Mal-
0 2 4 6 8 10 12 14 16 18
Days post-infection
d
AUC (0 - 18 dpi)
3.0
2.0
1.0
0.0
ns
Virgin Mal+
Gravid Mal+
e
AUC (0 - 18 dpi)
10.0
9.0
8.0
7.0
6.0
***
***
Virgin Mal+
Gravid Mal+
Gravid Mal-
f
AUC (0 - 18 dpi)
26
24
22
20
18
16
***
**
Virgin Mal+
Gravid Mal+
Gravid Mal-

Figure 2.2. Gravid Swiss Webster mice display a 10% or greater increase in body weight at GD 8 regardless of infection status.
Weight gain at GD 8 is presented for virgin Mal+, gravid Mal+, and gravid Mal- mice. Only gravid mice that produced live fetuses at term or delivered live pups are displayed. On the basis of the 10% minimum weight gain observed in these gravid mice, intended gravid mice were determined to be pregnant if they exhibited a 10% or greater increase in body weight at GD 8, regardless of the production of viable fetuses or live pups at term.
Virgin Mal+ $n = 11$; Gravid Mal+ $n = 23$; Gravid Mal- $n = 18$.

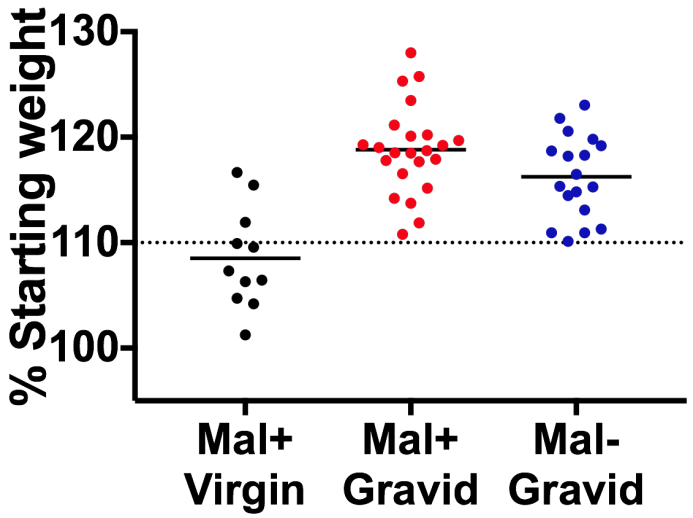
% Starting weight
130
120
110
100
Mal+
Virgin
Mal+
Gravid
Mal-
Gravid

Figure 2.3. Parasitemia, hematocrit, and weight change in aborting *P. chabaudi chabaudi* AS-infected Swiss Webster mice.

Data collected from intended gravid Mal+ mice that experienced spontaneous pregnancy loss at midgestation (gravid Mal+, aborting) are presented with data collected from gravid Mal+ mice that carried their pregnancies to term for comparison.

a) Parasitemia in gravid Mal+ mice is presented as the percentage of iRBCs in the peripheral blood.
b) Percent hematocrit was measured throughout infection.
c) Weight change is presented as the percentage of body weight relative to 0 days post-infection.
d) Area under the curve (AUC) was calculated for the parasitemia curve of each individual mouse. A statistically significant difference in parasite burden is not detected between aborting and non-aborting gravid Mal+ mice ($P = 0.4140$; Mann Whitney test).
e) AUC was calculated for the hematocrit curve of each individual mouse. A statistically significant difference in hematocrit is not detected between aborting and non-aborting gravid Mal+ mice ($P = 0.4451$; Mann Whitney test).
f) AUC was calculated for the weight change curve of each individual mouse. A statistically significant difference in weight change is detected between aborting and non-aborting gravid Mal+ mice ($P < 0.0001$; Mann Whitney test).

Gravid Mal+, aborting $n = 6$; Gravid Mal+ $n = 23$; *** $P \leq 0.001$; ns $P > 0.05$.

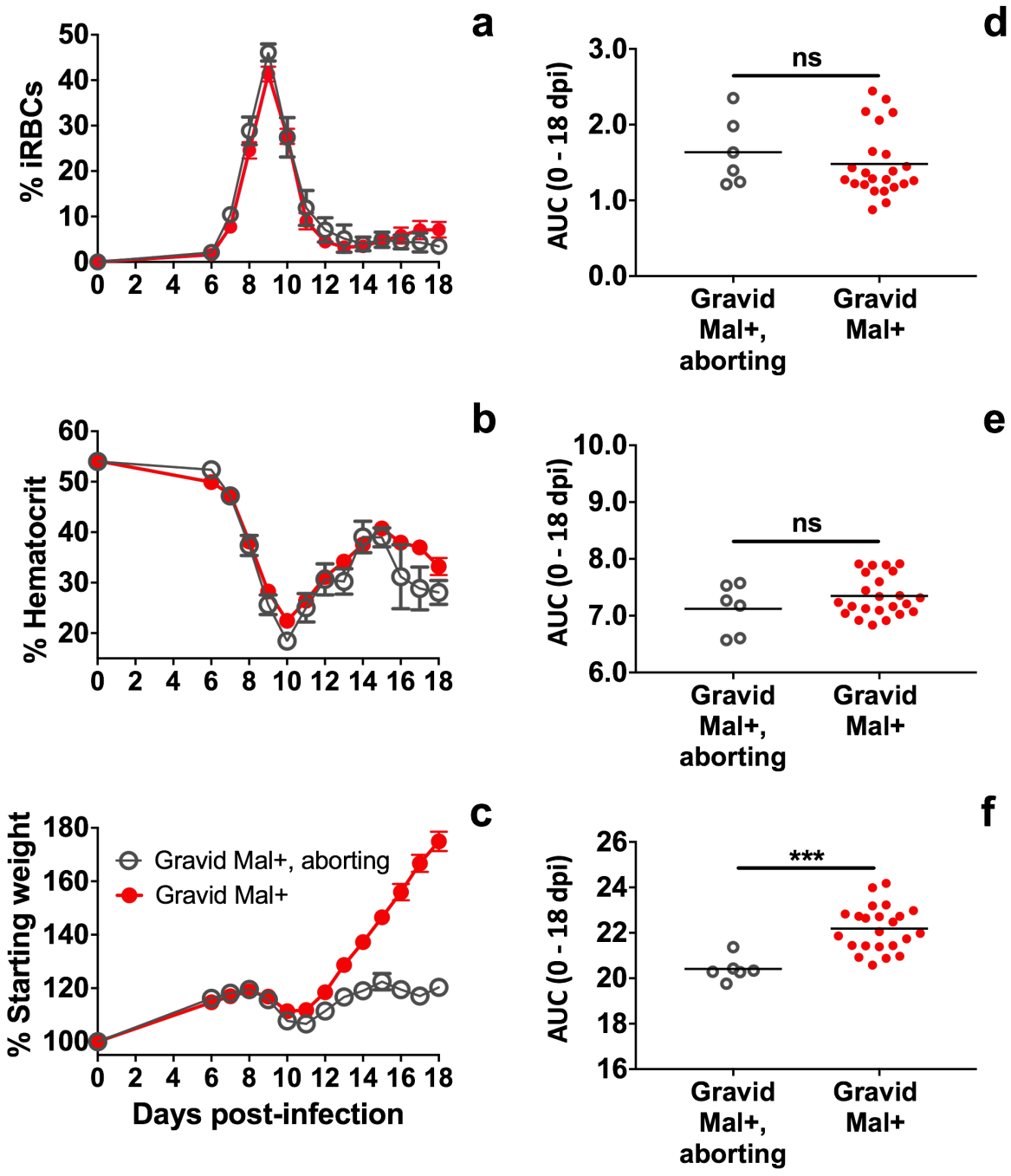
a
% iRBCs
50
40
30
20
10
0
0 2 4 6 8 10 12 14 16 18
b
% Hematocrit
60
50
40
30
20
0 2 4 6 8 10 12 14 16 18
c
% Starting weight
180
160
140
120
100
Gravid Mal+, aborting
Gravid Mal+
0 2 4 6 8 10 12 14 16 18
Days post-infection
d
AUC (0 - 18 dpi)
3.0
2.0
1.0
0.0
ns
Gravid Mal+, aborting
Gravid Mal+
e
AUC (0 - 18 dpi)
10.0
9.0
8.0
7.0
6.0
ns
Gravid Mal+, aborting
Gravid Mal+
f
AUC (0 - 18 dpi)
26
24
22
20
18
16
***
Gravid Mal+, aborting
Gravid Mal+

Figure 2.4. Impact of maternal infection status on fetal number, fetal weight, and placental weight at term.

Mal+ and Mal- dams were sacrificed at GD 18 for assessment of pregnancy outcome.

a) Number of total number of fetuses and number of viable fetuses produced by Mal+ and Mal- dams. Neither a statistically significant difference in the number of viable fetuses ($P > 0.05$; Student's *t* test) nor a significant difference in the number of total fetuses ($P > 0.05$; Student's *t* test) is observed as a function of infection status.
b) Weights of viable fetuses pooled by dam infection group.
c) Weights of placentae associated with viable fetuses, pooled by dam infection group.

Gravid Mal+ $n = 109$ fetuses and placentae, 13 litters; Gravid Mal- $n = 106$ fetuses and placentae, 11 litters; ns $P > 0.05$.

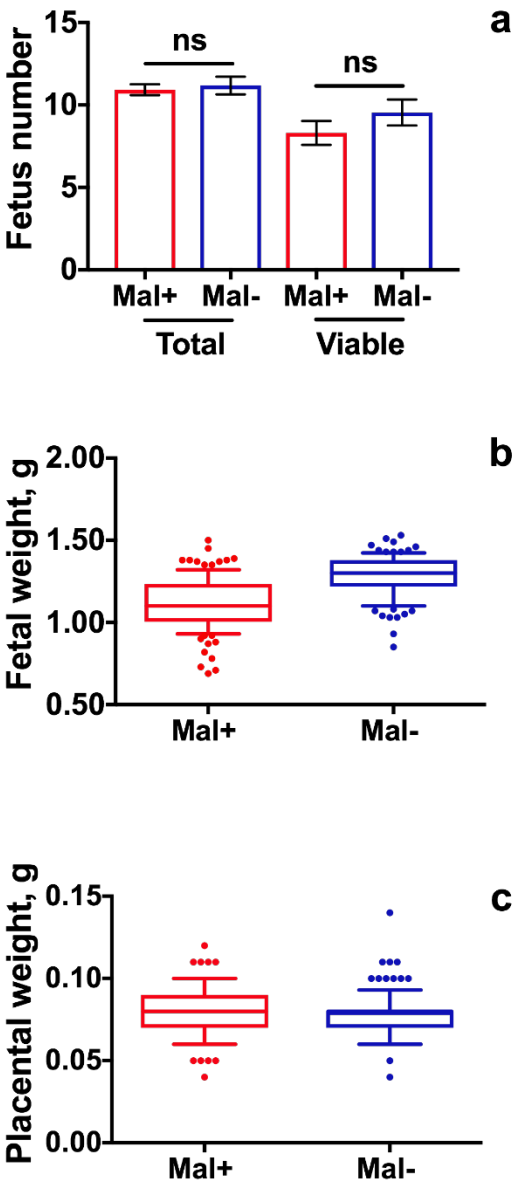
a
Fetus number
15
10
5
0
ns
ns
Mal+
Mal-
Mal+
Mal-
Total
Viable
b
Fetal weight, g
2.00
1.50
1.00
0.50
Mal+
Mal-
c
Placental weight, g
0.15
0.10
0.05
0.00
Mal+
Mal-

Figure 2.5. Fetal and placental weights by dam at GD 18.
Numbers on the X-axis represent the unique identifier assigned to each dam.
a) Weights of viable fetuses per dam.
b) Weights of placentae associated with viable fetuses per dam.

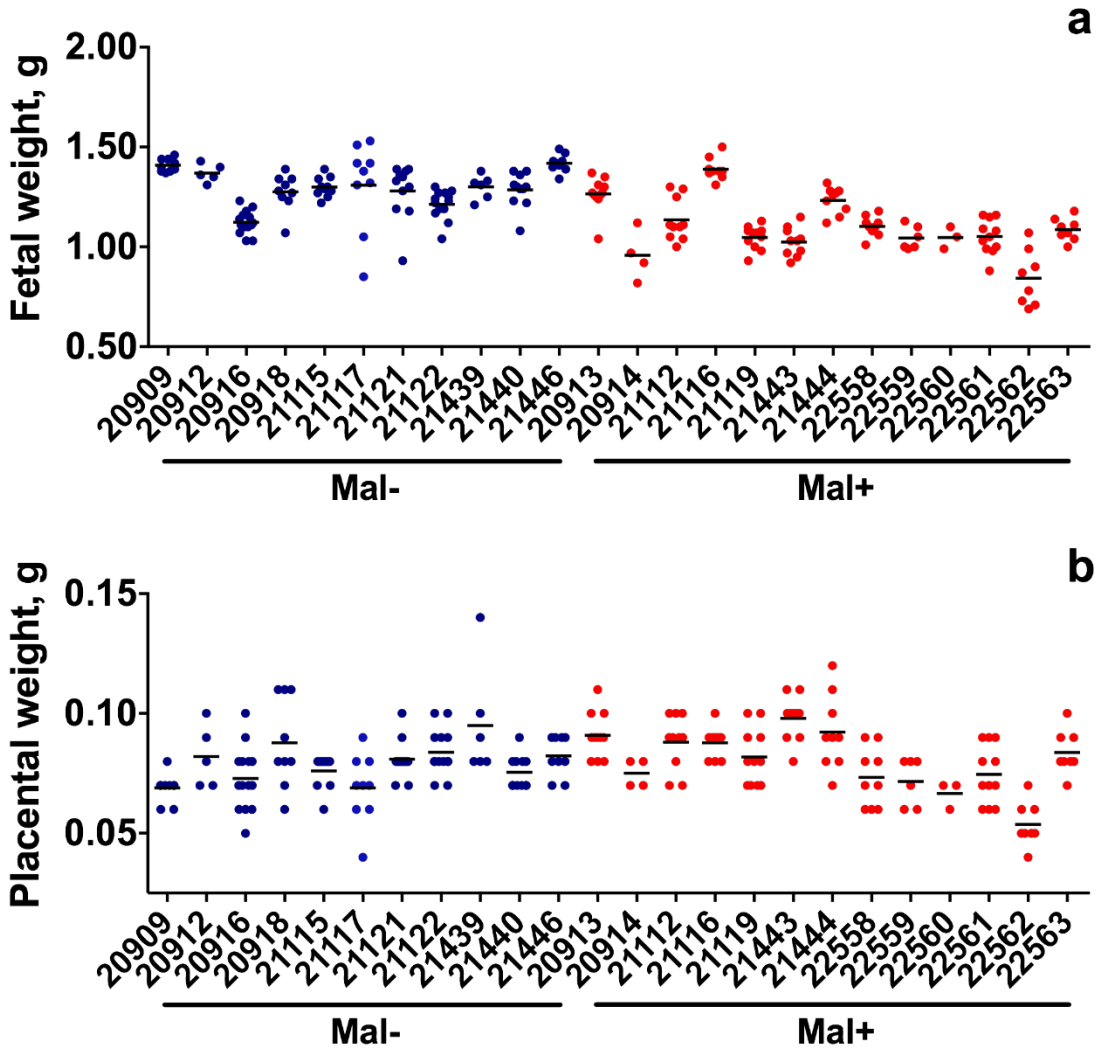
a
Fetal weight, g
2.00
1.50
1.00
0.50
20909
20912
20916
20918
21115
21117
21121
21122
21439
21440
21446
20913
20914
21112
21116
21119
21443
21444
22558
22559
22560
22561
22562
22563
Mal-
Mal+
b
Placental weight, g
0.15
0.10
0.05
20909
20912
20916
20918
21115
21117
21121
21122
21439
21440
21446
20913
20914
21112
21116
21119
21443
21444
22558
22559
22560
22561
22562
22563
Mal-
Mal+

Figure 2.6. Dam weights at GD 0.
No significant difference in mean body weight is observed between mice assigned to Mal+ and Mal- cohorts at the time of infection ($P = 0.7296$, two-tailed Student's *t* test).
Gravid Mal+ $n = 23$; Gravid Mal- $n = 18$; ns $P > 0.05$.

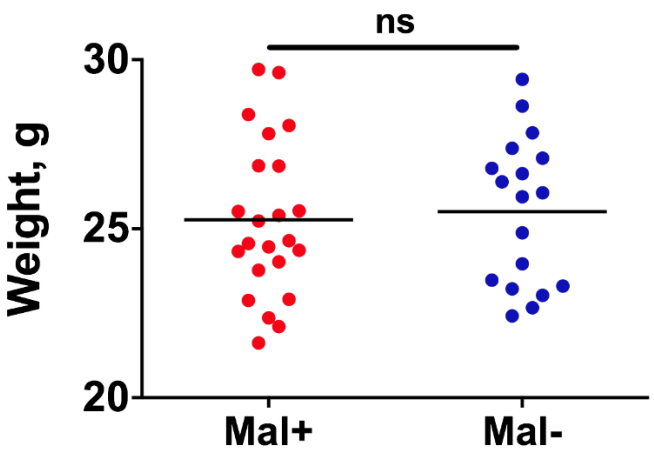
ns
30
25
20
Weight, g
Mal+
Mal-

2.7. Duration of gestation in *P. chabaudi chabaudi* AS-infected and uninfected gravid mice. Infection does not significantly impact the duration of gestation ($P = 0.1188$; Mantel-Cox test). Gravid Mal- $n = 7$; Gravid Mal+ $n = 11$.

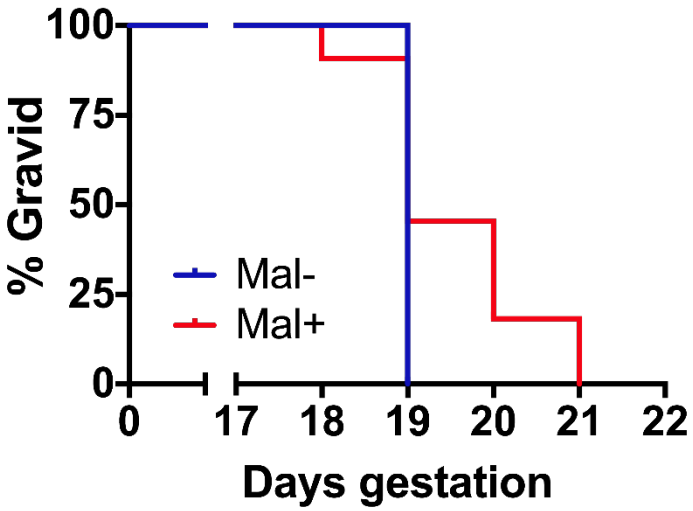
100
75
50
25
0
% Gravid
Mal-
Mal+
0
17
18
19
20
21
22
Days gestation

Figure 2.8. Postnatal pup growth.
Weights between 4 and 22 days of age are presented for the progeny of Mal+ and Mal- dams. Gravid Mal- $n = 7$ litters; Gravid Mal+ $n = 9$ litters. Pup numbers per group are as follows: Gravid Mal- female progeny $n = 47$; Gravid Mal- male progeny $n = 39$; Gravid Mal+ female progeny $n = 18$; Gravid Mal+ male progeny $n = 33$.

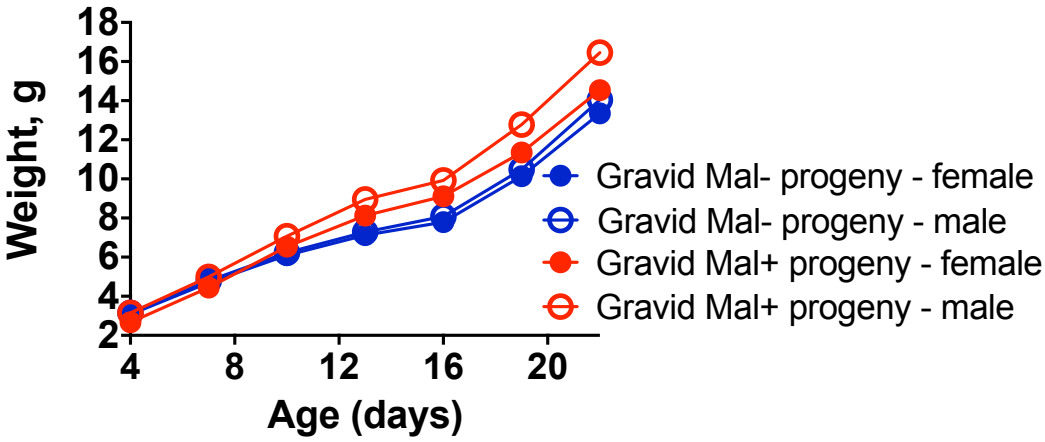
Weight, g
18
16
14
12
10
8
6
4
2
4
8
12
16
20
Age (days)
Gravid Mal- progeny - female
Gravid Mal- progeny - male
Gravid Mal+ progeny - female
Gravid Mal+ progeny - male

Figure 2.9. Relationship between litter size and average pup size at weaning.
The number of pups in a litter versus the mean weight of a pup in a litter is presented for the litters of Mal+ and Mal- dams.
Gravid Mal+ $n = 9$ litters; Gravid Mal- $n = 7$ litters.

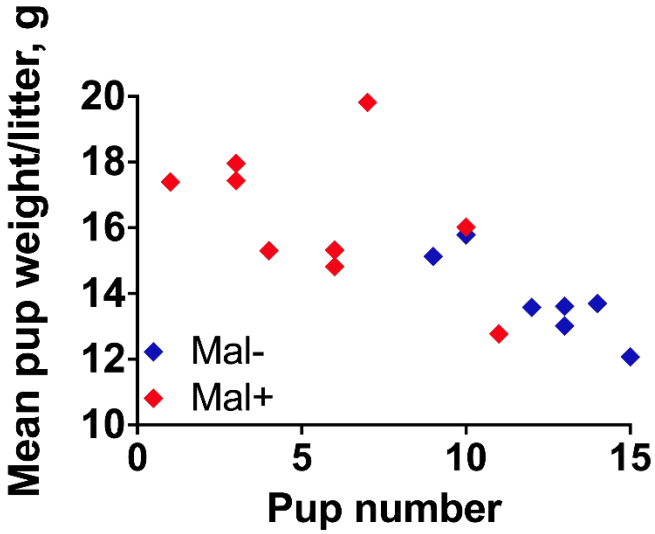
Mean pup weight/litter, g
20
18
16
14
12
10
0
5
10
15
Pup number
Mal-
Mal+

CHAPTER 3

COMPOSITION OF THE GUT MICROBIOTA TRANSCENDS GENETIC DETERMINANTS OF MALARIA INFECTION SEVERITY AND PREGNANCY OUTCOME IN AN OUTBRED MOUSE MODEL FOR TRANSGESTATIONAL MALARIA INFECTION

Introduction

Malaria poses a tremendous threat to the millions of pregnant women at risk for acquiring *Plasmodium falciparum* infections each year. In 2015, approximately 9.5 million pregnant women would have been exposed to malaria infection in the absence of malaria control programs seeking to prevent gestational malaria [11, 12]. In pregnant women, *P. falciparum* infection is associated with the sequestration of infected red blood cells (iRBCs) in the placenta [58]. The function of the parasitized placenta is compromised by inflammation, coagulation, and tissue damage resulting from the maternal immune response to infection [37-39, 41, 42, 56]. The extent to which normal placental mechanisms and processes are disrupted by infection is unknown; however, abnormal uteroplacental blood flow [92], amino acid transport [93, 94], glucose transport [97, 98], and autophagy [95], have been identified in malaria-infected placentae. As a result of these disruptions in normal placental function, gestational malaria is associated with poor birth outcomes, including low birth weight due to intrauterine growth restriction or preterm delivery, abortion, and stillbirth [3-8]. Furthermore, maternal malaria infection profoundly impacts the postnatal health and survival of the infant. Malaria-associated low birth weight is estimated to have a fatality rate of 37.5% [10], and infants born to malaria-infected women are more susceptible to malaria in early life [14, 16, 139]. Therefore, understanding the pathogenesis

of malaria in pregnancy is critical for improving maternal and child health outcomes in malarious areas.

Mouse models are important for the study of gestational malaria because the dysfunctional mechanisms linking maternal malaria infection and poor birth outcomes are incompletely understood, stymieing efforts to reduce the impact of malaria infection on pregnant women and their babies. Different parasite-mouse combinations best recapitulate different features of gestational malaria. Many mouse models for malaria in pregnancy result in spontaneous abortion or stillbirth [57, 101, 104, 106, 109, 111, 115], outcomes that are rarely observed in malaria-infected pregnant women [112]. For this reason, we have developed a novel model for transgestational malaria infection utilizing Swiss Webster mice infected with *Plasmodium chabaudi chabaudi* AS [Ch. 2]. Swiss Webster dams infected with *P. chabaudi chabaudi* AS on gestational day (GD) 0 carry their pregnancies to term and deliver live pups, allowing for the exploration of the impact of prolonged maternal malaria infection on postnatal outcomes [Ch. 2].

In addition to modeling live birth following malaria infection throughout pregnancy, the use of outbred mice allows this model to act as a bridge between completely homogenous inbred mouse populations and genetically diverse human populations. However, genetic traits are not the only determinants of malaria severity in experimentally infected mice. In inbred mice, the composition of the gut microbiota has been identified as a major determinant of susceptibility to malaria [125, 126]. Previous research has demonstrated that vendor-associated communities of gut microbes confer susceptibility or resistance to infection with multiple murine malaria species [125, 126]. To our knowledge, the ability of the gut microbiota to inform the susceptibility of

pregnant mice to malaria and subsequently influence fetal and postnatal outcomes has not been explored.

Remarkably, we find that the composition of the gut microbiota supersedes the diverse genetics of the outbred Swiss Webster mouse stock as a determinant of susceptibility to murine malaria infection. We describe how the manipulation of the gut microbiota in a cohort of mice sourced from a single vendor allows for the modulation of infection severity, as well as fetal and postnatal outcomes. Swiss Webster mice purchased from NCI are extremely susceptible to *P. chabaudi chabaudi* AS infection [Ch. 2]. The alteration of the microbial communities within Swiss Webster mice via antibiotic treatment and the administration of a fecal microbiota transplant (FMT) consisting of fecal microbes from mice reported to display microbiota-mediated resistance to malaria (from the Jackson Laboratory, FMT^{JAX}) [125] significantly impacts disease outcomes. Maternal infection is less severe in mice receiving FMT^{JAX}, and postnatal survival is improved relative to antibiotic-treated mice reconstituted with endogenous gut microbes (FMT^{NCI}). Therefore, we believe that the manipulation of the gut microbiota is an important tool for modulating malaria infection severity and pregnancy outcomes in *P. chabaudi chabaudi* AS-infected outbred Swiss Webster mice. We anticipate that this will expand the Swiss Webster model for transgestational malaria infection by enabling the exploration of pregnancy outcomes following severe and moderate parasite burdens using the same mouse-parasite combination.

Materials & Methods

Mice

Three-week-old Swiss Webster female mice, 5- to 6-week-old Swiss Webster male mice, and sexually mature Swiss Webster mice of both sexes (Clr:CFW) were purchased from NCI

(Fredrick, MD), a facility managed by Charles River Laboratory. Male and female B6 mice were purchased from the JAX as breeder stock and replaced at least every 10 generations. Animals were housed in *Helicobacter* species and norovirus-free rooms and maintained under specific-pathogen-free conditions at the University of Georgia (UGA) Coverdell Vivarium, a barrier facility. Mice were provided with food (PicoLab Mouse Diet 20 5053; St. Louis, MO) and water ad libitum. Mice were acclimated to a 14-hour light/10-hour dark cycle, and rooms were maintained at a temperature between 65-75ºF and humidity between 40-60%. All animal protocols were approved by the UGA Institutional Animal Care and Use Committee.

Antibiotic treatment and fecal microbiota transplantation

To induce dysbiosis of the native gut microbiota, 4-week-old female and 6- to 7-week-old male mice were treated with a broad spectrum antibiotic cocktail (ABX) consisting of 100mg/kg ampicillin (Gold Biotechnology; St. Louis, MO), 100mg/kg metronidazole (MP Biomedicals; Santa Ana, CA), 100mg/kg neomycin sulfate (Gold Biotechnology; St. Louis, MO), and 50mg/kg vancomycin hydrochloride (Gold Biotechnology; St. Louis, MO) in sterile water for 4 consecutive days and on alternate days thereafter, until 9 doses of antibiotic had been administered [140, 141]. The antibiotic cocktail was compounded fresh daily to minimize the degradation of antibiotics in aqueous solution and was administered by oral gavage to ensure that each mouse received the appropriate dose of each drug. Antibiotics were not provided in drinking water because mice find metronidazole unpalatable and will refuse water to the point of fatal dehydration [141]. Control (CTRL) animals were not antibiotic treated.

Fecal microbiota transplantation (FMT) was performed on the three consecutive days immediately following the final antibiotic dose. Donor feces were collected from sexually mature NCI-sourced Swiss Webster mice and JAX-lineage B6 breeder pairs and administered to

both ABX and CTRL mice. Briefly, a fecal slurry was generated by homogenizing freshly deposited fecal pellets from donor mice in sterile 1x phosphate-buffered saline (PBS) at a concentration of 50mg feces per 1ml PBS [142]. Undigested fibrous material was removed from the slurry by centrifugation (380xg, 30 seconds), and 200µl of the resulting supernatant was administered to each recipient mouse by oral gavage. Following each antibiotic and fecal slurry treatment, mice were moved to clean cages with fresh bedding in an attempt to reduce coprophagy and the bias in environmental exposure introduced by the outgrowth of some types of bacteria in heavily soiled bedding [143]. Following FMT completion, animals were not handled for at least one week to allow mice to recover from the stress of the ABX and FMT protocols.

Four groups of experimental females were produced by this treatment protocol. First, mice were randomly assigned to either CTRL or ABX treatment groups. Subsequently, CTRL animals were randomly assigned to receive FMT consisting of NCI (FMT^{NCI}) or JAX (FMT^{JAX}) feces, yielding the CTRL-FMT^{NCI} and CTRL-FMT^{JAX} experimental groups, respectively. Similarly, ABX-treated animals were randomly assigned to receive either FMT^{NCI} and FMT^{JAX}, resulting in the creation of ABX-FMT^{NCI} and ABX-FMT^{JAX} experimental groups.

Fecal microbiome analysis

Fecal pellets were collected from all experimental mice immediately prior to the administration of the first antibiotic dose and 7 to 10 days following the completion of the FMT protocol. A subset of fecal samples produced by ABX-FMT^{NCI} and ABX-FMT^{JAX} mice were processed for microbiome analysis. All processing and analyses were performed in the laboratory of Dr. Mansour Mohamadzadeh (Department of Infectious Diseases & Immunology,

University of Florida College of Veterinary Medicine; Gainesville, FL). Bioinformatic analyses were performed by Minghao Gong.

DNA was isolated from fecal samples using the ZymoBIOMICS DNA Mini Kit (Zymo Research; Irvine, CA) and the 16S rDNA V4-V5 region was PCR amplified using Illumina Miseq compatible primers described by Lightfoot et al. [144, 145]. Amplicons were gel purified using the Omega E.Z.N.A Gel Extraction Kit (Omega; Norcross, GA) and quantified using a Qubit 2.0 Fluorometer (Invitrogen; Grand Island, NY) and Qubit dsDNA HS Assay Kit (Invitrogen; Grand Island, NY), and by Kapa Library Quantification Kit (Kapa; Wilmington, MA) [144, 145]. Equal amounts of amplicons were pooled with 10% of Phix control from the Illumina Miseq Phix Control Kit v3 (Illumina, Inc.; San Diego, CA) [144, 145]. Pooled samples were analyzed using the Illumina Miseq machine using the Illumina Miseq Kit v2 (Illumina, Inc.; San Diego, CA) [144, 145]. Sequence analyses were performed using QIIME v.1.9.0 [146]. Operational taxonomic unit (OTU) picking was performed using an open reference OTU picking strategy [147]. Taxonomy was assigned using the Greengenes reference database [148]. Sequencing data were statistically analyzed as previously described [149]. Briefly, weighted UniFrac analyses [150] were used to measure β-diversity between microbial communities, and three-dimensional scatterplots were generated using principal coordinate analysis (PCoA).

Parasites, infection, and infection monitoring

The following reagent was obtained through BEI Resources Repository, NIAID, NIH: *Plasmodium chabaudi chabaudi*, Strain AS, MRA-741, contributed by David Walliker. Parasites were maintained as frozen stock according to BEI Resource Repository guidelines and amplified in A/J mice for the purposes of infecting experimental mice.

Gravid Mal+ and uninfected (Mal-) mice were generated by pairing experimental females with sexually mature Swiss Webster stud males. All experimental female mice were paired with male mice with concordant fecal microbe exposures. CTRL-FMT^{JAX} and ABX-FMT^{JAX} experimental females were exclusively paired with ABX-FMT^{JAX} stud males, while autologously transplanted CTRL-FMT^{NCI} and ABX-FMT^{NCI} experimental females were paired with unmanipulated NCI-sourced studs. Paired females were examined each morning for the presence of a copulatory plug, indicative of successful mating. The day a plug was detected was considered GD 0. Successfully mated females were randomized into Mal+ and Mal- cohorts. Mated females were considered pregnant if they exhibited at least a 10% increase in body weight by GD 8.

Infections were initiated as previously described [88, 101, 109-111]. Briefly, mice were infected intravenously with 10^3 iRBCs diluted in 200µl of 1x PBS per 20 grams of body weight. Virgin Mal+ mice were infected alongside gravid animals as controls. Gravid Mal- mice received an intravenous injection of 200µl 1xPBS per 20 grams of body weight to control for handling. Body weight and hematocrit were measured at the time of infection, experimental day (ED) 0. Thus, in gravid mice, GD 0 is also ED 0. Regardless of pregnancy status, animals were transitioned to a higher fat breeder chow (PicoLab Mouse Diet 20 5058; St. Louis, MO) at GD/ED 0.

Infection and pregnancy progression were monitored by measuring peripheral parasitemia, hematocrit, and body weight daily between GD/ED 6 and GD/ED 18. Peripheral parasitemia was measured by flow cytometry as previously described [134]. A drop of blood was collected by tail snip [135]. Within 4 hours of collection, blood was diluted 1:50 in normal saline, and stained with 2.5µM SYTO 16 Green Florescent Nucleic Acid Stain (ThermoFisher

Scientific; Waltham, MA) for 20 minutes at room temperature protected from light. Stained blood was diluted 1:9 in normal saline and analyzed using a CyAn ADP Flow Cytometer (Beckman Coulter; Brea, CA) within 4.5 hours of collection. iRBCs were identified based on size and fluorescence intensity, and a stained sample of uninfected blood was included each day as an internal control. Parasitemia is reported as the percentage of iRBCs in the peripheral blood.

Assessment of fetal and postnatal outcomes

At GD/ED 18, gravid Mal+ and Mal- CTRL-FMT^{NCI}, CTRL-FMT^{JAX}, ABX-FMT^{NCI}, and ABX-FMT^{JAX} mice, as well as identically treated Mal+ virgin controls, were anesthetized using 2.5% Tribromoethanol and sacrificed by cervical dislocation. The uteri of gravid mice were removed and dissected. Fetuses and resorptions were counted and fetal viability was assessed by reactive movement to prodding with forceps. Viable pups and their placentae were individually weighed.

To evaluate postnatal fitness, we generated additional gravid Mal+ and Mal- ABX-FMT^{NCI} and ABX-FMT^{JAX} mice for the production of malaria-exposed and unexposed progeny. Neonates were fostered such that this assessment could be performed in the absence of variable maternal morbidity. Postnatal fitness was explored using the progeny of gravid Mal+ and Mal- ABX-FMT^{NCI} and ABX-FMT^{JAX} mice because these cohorts of dams display the most striking differences in infection severity and fetal outcomes. At gestational term (GD 18), donor pups produced by donor Mal+ and Mal- ABX-FMT^{NCI} and ABX-FMT^{JAX} dams were delivered by caesarean section, dissected out of the uterus, individually weighed, and massaged with cotton swabs until clean and fully resuscitated. Donor pups were considered fully resuscitated when they were breathing regularly, pink in color, and displaying spontaneous wriggly movement. Fully resuscitated donor pups were mixed with the native litter of an uninfected, unmanipulated

Swiss Webster foster dam. Native litters were 0 to 3 days of age at the time of fostering. The foster dam's native pups received footpad tattoos using a nontoxic carbon pigment ink (Super Black Speedball India Ink; Statesville, NC) at the time of fostering so that they could be differentiated from the donor pups [136, 137]. Litter size was capped at 15 pups, with a minimum of 3 native pups retained in the final litter. Following fostering, the cage was not disturbed for four days to maximize foster dam acceptance of the donor pups. When the donor pups were 4 days old, they were counted, individually identified by footpad tattooing [136, 137], and individually weighed. Individual donor pups were weighed every three days between 4 days of age and weaning at 22 days of age. Sex was determined visually at weaning.

Statistics

Descriptive statistical analyses were performed using GraphPad Prism 7 (GraphPad Software; La Jolla, California). All raw clinical data are presented as mean ± SEM. Error bars are not depicted if the error bars are shorter than the height of the symbol. Area under the curve of parasitemia, hematocrit, and percent starting weight was calculated for each mouse between GD 0 and GD 18. Individual AUC values are presented as a scatter plot with a bar representing the group mean. AUC values were compared between groups using the statistical tests indicated in figure legends. Dam weights at infection day are presented as a scatter plot with a bar representing group means. Starting weights were compared by Kruskal-Wallis test with Dunn's post-test for multiple comparisons. Total and viable litter sizes are presented as mean ± SEM. Litter sizes were compared by Kruskal-Wallis test with Dunn's post-test for multiple comparisons. Fetal, placental, and pup weights, pooled by dam group, are shown as box and whisker plots with whiskers indicating the 10^{th} and 90^{th} percentile for visualization only. Outliers are shown as individual points. Fetal and placental weights for each dam are presented as a

scatter plot with a bar representing the litter mean. Fetal viability and pup sex were compared between dam groups using the two-tailed Fisher exact test. *P* values ≤ 0.05 were considered statistically significant.

Mixed linear models analysis (SAS 9.4) was used to estimate differences in term fetal and placental weights as a function of dam infection severity and postnatal pup growth as a function of dam treatment and infection severity. In both cases, the interrelatedness of pups born to the same dam was controlled with a random term for the dam. Best fit for the former model was obtained with the inclusion of antibiotic treatment (binary variable), FMT group (binary variable), and parasitemia AUC value (continuous variable). The latter model assessed trends over time for changes in pup growth; repeated measures in the pups were accommodated with a repeat command and the relatedness of pups born to the same dam was accounted for with a random term for the dam. Model fitting revealed that the number of pups at weaning, and age at weight measurement, with associated interaction terms with the latter, influenced trends in weight gain. Maternal infection status and maternal treatment group were not significant in initial models but are depicted in the figure for illustration purposes.

Results

The composition of the gut microbiota is shaped by FMT administration following broad-spectrum antibiotic treatment

Fecal samples were collected from experimental mice prior to antibiotic treatment and approximately 1 week following the completion of the ABX-FMT treatment protocol. A subset of these samples, from animals that were later allocated to Mal+ virgin or gravid cohorts, were utilized to determine the impact of treatment on the composition of the gut microbiota. Global changes in the composition of the gut microbiota were analyzed by the UniFrac method. By

PCoA, no separation between microbial communities collected from individual mice is observed prior to treatment, likely reflecting the shared origin of the mice (Fig. 3.1a). One week after the completion of treatment, mice receiving ABX-FMT^{NCI} and ABX-FMT^{JAX} cluster separately, indicating that antibiotic treatment followed by FMT from different donors results in distinct populations of mice with different communities of gut microbes (Fig. 3.1b).

Composition of the gut microbiota determines malaria infection severity in outbred Swiss Webster mice

In gravid and virgin Swiss Webster mice, the composition of the gut microbiota determines susceptibility to malaria infection. On average, gravid Mal+ ABX-FMT^{NCI} mice achieved a peripheral peak parasitemia of approximately 40% (Fig. 3.2a), consistent with the parasite burdens observed in unmanipulated Swiss Webster mice purchased from NCI [Ch. 2]. In contrast, gravid Mal+ ABX-FMT^{JAX} mice achieved a peripheral peak parasitemia of approximately 13% (Fig. 3.2a). The average achievement of peripheral peak parasitemia was delayed by one day in gravid Mal+ ABX-FMT^{JAX} mice compared to gravid Mal+ ABX-FMT^{NCI} mice (Fig. 3.2a). Over the course of infection, a statistically significant reduction in parasite burden was observed in gravid Mal+ ABX-FMT^{JAX} mice compared to gravid Mal+ ABX-FMT^{NCI} mice (Fig. 3.2d).

Malaria infection was associated with the development of malarial anemia in gravid ABX-FMT^{NCI} and ABX-FMT^{JAX} mice around the time of peak infection (Fig. 3.2b). A significant reduction in hematocrit was observed in both gravid Mal+ ABX-FMT^{NCI} and ABX-FMT^{JAX} mice compared to Mal- controls (Fig. 3.2e). Over the course of infection, gravid Mal+ ABX-FMT^{NCI} mice displayed a statistically significant reduction in hematocrit compared to gravid Mal+ ABX-FMT^{JAX} mice (Fig. 3.2e), reflecting the higher parasite burdens observed in

gravid Mal+ ABX-FMT^{NCI} mice (Fig. 3.2d). In the absence of infection, treatment group did not significantly influence hematocrit over the course of infection (Fig. 3.2e).

Weight change over the course of gestation also reflected parasite burden. Gravid Mal+ ABX-FMT^{NCI} mice displayed a reduction in weight gain between GD/ED 9 and GD/ED 11, corresponding with the time of peak infection (Fig. 3.2c). This stasis in weight gain was not observed in gravid Mal+ ABX-FMT^{JAX} animals or gravid Mal- controls (Fig. 3.2c). This disruption in weight gain resulted in a significant reduction in weight change over the course of gestation in gravid Mal+ ABX-FMT^{NCI} mice compared to gravid Mal+ ABX-FMT^{JAX} mice and gravid Mal- ABX-FMT^{NCI} controls (Fig 3.2f). Among gravid ABX-FMT^{JAX} animals, malaria infection was not associated with a statistically significant reduction in weight change over the course of gestation (Fig. 3.2f). In the absence of infection, treatment group did not significantly impact weight gain (Fig. 3.2f). Furthermore, treatment group was not associated with a significant change in body weight at the time of infection, GD/ED 0 (Fig. 3.5).

In the absence of antibiotic pretreatment, FMT source did not influence infection severity (Fig. 3.3). Gravid Mal+ CTRL-FMT^{NCI} and CTRL-FMT^{JAX} mice developed similar parasite burdens over the course of gestation (Fig. 3.3d). Within treatment groups, malaria infection was associated with a significant reduction in hematocrit over the course of gestation; however, a significant difference in hematocrit was not observed between gravid Mal+ CTRL-FMT^{NCI} and CTRL-FMT^{JAX} mice, reflecting the similar parasite burdens observed in these cohorts (Fig. 3.3e). No significant changes in body weight were observed over the course of gestation either as a function of treatment group or infection status (Fig. 3.3f). Treatment group did not significantly alter hematocrit or weight change in gravid Mal- mice (Figure 3.3e, f). Significant differences in

body weight at the time of infection, GD/ED 0, were not observed between CTRL-FMT^{NCI} and CTRL-FMT^{JAX} dams or between CTRL and ABX dams (Fig. 3.5).

The results observed in virgin Mal+ mice were similar to those observed in identically treated gravid Mal+ mice (Fig. 3.4). Briefly, a statistically significant reduction in parasite burden over the course of the experiment was observed in virgin Mal+ ABX-FMT^{JAX} animals compared to virgin Mal+ ABX-FMT^{NCI} animals (Fig. 3.4d). This reduction in parasite burden in virgin Mal+ ABX-FMT^{JAX} mice was associated with a statistically significant increase in hematocrit compared to virgin Mal+ ABX-FMT^{NCI} mice over the course of the experiment (Fig. 3.4e). No significant change in weight as a function of infection severity was observed over the course of infection in the absence of pregnancy (Fig. 3.4f).

Maternal infection severity influences fetal viability at gestational term

Dams were sacrificed on GD/ED 18 and uteri were removed to count fetuses and assess fetal viability. Spontaneous midgestational pregnancy loss due to infection was infrequently observed in Mal+ dams. Of the dams sacrificed to assess fetal weight and viability at term, 9% (1/11) of gravid Mal+ ABX-FMT^{NCI} mice, 25% (2/8) of gravid Mal+ CTRL-FMT^{NCI} mice, and 29% (2/7) of gravid Mal+ CTRL-FMT^{JAX} mice displayed weight gain consistent with pregnancy at GD 8 but did not have fetuses or resorptions in the uterus at term. These mice were assumed to have suffered spontaneous pregnancy loss and expelled their embryos around the time of peak infection. As spontaneous pregnancy loss was observed relatively infrequently, these mice were excluded from analysis. No mated mice allocated to gravid Mal+ ABX-FMT^{JAX} or gravid Mal- cohorts failed to produce fetuses at term.

The mean numbers of total fetuses and viable fetuses produced by individual ABX-FMT^{NCI} and ABX-FMT^{JAX} dams did not differ significantly as a function of infection status or

infection severity (Fig. 3.6a). However, in populations of fetuses pooled by maternal treatment group and infection status, lower parasite burdens were associated with improved fetal outcomes. Gravid Mal+ ABX-FMT^{JAX} mice displayed a tendency towards higher fetal viability (n = 10 dams, 96/112 or 86% viability) than gravid Mal+ ABX-FMT^{NCI} dams (n = 11 dams, 90/132 or 68% viability; P = 0.0540, two-tailed Fisher exact test). No significant difference in fetal viability was observed between treatment groups in the absence of infection. Gravid Mal- ABX-FMT^{JAX} mice produced a similar proportion of viable fetuses (n = 10 dams, 112/126 or 89% viability) as gravid Mal- ABX-FMT^{NCI} mice (n = 9 dams, 101/116 or 87% viability; P = 0.6959, two-tailed Fisher exact test).

The mean numbers of total and viable fetuses produced by individual CTRL-FMT^{NCI} and CTRL-FMT^{JAX} dams did not differ significantly as a function of infection status or treatment group (Fig. 3.7a). When fetuses were pooled by dam group, a significant difference in fetal viability was not observed between gravid Mal+ CTRL-FMT^{JAX} mice (n = 5 dams, 57/69 or 83% viability) and gravid Mal+ CTRL-FMT^{NCI} mice (n = 6 dams, 68/81 or 84% viability; P = 0.8300, two-tailed Fisher exact test), consistent with the similar parasite burdens observed in these animals (Fig. 3.3d). In addition, no significant difference in fetal viability was observed between gravid Mal- CTRL-FMT^{NCI} mice (n = 6 dams, 72/79 or 91% viability) and gravid Mal- CTRL-ABX^{JAX} mice (n = 6 dams, 67/71 or 94% viability; P = 0.5400, two-tailed Fisher exact test).

Maternal infection severity influences fetal weight at gestational term

Following the sacrifice of Mal+ and Mal- dams at GD/ED 18, viable fetuses and placentae were weighed to assess the impact of maternal infection on fetal growth. Mixed linear models were utilized to assess the impact of maternal infection severity, maternal antibiotic treatment status, and maternal FMT group on fetal weights while accounting for the lack of

independence between littermates. Parasite burden, represented by parasitemia AUC value (Fig. 3.2d, Fig. 3.3d), ABX treatment status, and FMT group account for 34.3% of the variance in fetal weight between dams ($P < 0.001$). If ABX treatment status and FMT treatment group are held constant, each unit increase in AUC is associated with a -0.0003g reduction in the weight of each fetus on average ($P = 0.0027$). Summary data depicting fetal weights pooled by dam cohort for all groups of Mal+ and Mal- ABX (Fig. 3.6b) and CTRL dams (Fig. 3.7b) are presented for the purposes of visualization.

Maternal antibiotic treatment status also exerts a significant influence on fetal weight. Antibiotic treatment is associated with a 0.1417g increase in the weight of each fetus on average ($P = 0.0009$) when parasitemia AUC value and FMT treatment group are held constant. Fetal weights, pooled by dam antibiotic treatment status, are shown in summary form to depict the impact of maternal antibiotic treatment on fetal weight (Fig. 3.8).

Placental weight was not significantly influenced by any of the variables included in analysis. For visualization, placental weight data are shown in summary form, pooled by maternal infection status and treatment group (Fig. 3.6c, 3.7c). Fetal and placental weights are also depicted by individual dams (Fig. 3.9) to demonstrate the variability within and between dams in a cohort.

Maternal infection severity influences neonatal survival in the first days of life, but surviving pups develop normally prior to weaning

To evaluate postnatal growth in the absence of variable maternal morbidity, pups produced by ABX-FMT^{NCI} and ABX-FMT^{JAX} donor dams were delivered by caesarean section and placed with unmanipulated NCI-sourced Swiss Webster foster dams with 0- to 3-day-old litters. Fostering success and fostered pup survival at weaning are described in Table 3.1. Of the

successfully mated females that met the weight gain threshold for pregnancy, pregnancy loss was only observed within the gravid Mal+ ABX-FMT^{NCI} cohort (Table 3.1). A large proportion of the gravid Mal+ ABX-FMT^{NCI} mice intended as donor dams for fostering were not pregnant at GD 18. The reason for the high rate of pregnancy loss in this group is unknown.

Although foster dams were not disturbed for 3 days following fostering to minimize pup loss, foster pup attrition during this time was significant in all groups (Table 3.1). Survival to weaning age did not differ significantly between the fostered progeny of Mal- ABX-FMT^{NCI} dams and Mal- ABX-FMT^{JAX} dams (Table 3.1). A significant reduction in fostered pup survival was observed in the progeny of Mal+ ABX-FMT^{NCI} dams compared to Mal+ ABX-FMT^{JAX} dams (Table 3.1), suggesting that maternal infection severity is inversely related to postnatal fitness. Compared to the progeny of gravid Mal+ ABX-FMT^{JAX} mice, the progeny of gravid Mal+ ABX-FMT^{NCI} weighed less at the time of fostering (Fig. 3.10).

When the fostered pups reached 4 days of age, they were individually identified by footpad tattooing and weighed. Individual pup weights were measured every 3 days until weaning at 22 days of age. Trends in pup growth were analyzed by linear mixed models. No significant relationships between maternal parasite burden or maternal treatment group and pup growth trends were detected. The model revealed that the number of total pups (native and fostered) in the litter at weaning significantly influenced the pup growth trajectory. Furthermore, the sex of the pup exerted an effect that varied over time (interaction term, $P = 0.0277$). Raw pup weights are depicted in Fig. 3.11 for the purposes of data visualization only. Although neither dam infection severity nor dam treatment group influenced trends in pup growth, pup weights are presented grouped by dam cohort for the purposes of illustration.

Pups were visually sexed at weaning. Maternal infection severity does not significantly influence the proportion of male progeny produced by infected dams. No significant difference in sex ratio was observed between Mal+ dams (Mal+ ABX-FMT^{NCI} 5 male/9 total pups; Mal+ ABX-FMT^{JAX} 19 male/44 total pups; $P = 0.2247$, two-tailed Fisher exact test) nor between Mal- dams (Mal- ABX-FMT^{NCI} 31 male/47 total pups; Mal- ABX-FMT^{JAX} 14 male/28 total pups; $P = 0.7153$, two-tailed Fisher exact test).

Discussion

We report that the composition of the gut microbiota supersedes genetic determinants of malaria infection severity and pregnancy outcome in an outbred mouse model for gestational malaria. Compared to Swiss Webster dams that received a susceptibility-conferring FMT (ABX-FMT^{NCI}), Swiss Webster dams that received a resistance-conferring FMT (ABX-FMT^{JAX}) developed lower parasite burdens and were protected from malarial anemia and an infection-associated reduction in gestational weight gain. Furthermore, the reduction in parasite burden observed in ABX-FMT^{JAX} mice was associated with improved fetal viability and postnatal survival.

Increasing maternal parasite burdens were associated with significant, but modest, reductions in fetal weight at term. Intriguingly, maternal antibiotic treatment was associated with a relatively large increase in fetal weight at term, regardless of FMT donor or parasite burden. The mechanism by which maternal antibiotic treatment prior to pregnancy enhances fetal growth is unknown. Previous research in mice has demonstrated that maternal antibiotic treatment can promote adiposity in offspring after birth, although these studies entail the peripartum antibiotic treatment of dams [151, 152]. In contrast, in the experiments described here, dams complete the antibiotic treatment course approximately two weeks prior to mating and the initiation of the

experiment, so the antibiotic exposure of the fetus is minimal. Furthermore, the impact of antibiotic treatment on postnatal growth was not assessed in this study, so it is not possible to directly compare the results presented here with previously published work.

Postnatal survival was significantly reduced in the progeny of Mal+ ABX-FMT^{NCI} dams compared to Mal+ ABX-FMT^{JAX} dams. The majority of pup loss occurred within the neonatal period, between 0 and 4 days of age. The high rate of neonatal mortality observed among the progeny of Mal+ ABX-FMT^{NCI} dams is consistent with the contraction in litter size observed in the litters of Mal+ NCI-sourced dams [Ch. 2]. As fostering was performed to control for the potential impact of abnormal maternal behavior due to infection, we cannot attribute neonatal mortality among the progeny of Mal+ ABX-FMT^{NCI} dams to maternal illness. Instead, these data suggest that the progeny of Mal+ ABX-FMT^{NCI} dams are less fit at the time of delivery, although the impact of higher maternal parasite burdens on term fetal weights are minimal. We speculate that fostered pups produced by Mal+ ABX-FMT^{NCI} dams are less able to compete for limited maternal resources, especially in a litter that contains older and larger native pups. However, the mechanisms by which high maternal parasite burdens reduce postnatal survival in the progeny of Mal+ ABX-FMT^{NCI} dams compared to the progeny of Mal+ ABX-FMT^{JAX} dams is unclear.

The divergent infection trajectories reported in ABX-FMT^{NCI} and ABX-FMT^{JAX} mice are associated with the establishment of distinct communities of gut microbes in these cohorts of mice. The composition of the gut microbiotas of CTRL-FMT^{NCI} and CTRL-FMT^{JAX} mice were not interrogated. We speculate that the composition of the gut microbiota in CTRL-FMT^{NCI} and CTRL-FMT^{JAX} mice closely resembles the composition of the gut microbiota in NCI-sourced Swiss Webster mice. Consistent with this, CTRL-FMT^{NCI} and CTRL-FMT^{JAX} mice develop high parasite burdens similar to those observed in ABX-FMT^{NCI} animals and unmanipulated NCI-

sourced Swiss Webster mice [Ch. 2]. Furthermore, previous work has demonstrated that fecal microbes administered by oral gavage do not consistently colonize the gut in the absence of a niche created by antibiotic pretreatment [125, 153].

We speculate that the differences in malaria infection severity observed between ABX-FMT^{NCI} and ABX-FMT^{JAX} mice reflect vendor-dependent differences in the composition of the gut microbiota of the NCI-sourced and JAX-derived mice used as fecal donors for FMT. However, NCI-sourced Swiss Webster mice were used as fecal donors for mice receiving FMT^{NCI} while JAX-derived B6 mice were used as fecal donors for mice receiving FMT^{JAX}. It is possible that the differences in gut microbiota that we observe between ABX-FMT^{NCI} and ABX-FMT^{JAX} recipient mice reflect mouse strain- or stock-specific, not vendor-specific, differences in donor microbial communities. The innate immunological differences between mouse strains shapes the composition of the gut microbiota, so the composition of the gut microbiota may vary between strains of mice purchased from the same vendor [142]. Furthermore, gut-resident eukaryotic commensals can have immunomodulatory capabilities [154], and we cannot eliminate the possibility that non-microbial gut-resident organisms contribute to the modulation of malaria infection severity in mice receiving different FMT.

Although we did not explore the relationships between specific bacterial families and infection severity, associations between the relative abundance of specific bacterial families and susceptibility to murine malaria infection have been identified. In inbred mice sourced from different vendors, an increased abundance of Clostridiaceae, Erysipelotrichaceae, Lactobacillaceae, and Peptostreptococcaceae family members has been linked to lower parasite burdens following infection with multiple murine malaria species, while a greater abundance of Bacteroidaceae, Prevotellaceae, and Sutterellaceae family members has been associated with

susceptibility to murine malaria [125, 126]. The mechanisms by which some vendor-associated gut microbiotas reduce susceptibility to murine malaria infection are not known. Villarino et al. attribute this difference to an accelerated T-follicular helper cell response in mice colonized with resistance-associated microbes, although the microbial products or antigens that drive this acceleration have not been identified [125]. The gut microbiota could influence the systemic immune system by direct interaction with immune cells or the production of bacterial products absorbed out of the gut lumen. It is also possible that cross-reactive antibodies raised against specific members of the gut microbiota present in JAX-associated feces and absent in NCI-associated feces could neutralize blood-stage malaria parasites. A similar phenomenon is observed in mice colonized with *Escherichia coli* O86:B7, an isolate that expresses Galα1-3Galβ1-4GlcNAc-R (α-gal). The antibodies produced in response to E. coli O86:B7 target malaria sporozoites, which also bear α-gal on their surface, and protect mice against transmission [123].

The extent to which the composition of the gut microbiota influences human susceptibility to malaria infection has not been extensively explored. At this time, a single study explores the relationship between the composition of the gut microbiota and malaria infection in humans. Malian children with a taxonomic profile characterized by an elevated abundance of *Bifidobacterium* and *Streptococcus* species are more likely to be infected with *P. falciparum* than children with a gut microbiota characterized by an elevated abundance of Ruminococcaceae and Lachnospiraceae family members [128]. However, children in both groups are equally likely to develop febrile malaria following infection [128]. Although the identification of specific bacterial families or genera associated with relative resistance to malaria infection in humans is tantalizing, relationships between specific microbial community members and susceptibility to

malaria remain challenging to pinpoint due to the extreme diversity between individuals. In addition, identification of resistance-associated microbial community members in pregnant women will be further complicated by the changes observed in the human gut microbiota over the course of the pregnancy [131]. While research aiming to better understand the relationship between the gut microbiota and the antimalarial immune response may ultimately pave the way for the development of probiotic adjunctive therapies for malaria infection, we envision a more immediate application for our findings as a tool for model development and expansion.

The ability to alter susceptibility to malaria infection in the context of pregnancy allows for the exploration of the relationship between maternal infection burden and fetal or postnatal outcomes. We anticipate that fecal exposure-mediated modulation of infection severity will be an increasingly useful tool for the tuning of infection severity in systemic disease models. Both malaria infection severity and pregnancy outcome can by influenced by exposure different fecal contents in an outbred mouse model for malaria in pregnancy demonstrating the utility of this strategy. Furthermore, this model allows for the exploration of the mechanisms by which the gut microbiota shapes susceptibility to a systemic infection in the context of a genetically diverse population of animals, perhaps providing insights into the modulation of human infection responses by the microbial communities within the gut.

Acknowledgments

We thank Dr. Mansour Mohamadzadeh and his lab at the University of Florida for performing fecal microbiome analyses and providing guidance for the processing of fecal samples. Specifically, we thank Minghao Gong for performing bioinformatic analyses. We also thank Simon Owino for processing fecal samples. In addition, we thank Alicer K. Andrew, Caitlin A. Cooper, Tara C. Bracken, Vivian Anderson, and Trisha Dalapati for their assistance

performing mouse experiments. Finally, we thank Julie Nelson at the Flow Cytometry Facility of the Center for Tropical and Emerging Global Diseases for flow cytometry services and technical assistance. Research reported in this manuscript was supported by the National Institute of Allergy and Infectious Diseases and the Eunice Kennedy Shriver National Institute of Child Health and Human Development of the National Institutes of Health under award numbers T32AI060546 (to CDMS), and R01HD46860 and R21AI111242 (to JMM). The content is solely the responsibility of the authors and does not necessarily represent official views of the Eunice Kennedy Shriver National Institute of Child Health and Human Development, the National Institute of Allergy and Infectious Diseases, or the National Institutes of Health.

Table 3.1. Fostering success and survivorship.
A significant difference in the proportion of total pups suitable for fostering was observed between maternal treatment groups only between cohorts of Mal+ mice (two-tailed Fisher exact test). Similarly, a significant difference in the proportion of fostered pups surviving to weaning was observed between maternal treatment groups only between cohorts of Mal+ mice (two-tailed Fisher exact test).

Group	Dams producing live fetuses/ Total dams	Resuscitated, fostered pups	Fostered/ Total pups	Sig.	Pup no. 4, 22 days of age	Weaned/ Fostered pups	Sig.
Mal- ABX-FMT^{NCI}	8/8	82, 81	81/96 (84%)	0.8160	48, 47	47/81 (58%)	0.4365
Mal- ABX-FMT^{JAX}	5/5	42, 42	42/51 (82%)		29, 28	28/42 (67%)	
Mal+ ABX-FMT^{NCI}	7/13	28, 26	26/61 (43%)	**< 0.0001**	10, 9	9/26 (35%)	**0.0014**
Mal+ ABX-FMT^{JAX}	6/6	61, 60	60/64 (94%)		45, 44	44/60 (73%)	

Figure 3.1. Composition of the gut microbiota pre- and post-treatment.
a) Weighted UniFrac analysis of pre-treatment fecal samples.
b) Weighted UniFrac analysis of post-treatment fecal samples.
Red symbols represent mice in the ABX-FMT^{NCI} treatment group. Blue symbols represent mice in the ABX-FMT^{JAX} treatment group. Fainter colors correspond to points that are further from the page along the z-axis.
ABX-FMT^{NCI} $n = 14$; ABX-FMT^{JAX} $n = 13$.

a

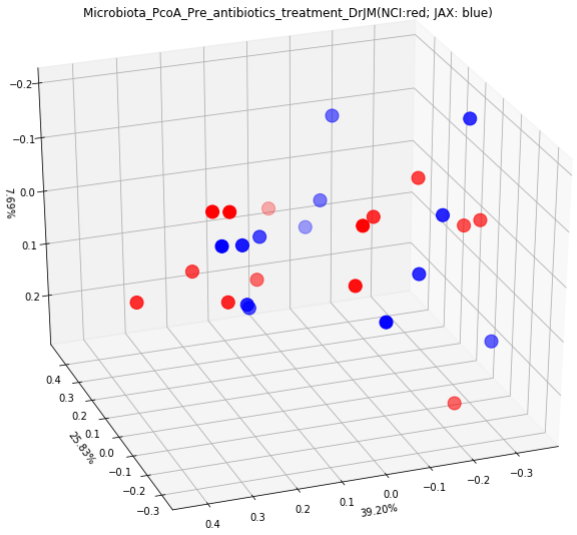
Microbiota_PcoA_Pre_antibiotics_treatment_DrJM(NCI:red; JAX: blue)
7.69%
25.83%
39.20%

b

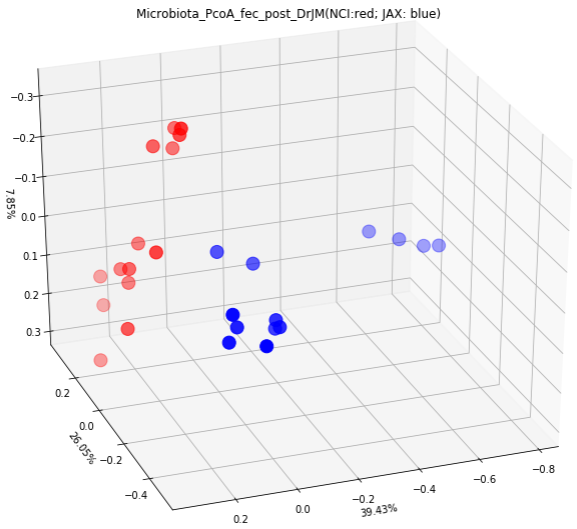
Microbiota_PcoA_fec_post_DrJM(NCI:red; JAX: blue)
7.85%
26.05%
39.43%

Figure 3.2. Parasitemia, hematocrit, and weight change in gravid ABX-FMT^{NCI} and ABX-FMT^{JAX} Swiss Webster mice.

a) Parasitemia in gravid Mal+ mice was estimated by flow cytometry and is presented as the percentage of iRBCs in the peripheral blood.
b) Percent hematocrit was measured throughout infection in gravid Mal+ mice and Mal- controls.
c) Weight change in gravid Mal+ mice and Mal- controls is presented as the percentage of body weight relative to 0 days post-infection or post-mock infection.
d) Area under the curve (AUC) was calculated for the parasitemia curve of each individual animal. A statistically significant difference in parasite burdens is observed between Mal+ ABX-FMT^{NCI} and ABX-FMT^{JAX} dams (Mann Whitney test, $P < 0.001$).
e) AUC was calculated for the hematocrit curve of each individual dam. Statistically significant differences in hematocrit are observed between Mal+ and Mal- ABX-FMT^{NCI} dams ($P < 0.001$), between Mal+ and Mal- ABX-FMT^{JAX} dams ($P < 0.001$), and between Mal+ ABX-FMT^{NCI} and Mal+ ABX-FMT^{JAX} dams ($P < 0.001$; one-way ANOVA with Bonferroni multiple group comparisons).
f) AUC was calculated for the weight change curve of each individual animal. Statistically significant differences in weight change are observed between Mal+ and Mal- ABX-FMT^{NCI} dams ($P < 0.001$), and between Mal+ ABX-FMT^{NCI} and Mal+ ABX-FMT^{JAX} dams ($P < 0.001$; one-way ANOVA with Bonferroni multiple group comparisons).

Gravid Mal+, ABX-FMT^{NCI} $n = 18$; Gravid Mal-, ABX-FMT^{NCI} $n = 18$; Gravid Mal+, ABX-FMT^{JAX} $n = 16$; Gravid Mal-, ABX-FMT^{JAX} $n = 15$; *** $P \leq 0.001$; ns $P > 0.05$.

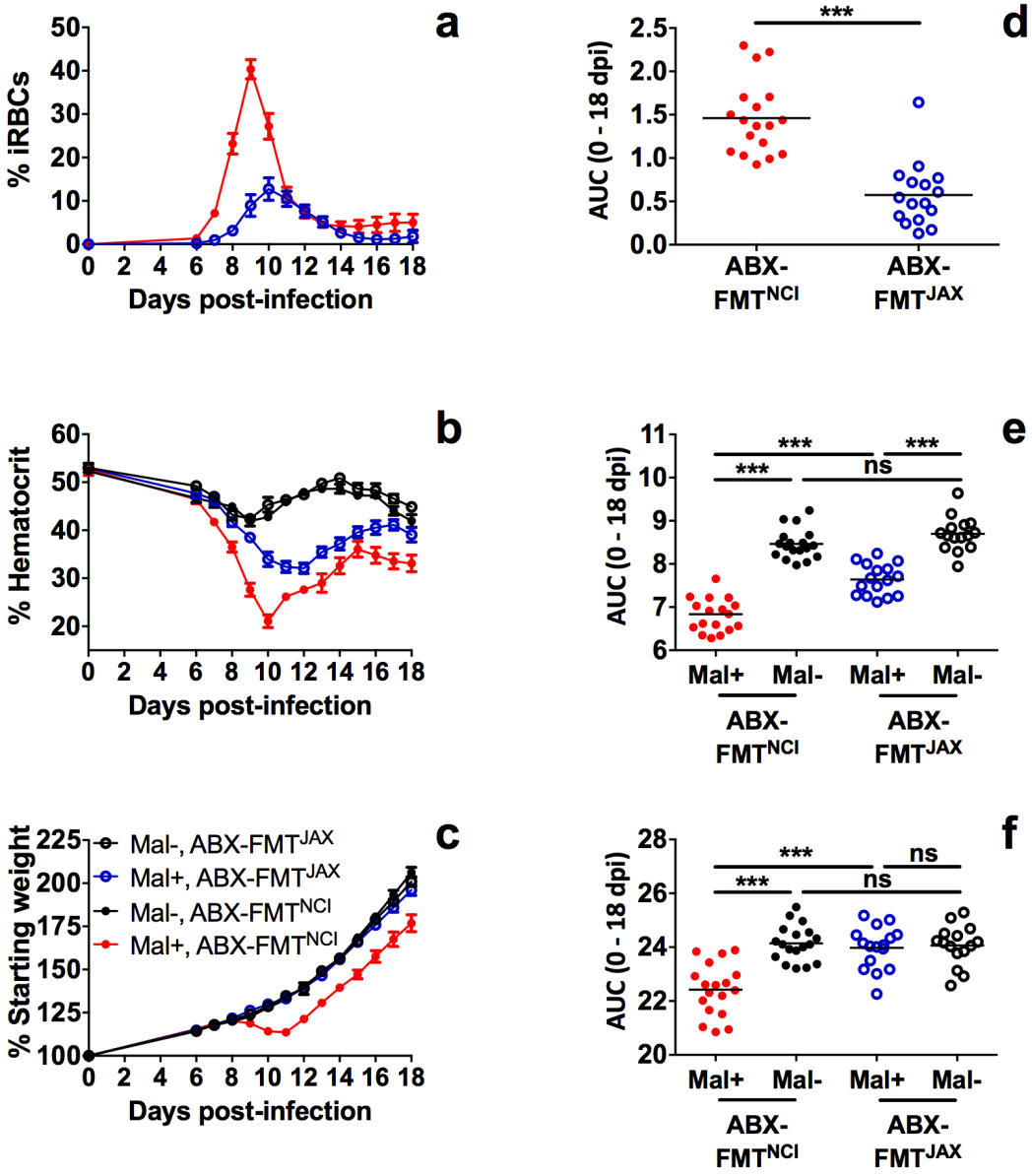
a
% iRBCs
Days post-infection
b
% Hematocrit
Days post-infection
c
% Starting weight
Mal-, ABX-FMT^JAX
Mal+, ABX-FMT^JAX
Mal-, ABX-FMT^NCI
Mal+, ABX-FMT^NCI
Days post-infection
d
AUC (0 - 18 dpi)
***
ABX-FMT^NCI
ABX-FMT^JAX
e
AUC (0 - 18 dpi)
***
ns
Mal+
Mal-
ABX-FMT^NCI
ABX-FMT^JAX
f
AUC (0 - 18 dpi)
***
ns
Mal+
Mal-
ABX-FMT^NCI
ABX-FMT^JAX

Figure 3.3. Parasitemia, hematocrit, and weight change in gravid CTRL-FMT^{NCI} and CTRL-FMT^{JAX} Swiss Webster mice.

a) Parasitemia in gravid Mal+ mice was estimated by flow cytometry and is presented as the percentage of iRBCs in the peripheral blood.
b) Percent hematocrit was measured throughout infection in gravid Mal+ mice and Mal- controls.
c) Weight change in gravid Mal+ mice and Mal- controls is presented as the percentage of body weight relative to 0 days post-infection or post-mock infection.
d) Area under the curve (AUC) was calculated for the parasitemia curve of each individual animal. Statistically significant differences in parasite burden are not observed between Mal+ gravid CRTL-FMT^{NCI} and CRTL-FMT^{JAX} mice by AUC analysis (Mann Whitney test, $P > 0.05$).
e) AUC was calculated for the hematocrit curve of each individual dam. Statistically significant differences in hematocrit are observed between Mal+ and Mal- CRTL-FMT^{NCI} dams ($P \leq 0.05$) and Mal+ and Mal- CRTL-FMT^{JAX} dams ($P \leq 0.05$) by AUC analysis (Kruskal-Wallis test with Dunn's post-test).
f) AUC was calculated for the weight change curve of each individual animal. There are no statistically significant differences in weight change either as a function of infection status or treatment group by AUC analysis ($P > 0.05$; Kruskal-Wallis test with Dunn's post-test).

Gravid Mal+, CTRL-FMT^{NCI} $n = 6$; Gravid Mal-, CTRL-FMT^{NCI} $n = 6$; Gravid Mal+, CTRL-FMT^{JAX} $n = 5$; Gravid Mal-, CTRL-FMT^{JAX} $n = 6$; * $P \leq 0.05$; ns $P > 0.05$.

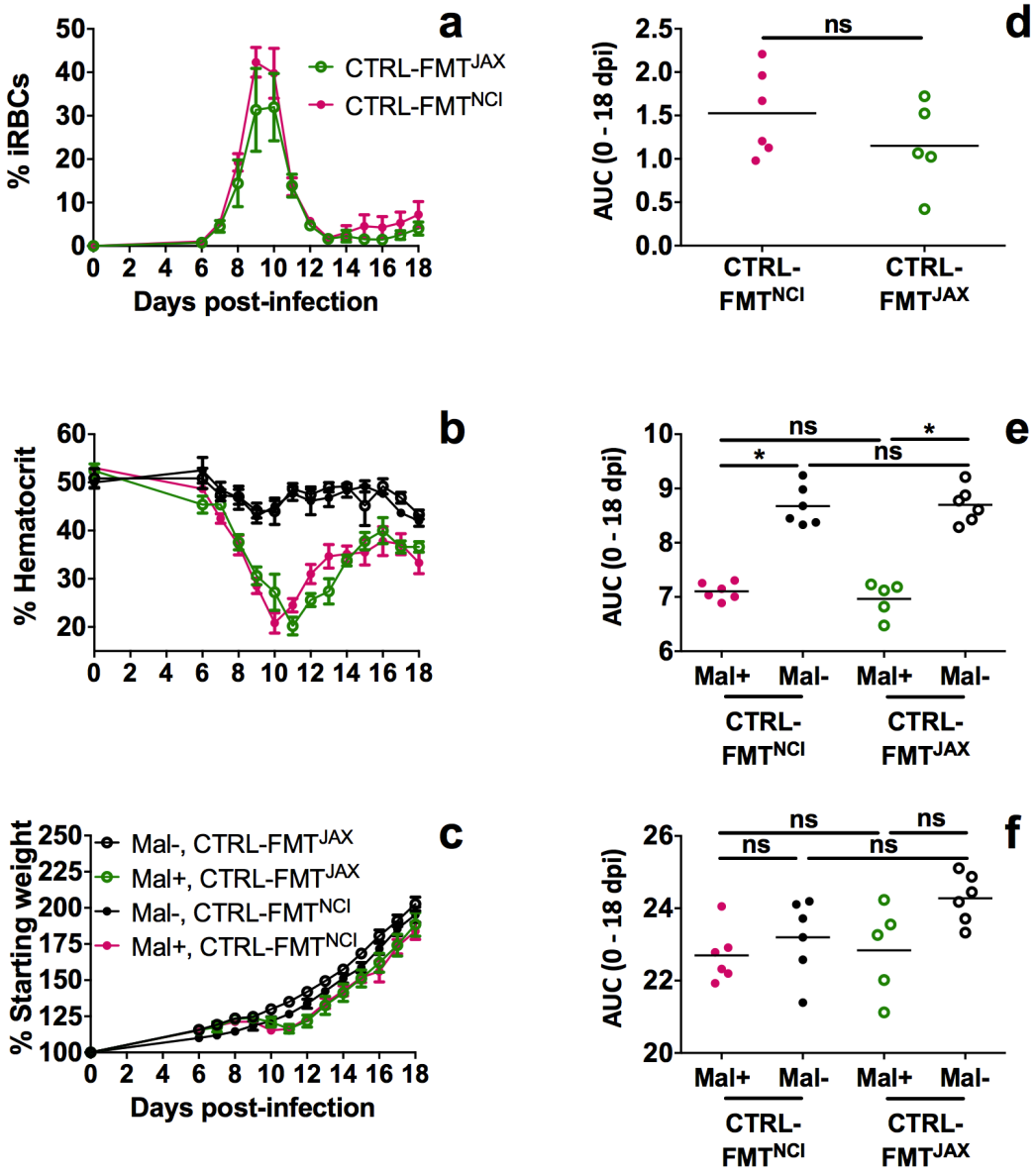
a
% iRBCs
Days post-infection
CTRL-FMT^JAX
CTRL-FMT^NCI
b
% Hematocrit
c
% Starting weight
Mal-, CTRL-FMT^JAX
Mal+, CTRL-FMT^JAX
Mal-, CTRL-FMT^NCI
Mal+, CTRL-FMT^NCI
d
AUC (0 - 18 dpi)
ns
e
*
f
Mal+
Mal-

Figure 3.4. Parasitemia, hematocrit, and weight change in virgin ABX-FMT^{NCI}, ABX-FMT^{JAX}, CTRL-FMT^{NCI}, and CTRL-FMT^{JAX} Swiss Webster mice.

a) Parasitemia in virgin Mal+ mice was estimated by flow cytometry and is presented as the percentage of iRBCs in the peripheral blood.
b) Percent hematocrit was measured through infection in virgin Mal+ mice.
c) Weight change in virgin Mal+ mice is presented as the percentage of body weight relative to 0 days post-infection.
d) AUC was calculated for the parasitemia curve of each individual animal. A statistically significant difference in parasite burden is only observed between virgin Mal+ ABX-FMT^{NCI} and ABX-FMT^{JAX} mice ($P \leq 0.01$; Kruskal-Wallis test with Dunn's post-test for multiple comparisons).
e) AUC was calculated for the hematocrit curve of each individual dam. A statistically significant difference in hematocrit is only observed between virgin Mal+ ABX-FMT^{NCI} and ABX-FMT^{JAX} mice ($P \leq 0.05$; Kruskal-Wallis test with Dunn's post-test for multiple comparisons).
f) AUC was calculated for the weight change curve of each individual animal. No statistically significant differences in weight change are observed between groups ($P > 0.05$, Kruskal-Wallis test with Dunn's post-test for multiple comparisons).

Virgin Mal+, CTRL-FMT^{NCI} $n = 6$; Virgin Mal+, CTRL-FMT^{JAX} $n = 5$; Virgin Mal+, ABX-FMT^{NCI} $n = 7$; Virgin Mal+, ABX-FMT^{JAX} $n = 6$; * $P \leq 0.05$; ** $P \leq 0.01$; ns $P > 0.05$**.**

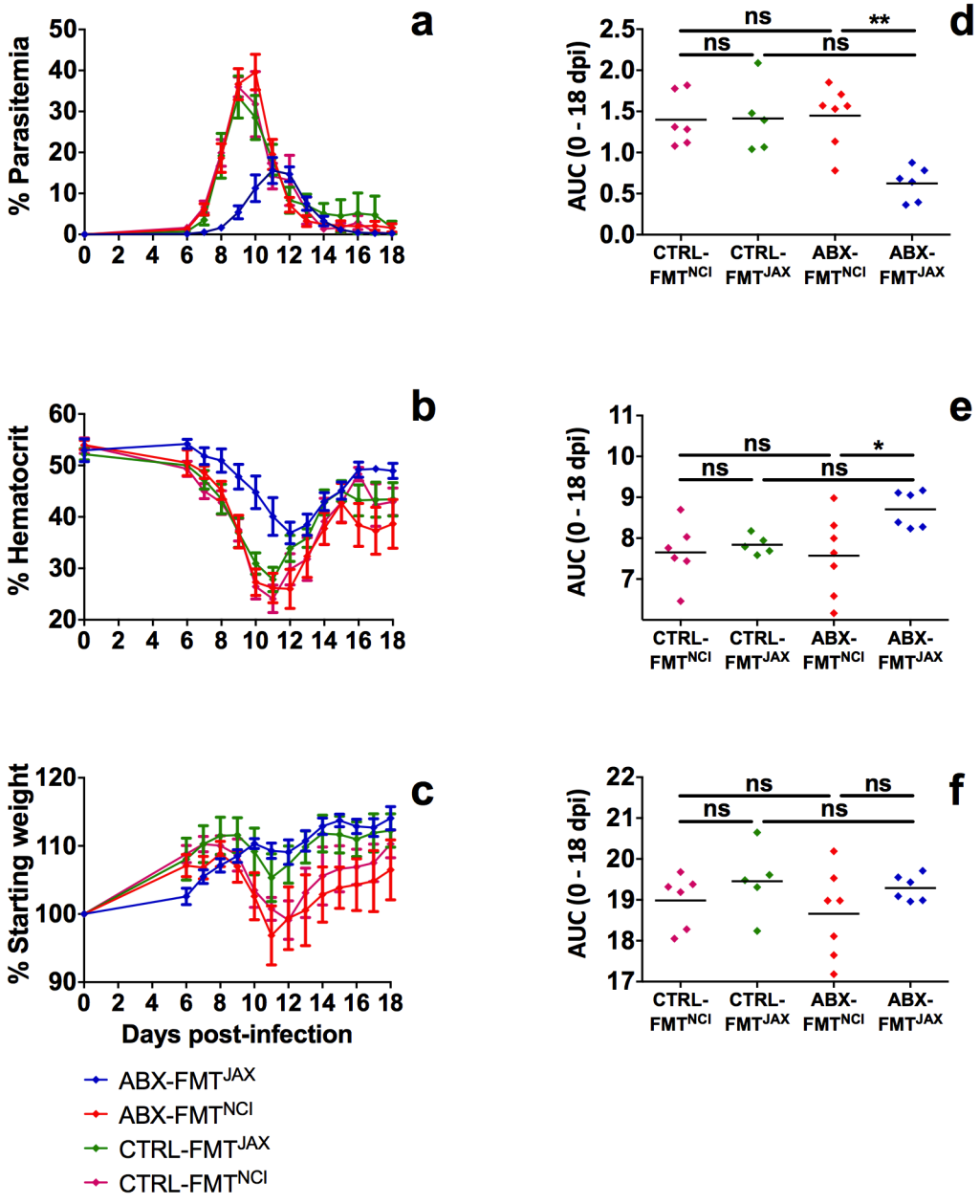
a
% Parasitemia
50
40
30
20
10
0
0 2 4 6 8 10 12 14 16 18
b
% Hematocrit
60
50
40
30
20
0 2 4 6 8 10 12 14 16 18
c
% Starting weight
120
110
100
90
0 2 4 6 8 10 12 14 16 18
Days post-infection
ABX-FMTJAX
ABX-FMTNCI
CTRL-FMTJAX
CTRL-FMTNCI
d
AUC (0 - 18 dpi)
2.5
2.0
1.5
1.0
0.5
0.0
ns
ns
ns
**
CTRL-FMTNCI
CTRL-FMTJAX
ABX-FMTNCI
ABX-FMTJAX
e
AUC (0 - 18 dpi)
11
10
9
8
7
ns
ns
ns
*
CTRL-FMTNCI
CTRL-FMTJAX
ABX-FMTNCI
ABX-FMTJAX
f
AUC (0 - 18 dpi)
22
21
20
19
18
17
ns
ns
ns
ns
CTRL-FMTNCI
CTRL-FMTJAX
ABX-FMTNCI
ABX-FMTJAX

Figure 3.5. Dam weights at GD 0.
Individual dam weights prior to infection or mock infection are presented. No significant differences in starting weight are observed between groups ($P > 0.05$, Kruskal-Wallis test with Dunn's post-test for multiple comparisons).
Mal+ CTRL-FMT^{NCI} $n = 6$; Mal- CTRL-FMT^{NCI} $n = 6$; Mal+ CTRL-FMT^{JAX} $n = 5$; Mal- CTRL-FMT^{JAX} $n = 6$; Mal+ ABX-FMT^{NCI} $n = 18$; Mal- ABX-FMT^{NCI} $n = 18$; Mal+ ABX-FMT^{JAX} $n = 16$; Mal- ABX-FMT^{JAX} $n = 15$.

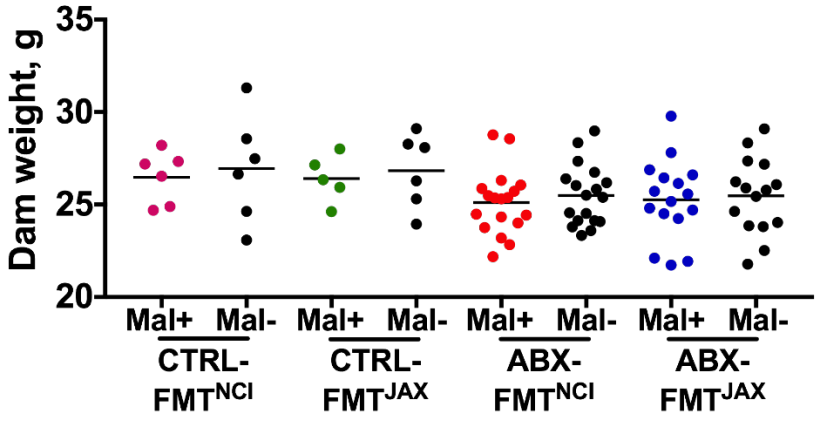
Dam weight, g
35
30
25
20
Mal+
Mal-
Mal+
Mal-
Mal+
Mal-
Mal+
Mal-
CTRL-
FMTNCI
CTRL-
FMTJAX
ABX-
FMTNCI
ABX-
FMTJAX

Figure 3.6. Fetal numbers, fetal weights, and placental weights at term in ABX-FMT^{NCI} and ABX-FMT^{JAX} dams.

a) No statistically significant difference in total or viable fetus number was observed as a function of treatment group or infection status ($P > 0.05$; Kruskal-Wallis test with Dunn's post-test).
b) Fetal weights are displayed pooled by dam group to show population-level patterns.
c) Placental weights are displayed pooled by dam group to show population-level patterns.

Gravid Mal+ ABX-FMT^{NCI} $n = 91$ fetuses/placentae, 11 litters; Gravid Mal- ABX-FMT^{NCI} $n = 101$ fetuses/placentae, 10 litters; Gravid Mal+ ABX-FMT^{JAX} $n = 96$ fetuses/placentae, 10 litters; Gravid Mal- ABX-FMT^{JAX} $n = 112$ fetuses/placentae, 10 litters.

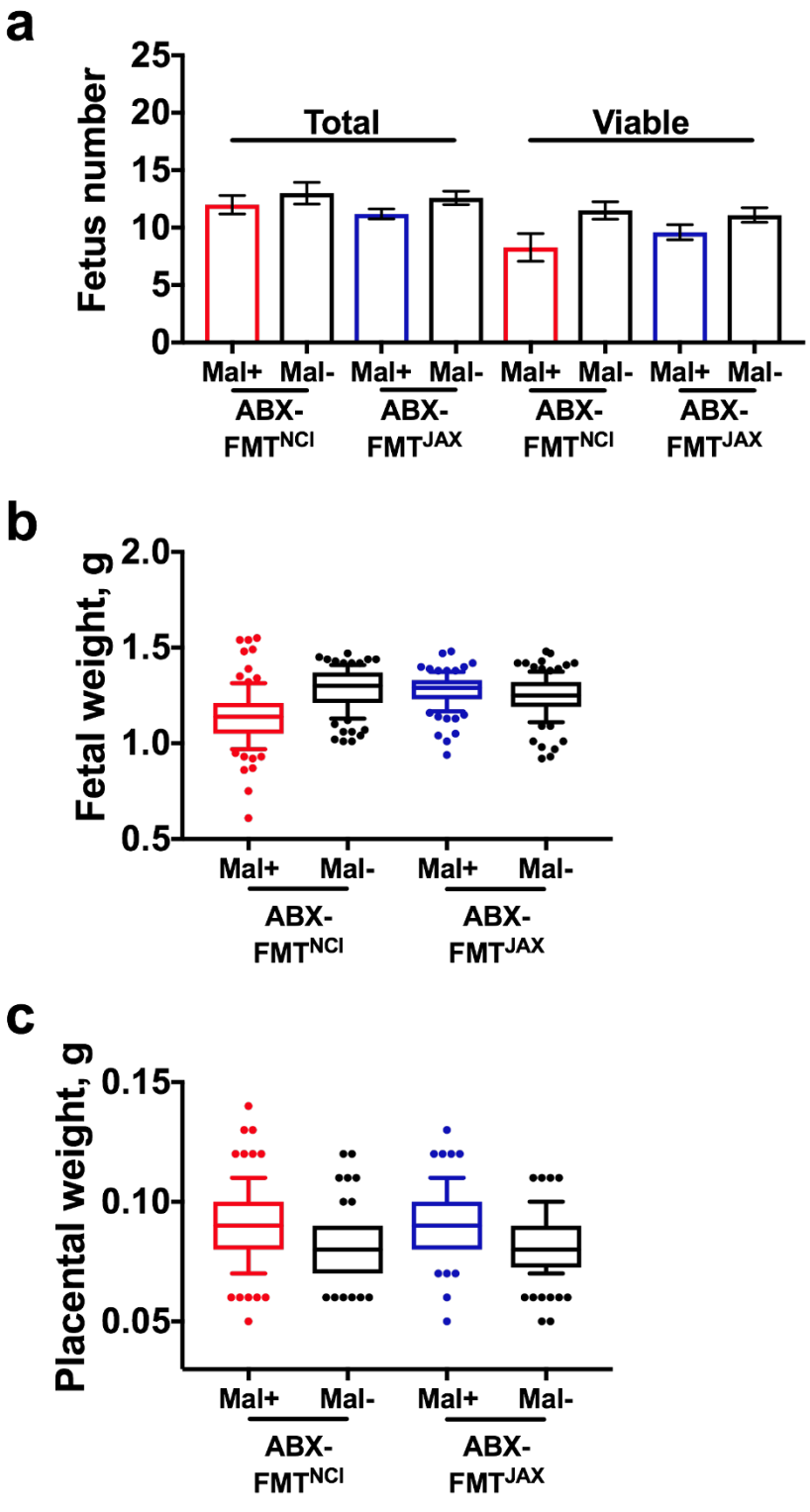
a
Fetus number
25
20
15
10
5
0
Total
Viable
Mal+
Mal-
Mal+
Mal-
Mal+
Mal-
Mal+
Mal-
ABX-
FMTNCI
ABX-
FMTJAX
ABX-
FMTNCI
ABX-
FMTJAX
b
Fetal weight, g
2.0
1.5
1.0
0.5
Mal+
Mal-
Mal+
Mal-
ABX-
FMTNCI
ABX-
FMTJAX
c
Placental weight, g
0.15
0.10
0.05
Mal+
Mal-
Mal+
Mal-
ABX-
FMTNCI
ABX-
FMTJAX

Figure 3.7. Fetal numbers, fetal weights, and placental weights at term in CTRL-FMT^{NCI} and CTRL-FMT^{JAX} dams.

a) No statistically significant difference in total or viable fetus number was observed as a function of treatment group or infection status ($P > 0.05$; Kruskal-Wallis test with Dunn's post-test).
b) Fetal weights are displayed pooled by dam group to show population-level patterns.
c) Placental weights are displayed pooled by dam group to show population-level patterns.

Gravid Mal+ CTRL-FMT^{NCI} $n = 68$ fetuses/placentae, 6 litters; Gravid Mal- CTRL-FMT^{NCI} $n = 72$ fetuses/placentae, 6 litters; Gravid Mal+ CTRL-FMT^{JAX} $n = 57$ fetuses/placentae, 5 litters; Gravid Mal- CTRL-FMT^{JAX} $n = 67$ fetuses/placentae, 6 litters.

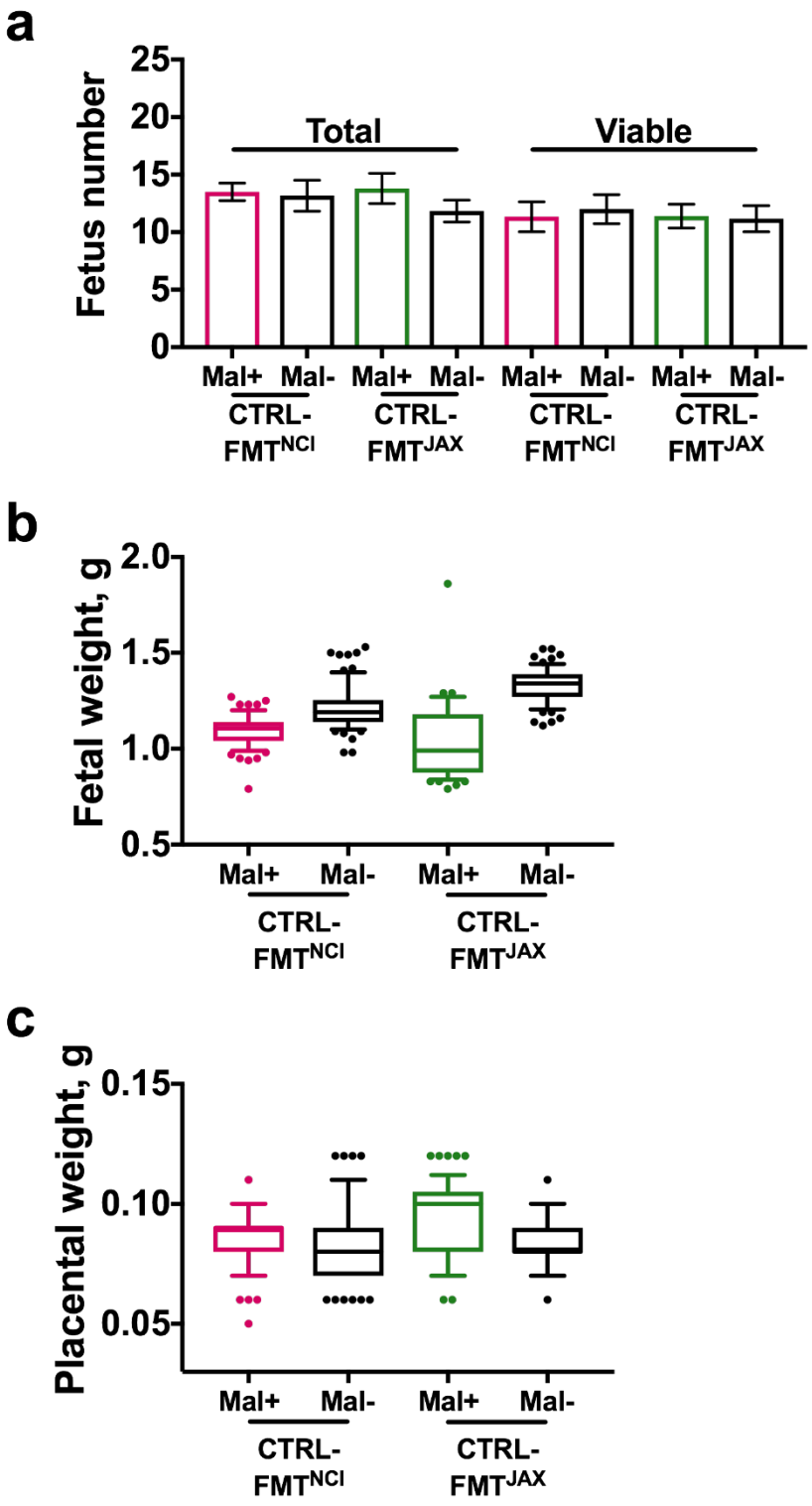
a
Fetus number
25
20
15
10
5
0
Total
Viable
Mal+ Mal- Mal+ Mal- Mal+ Mal- Mal+ Mal-
CTRL-FMTNCI
CTRL-FMTJAX
CTRL-FMTNCI
CTRL-FMTJAX
b
Fetal weight, g
2.0
1.5
1.0
0.5
Mal+ Mal- Mal+ Mal-
CTRL-FMTNCI
CTRL-FMTJAX
c
Placental weight, g
0.15
0.10
0.05
Mal+ Mal- Mal+ Mal-
CTRL-FMTNCI
CTRL-FMTJAX

Figure 3.8. Impact of maternal antibiotic treatment on fetal weight at GD 18.
FMT groups and infection status are collapsed within ABX and CTRL cohorts to demonstrate the impact of maternal antibiotic treatment regardless of subsequent FMT exposure or infection status on fetal weight at GD 18.
Mal+ CTRL *n* = 125 fetuses; Mal- CTRL *n* = 139 fetuses; Mal+ ABX *n* = 187 fetuses; Mal- ABX *n* = 213 fetuses.

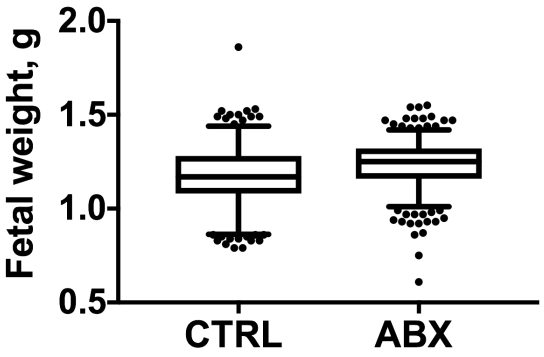
Fetal weight, g
2.0
1.5
1.0
0.5
CTRL
ABX

Figure 3.9. Fetal and placental weights by dam at GD 18.
Numbers on the X-axis are the unique identifier assigned to each dam.

a) Weights of viable fetuses are presented for each CTRL-FMT^{NCI} dam.
b) Weights of viable fetuses are presented for each CTRL-FMT^{JAX} dam.
c) Weights of viable fetuses are presented for each ABX-FMT^{NCI} dam.
d) Weights of viable fetuses are presented for each ABX-FMT^{JAX} dam.
e) Weights of placentae associated with viable fetuses are presented for each CTRL-FMT^{NCI} dam.
f) Weights of placentae associated with viable fetuses are presented for each CTRL-FMT^{JAX} dam.
g) Weights of placentae associated with viable fetuses are presented for each ABX-FMT^{NCI} dam.
h) Weights of placentae associated with viable fetuses are presented for each ABX-FMT^{JAX} dam.

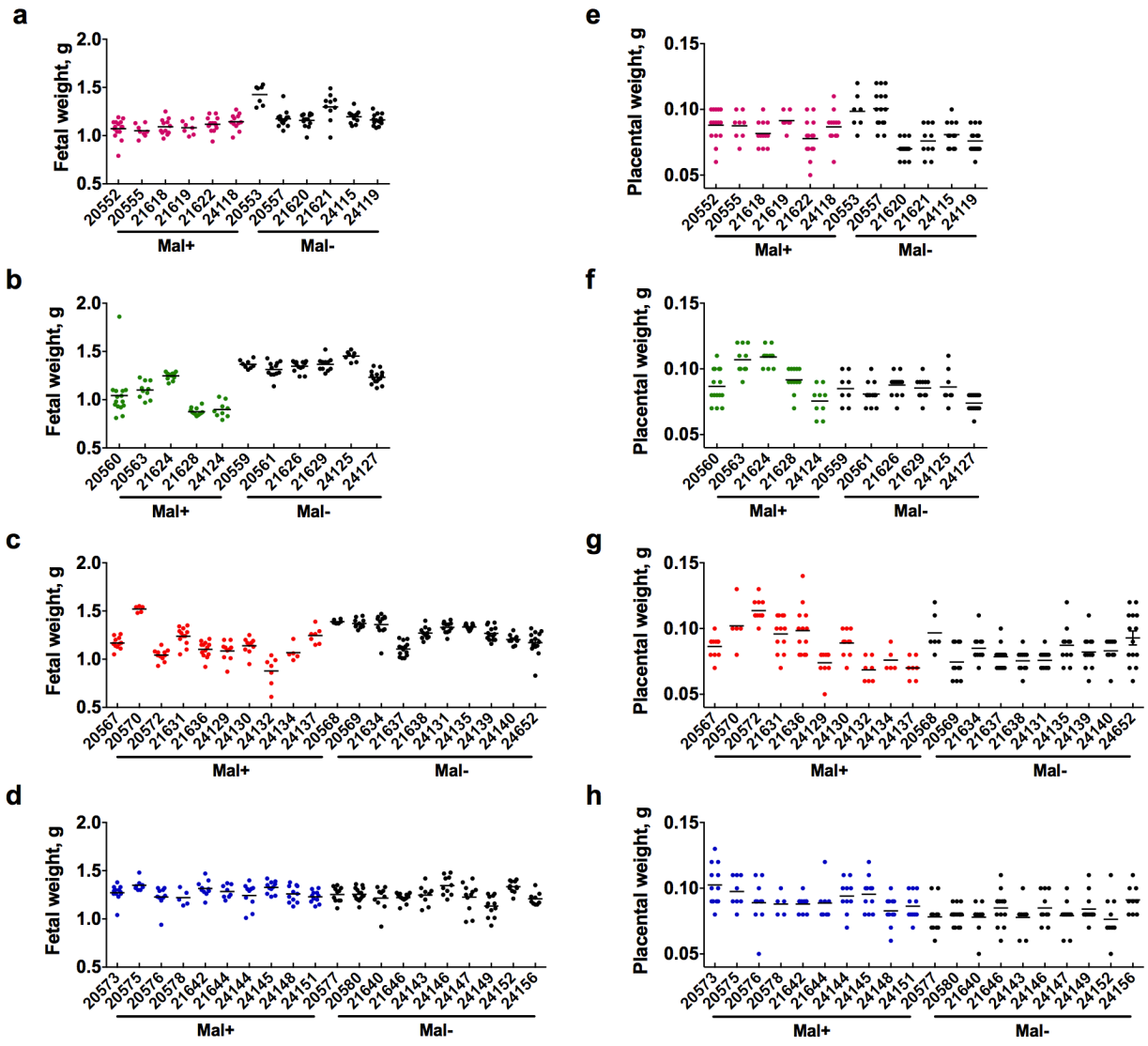
a
Fetal weight, g
2.0
1.5
1.0
0.5
20552 20555 21618 21619 21622 24118 20553 20557 21620 21621 24115 24119
Mal+
Mal-
e
Placental weight, g
0.15
0.10
0.05
20552 20555 21618 21619 21622 24118 20553 20557 21620 21621 24115 24119
Mal+
Mal-
b
Fetal weight, g
2.0
1.5
1.0
0.5
20560 20563 21624 21628 24124 20559 20561 21626 21629 24125 24127
Mal+
Mal-
f
Placental weight, g
0.15
0.10
0.05
20560 20563 21624 21628 24124 20559 20561 21626 21629 24125 24127
Mal+
Mal-
c
Fetal weight, g
2.0
1.5
1.0
0.5
20567 20570 20572 21631 21636 24129 24130 24132 24134 24137 20568 20569 21634 21637 21638 24131 24135 24139 24140 24652
Mal+
Mal-
g
Placental weight, g
0.15
0.10
0.05
20567 20570 20572 21631 21636 24129 24130 24132 24134 24137 20568 20569 21634 21637 21638 24131 24135 24139 24140 24652
Mal+
Mal-
d
Fetal weight, g
2.0
1.5
1.0
0.5
20573 20575 20576 20578 21642 21644 24144 24145 24148 24151 20577 20580 21640 21646 24143 24146 24147 24149 24152 24156
Mal+
Mal-
h
Placental weight, g
0.15
0.10
0.05
20573 20575 20576 20578 21642 21644 24144 24145 24148 24151 20577 20580 21640 21646 24143 24146 24147 24149 24152 24156
Mal+
Mal-

Figure 3.10. Fetal weights at GD 18 in fostered pups.
Weights of all viable pups were recorded at the time of fostering. Pup weights are presented pooled by donor dam group to show population-level patterns.
Mal+ ABX-FMT^{NCI} n = 56; Mal+ ABX-FMT^{JAX} n = 64; Mal- ABX-FMT^{NCI} n = 92; Mal- ABX-FMT^{JAX} n = 49.

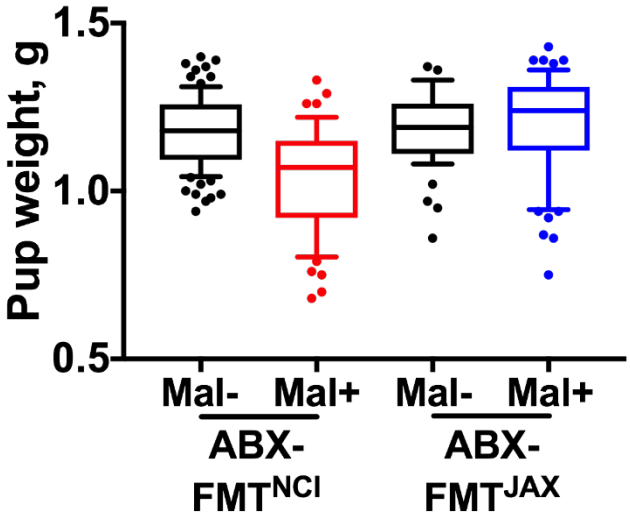
Pup weight, g
1.5
1.0
0.5
Mal-
Mal+
Mal-
Mal+
ABX-
FMT^NCI
ABX-
FMT^JAX

Figure 3.11. Postnatal growth of fostered pups.

a) Fostered female pups were individually identified and weighed every three days between 4 days of age and weaning at 22 days of age. Mal+ ABX-FMT^{NCI} n = 4; Mal+ ABX-FMT^{JAX} n = 25; Mal- ABX-FMT^{NCI} n = 16; Mal- ABX-FMT^{JAX} n = 14.

b) Fostered male pups were individually identified and weighed every three days between 4 days of age and weaning at 22 days of age. Mal+ ABX-FMT^{NCI} n = 5; Mal+ ABX-FMT^{JAX} n = 19; Mal- ABX-FMT^{NCI} n = 31; Mal- ABX-FMT^{JAX} n = 14.

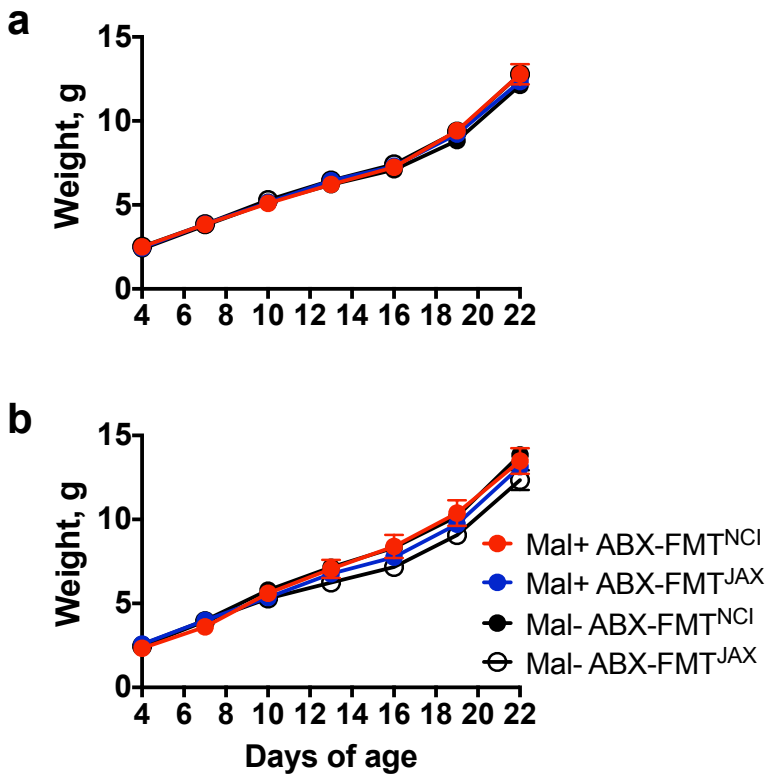
a
Weight, g
15
10
5
0
4 6 8 10 12 14 16 18 20 22
b
Weight, g
15
10
5
0
4 6 8 10 12 14 16 18 20 22
Days of age
Mal+ ABX-FMTNCI
Mal+ ABX-FMTJAX
Mal- ABX-FMTNCI
Mal- ABX-FMTJAX

CHAPTER 4

COMPARING THE IMMUNOLOGICAL AND PLACENTAL ENVIRONMENT IN PREGNANT MICE DISPLAYING GUT MICROBIOTA-ASSOCIATED RESISTANCE AND SUSCEPTIBILITY TO MALARIA INFECTION

Introduction

Gestational malaria infection causes severe maternal illness, poor birth outcomes, and increased infant mortality [3-9, 11, 12]. In humans, infection with *Plasmodium falciparum* compromises the health of the pregnancy by damaging the placenta, the connection between the mother and the fetus. The parasitized placenta is characterized by the sequestration of malaria-infected red blood cells (iRBCs) [39], the disruption of placental architecture [35, 36, 50, 133], and the development of a proinflammatory and pro-coagulant placental environment [56, 84]. As a result, gestational malaria is associated with placental dysfunction, including the disruption of normal uteroplacental blood flow [92], amino acid transport [93, 94], glucose transport [97, 98], and autophagy [95].

Mouse models are important for dissecting the relationships between the placental damage and dysfunction observed in PM and the resulting poor birth outcomes. The use of pregnant Swiss Webster mice infected with *Plasmodium chabaudi chabaudi* AS on gestational day (GD) 0 allows for exploration of fetal and postnatal outcomes following prolonged *in utero* exposure to malaria [Ch. 2]. This model can be expanded by altering the gut microbiota, which modulates both infection severity and subsequent pregnancy outcomes [Ch. 3]. Vendor-affiliated communities of fecal microbes known to confer susceptibility or resistance to malaria infection

were utilized to alter the composition of the murine gut microbiota. Gut microbial communities collected from Jackson Laboratory (JAX)-sourced mice are associated with resistance to infection, while the gut microbial communities of National Cancer Institute Mouse Repository (NCI)-sourced mice are associated with susceptibility to malaria infection [125]. Swiss Webster mice that are antibiotic-treated (ABX) prior to the administration of a fecal microbiota transplant (FMT) consisting of feces collected from JAX-derived stock (ABX-FMT^{JAX}), develop relatively low parasite burdens [Ch. 3], while mice purchased from NCI shortly prior to infection or mice that are antibiotic treated prior to receiving an autologous FMT consisting of feces collected from other untreated NCI-sourced mice (ABX-FMT^{NCI}) develop higher parasite burdens and greater morbidity [Ch. 2, Ch. 3]. Therefore, this model allows for the exploration of the maternal-fetal relationship during severe and moderate maternal malaria infection by enabling the modulation of susceptibility to *P. chabaudi chabaudi* AS infection via the manipulation of the gut microbiota.

The most profound differences in parasitemia, hematocrit, and weight gain between susceptible and resistant Swiss Webster dams are observed around the time of peak infection. Susceptible dams exhibit higher parasite burdens, lower hematocrit, and a stasis in weight gain at peak infection compared to resistant dams. The difference in weight gain at this timepoint is intriguing, because it may indicate impaired embryo growth in susceptible NCI-sourced and ABX-FMT^{NCI} dams compared to relatively resistant ABX-FMT^{JAX} dams. This stasis in weight gain cannot be attributed to embryo demise at peak infection because maternal infection is not associated with a significant reduction in the average number of total fetuses or the average number of viable fetuses produced by NCI-sourced, ABX-FMT^{NCI}, or ABX-FMT^{JAX} dams at gestational term (GD 18). However, severe infection in NCI-sourced and ABX-FMT^{NCI} dams is

associated with a significant reduction in fetal weight at term. Furthermore, susceptible malaria-infected (Mal+) NCI-sourced and ABX-FMT^{NCI} dams produce fewer pups that survive to weaning than uninfected (Mal-) controls or resistant Mal+ ABX-FMT^{JAX} dams, perhaps indicating that low birth weight contributes to neonatal death [Ch. 2, Ch. 3].

While the variable gestational outcomes observed in dams with gut microbiota-associated susceptibility or resistance to malaria infection have been characterized, the mechanisms determining these different outcomes have not been elucidated. To explore the immunological and placental environments of highly susceptible and relatively resistant mice at peak infection, susceptible NCI-sourced and resistant ABX-FMT^{JAX} dams were sacrificed at gestational day/experimental day (GD/ED) 10. Embryo number and embryo viability were not significantly different between Mal+ NCI-sourced and ABX-FMT^{JAX} dams at GD/ED 10, although uterine weights in Mal+ NCI-sourced dams were reduced compared to Mal- NCI-sourced controls. A statistically significant accumulation of iRBCs in the placenta was not observed in either Mal+ NCI-sourced or ABX-FMT^{JAX} dams, although Mal+ ABX-FMT^{JAX} dams displayed a tendency towards higher placental parasitemia compared to peripheral parasitemia. The levels of peripheral blood cytokines between virgin and gravid Mal+ NCI-sourced and ABX-FMT^{JAX} mice did not differ as a result of pregnancy status or infection severity. The expression of genes associated with inflammation, the response to hypoxia, and the oxidative stress response at the level of the conceptus were similar between gravid Mal+ NCI-sourced and ABX-FMT^{JAX} mice. However, conceptuses collected from susceptible Mal+ NCI-sourced dams displayed an increase in *Il10* transcription compared to conceptuses collected from Mal+ ABX-FMT^{JAX} dams, perhaps reflecting an elevated compensatory anti-inflammatory response in Mal+ NCI-sourced mice. Taken together, these data indicate that embryo growth is reduced in NCI-sourced dams

experiencing heavy parasite burdens compared to Mal+ ABX-FMT^{JAX} dams experiencing more modest parasite burdens. At this time, the reduction in embryo weight observed in Mal+ NCI-sourced dams cannot be attributed to iRBC accumulation within the placenta, elevated peripheral inflammation, or the transcriptional response of conceptuses at the time of sacrifice, GD/ED 10.

Materials & Methods

Mice

Seven-week-old female and eight- to ten-week-old male Swiss Webster mice (Clr:CFW) were purchased from the NCI Mouse Repository (Frederick, MD) to serve as NCI-sourced experimental females and studs. Three-week-old female and five-week-old male Swiss Webster mice were purchased from NCI to serve as ABX-FMT^{JAX} experimental females and studs. C57BL/6 (B6) mice used as FMT^{JAX} donors were derived from breeder stock purchased from JAX and maintained at the University of Georgia (UGA) for no more than ten generations. All mice were maintained at the UGA Coverdell Vivarium, a barrier facility, under specific-pathogen-free conditions in *Helicobacter* species and norovirus-free rooms. Mice were acclimated to a 14-hour light/10-hour dark cycle and rooms were maintained at 65-75°F and 40-60% humidity. All mice were given unrestricted access to food (PicoLab Mouse Diet 20 5053; St. Louis, MO) and water. Husbandry and experiments were performed in accordance with the guidelines and regulations set forth by the UGA Institutional Animal Care and Use Committee.

ABX-FMT^{JAX} mice were generated as previously described [Ch. 3]. Briefly, four-week-old female and six-week-old male mice were treated with a broad spectrum antibiotic cocktail consisting of 100mg/kg ampicillin (Gold Biotechnology; St. Louis, MO), 100mg/kg metronidazole (MP Biomedicals; Santa Ana, CA), 100mg/kg neomycin sulfate (Gold Biotechnology; St. Louis, MO), and 50mg/kg vancomycin hydrochloride (Gold Biotechnology;

St. Louis, MO) in sterile water by oral gavage [140, 141]. Mice were treated for four consecutive days, then every other day thereafter until 9 doses of antibiotic had been administered. Beginning on the day following the administration of the final dose of antibiotic, mice were treated for three consecutive days with a fecal slurry consisting of feces produced by JAX-derived B6 mice, 200µl 50mg/ml feces in 1x phosphate-buffered saline (PBS), by oral gavage [142]. Following the completion of the FMT treatment course, animals were not handled for seven to ten days.

To produce pregnant mice, mice were mated as previously described [Ch. 2, Ch. 3]. Briefly, NCI-sourced and ABX-FMT^{JAX} females were paired with NCI-sourced and ABX-FMT^{JAX} studs, respectively. Female mice were checked each morning for the presence of a copulation plug, indicating successful mating. The day a copulation plug was observed was considered GD 0. Infection in gravid mice was initiated the morning a plug was observed. The day of infection was considered experimental day (ED) 0, so GD and ED are aligned in gravid Mal+ mice. Mated mice were randomly assigned to Mal+ and Mal- cohorts, and virgin controls were infected alongside gravid mice. At GD/ED 0, all experimental animals were provided with a higher fat breeder chow (PicoLab Mouse Diet 20 5058; St. Louis, MO). Mated female mice displaying a 10% or greater increase in body weight between GD 0 and GD 8 were considered gravid.

Parasites, infection, and infection monitoring

The following reagent was obtained through BEI Resources Repository, NIAID, NIH: *Plasmodium chabaudi chabaudi*, Strain AS, MRA-741, contributed by David Walliker. Parasites were maintained as frozen stock in accordance with supplier guidelines and amplified in A/J mice for the purposes of infecting experimental mice.

To initiate infection, gravid and virgin Mal+ mice were injected intravenously with 10^3 *P. chabaudi chabaudi* AS-iRBCs in 200µl 1x phosphate-buffered saline (PBS) per 20 grams of body weight. Gravid Mal- controls were mock infected with 200µl 1x PBS per 20 grams of body weight. Immediately prior to infection, body weight and hematocrit were measured. Parasitemia, body weight, and hematocrit were measured daily between GD/ED 6 and GD/ED 10.

To measure peripheral parasitemia, blood samples were collected using a modified tail-clip technique [135] and analyzed by flow cytometry using a method adapted from Jimenez-Diaz et al. [134]. Within 4 hours of collection, blood samples were diluted 1:50 in isotonic saline and stained with 2.5µM SYTO® 16 Green Florescent Nucleic Acid Stain (ThermoFisher Scientific; Waltham, MA). After 20 minutes incubation at room temperature and protected from light, stained blood was diluted 1:9 in isotonic saline and analyzed using a CyAn ADP Flow Cytometer (Beckman Coulter; Brea, CA). Thirty thousand cells were analyzed per mouse, and all samples were analyzed within 4.5 hours of collection. iRBCs were identified based on size and fluorescence intensity. Blood was collected from an uninfected mouse and stained to serve as an internal control. Parasitemia is reported as the percentage of iRBCs in the total population of red blood cells.

Plasma and tissue collection

All mice were sacrificed for plasma and tissue collection at GD/ED 10. Mice were anesthetized with 2.5% Tribromoethanol. Blood was collected by venipuncture of the caudal vena cava [155] using an Anticoagulant Citrate-Dextrose (ACD) charged syringe. Platelet-poor plasma was isolated by double centrifugation of whole blood containing 10% ACD v/v [156], snap frozen, and stored at -80°C. Following blood collection, non-exsanguinated mice were euthanized by cervical dislocation. The uterus was removed and weighed. Viable embryos,

nonviable embryos, and resorption scars were counted. Plump, pink, well-vascularized embryos without hemorrhaging were considered viable. Nonviable embryos and resorptions were included in the count of total embryos. Approximately half of the conceptuses were removed from the uterus and snap frozen for gene expression analysis, while the remaining conceptuses were preserved in formalin within the uterus for histology.

Placental parasitemia

Uterine segments containing conceptuses were harvested at sacrifice and fixed overnight in 4% buffered formalin. Following overnight fixation, uterine segments were bisected longitudinally and allowed to fix for another 24 hours to complete fixation of tissues. Tissues were then dehydrated with ethanol, cleared in xylenes, and infiltrated in melted paraffin prior to embedding. Seven micron sections were Giemsa-stained, and parasite burden in the placenta was measured by counting iRBCs in maternal blood sinusoids in Giemsa-stained tissue sections. At least 10^3 erythrocytes were counted for each dam across a minimum of three conceptuses. Placental parasitemia is presented as the percentage of iRBCs counted in the maternal blood.

Peripheral cytokine titers

Cytokine levels in plasma collected at sacrifice were measured using the Bio-Plex Pro™ Mouse Cytokine Th17 Panel A 6-Plex kit (Bio-Rad; Hercules, CA), read using the Bio-Rad Bio-Plex® 200 system (Bio-Rad; Hercules, CA), and analyzed with Bio-Plex Manager™ software (Bio-Rad; Hercules, CA).

Gene expression

Total RNA was isolated from GD/ED 10 mouse conceptuses using the RNeasy Plus Mini Kit (Qiagen; Germantown, MD) following homogenization in lysis buffer using the TissueMiser (Fisher Scientific; Waltham, MA) or Bullet Blender Gold (Next Advance; Troy, NY). A

minimum of 3 conceptuses were pooled per dam. Reverse transcription was performed using the High-Capacity cDNA Reverse Transcription Kit (Applied Biosystems; Foster City, CA). Relative transcript abundance was measured using Power SYBR® Green Supermix (Applied Biosystems; Foster City, CA) with the C1000 Touch Thermal Cycler (CFX96 Real Time Systems; Bio-Rad, Hercules, CA). Each sample was assayed in duplicate for all target and housekeeping genes. Average threshold cycle (Ct) values were normalized to average *Ubc* Ct values. Relative transcript abundance of each gene of interest was determined using the ΔΔCt method [157]. Briefly, transcript expression in Mal+ NCI-sourced, Mal- ABX-FMT^{JAX}, and Mal+ ABX-FMT^{JAX} mice is presented relative to the mean expression value in Mal- NCI-sourced mice. Columns and bars represent mean ± SEM of the fold change for each gene. The dashed line at y = 1 represents the baseline fold change represented by the mean expression value in Mal- NCI-sourced mice. When possible, primer pairs were designed to span large introns such that amplification exclusively represented cDNA template. Primer sequences, amplicon size, and total intron size are listed in Table 1. *Ubc*, the gene encoding murine ubiquitin C, was selected as a housekeeping gene due to its relatively high stability in the embryo [158] and placenta [159].

Statistics

Descriptive statistical analyses were performed using GraphPad Prism 7 (GraphPad Software; La Jolla, California). All raw clinical data are presented as mean ± SEM. Error bars are not depicted if the error bars are shorter than the height of the symbol. Area under the curve of parasitemia, hematocrit, and percent starting weight was calculated for each mouse between GD 0 and GD 10. Individual AUC values are presented as scatterplots with bars representing group means. Parasitemia AUC values were compared between gravid Mal+ and virgin Mal+ cohorts by two-tailed Student's *t* test and by Mann-Whitney test, respectively. Hematocrit and

weight change AUC values were compared between gravid Mal+ and virgin Mal+ cohorts by Kruskal-Wallis test with Dunn's multiple comparisons test or by Mann-Whitney test as appropriate. The numbers of total and viable embryos produced by dams in a cohort are presented as bars depicting group means, with error bars depicting SEM. Total and viable embryo numbers are compared between Mal+ and Mal- dams within maternal treatment groups and between infection status-matched dams across maternal treatment group by Kruskal-Wallis test with Dunn's multiple comparisons test. Raw uterine weights are presented as a scatterplot with a bar representing the group mean. Uterine weights were compared across cohorts by Kruskal-Wallis test with Dunn's multiple comparisons test. Paired peripheral and placental parasitemias, representing individual mice, were compared by Wilcoxon matched-pairs signed rank test. Peripheral cytokine titers are presented for each individual mouse and compared by Kruskal-Wallis test with Dunn's multiple comparisons test. P values ≤ 0.05 were considered statistically significant.

Results

NCI-sourced Swiss Webster mice are more susceptible to *P. chabaudi chabaudi* AS infection than ABX-FMT^{JAX} Swiss Webster mice

Parasitemia, hematocrit, and body weight were measured daily between GD/ED 6 and sacrifice at GD/ED 10 in Mal+ mice and Mal- controls to track infection progression and pregnancy development. Compared to gravid Mal+ ABX-FMT^{JAX} mice, gravid Mal+ NCI-sourced animals developed significantly greater parasite burdens over the course of the experiment (Fig. 4.1d). On average, gravid Mal+ NCI-sourced mice achieved peak parasitemia at GD/ED 9 (Fig. 4.1a). Descending parasitemia was not observed in gravid Mal+ ABX-FMT^{JAX} animals during the experimental period, indicating that peak infection was delayed compared to

gravid Mal+ NCI-sourced mice (Fig. 4.1a). A significant reduction in hematocrit was observed in susceptible gravid Mal+ NCI-sourced mice compared to gravid Mal- NCI-sourced controls (Fig. 4.1e). However, infection did not significantly reduce hematocrit among gravid ABX-FMT^{JAX} mice. Hematocrit does not rebound during the experimental period in either gravid Mal+ cohort, indicating that gravid Mal+ mice are experiencing significant disease at GD/ED 10 (Fig. 4.1b). No significant differences in weight change are observed between gravid cohorts over the course of the experiment (Fig. 4.1f). However, gravid Mal+ NCI-sourced mice do not adhere to the weight gain trajectory observed in the other cohorts at GD/ED 9 and GD/ED 10 (Fig. 4.1c), suggesting that these animals may experience a stasis in weight gain at peak infection as previously observed in NCI-sourced mice followed throughout gestation [Ch. 2]. Differences in hematocrit and weight change were not observed between Mal- NCI-sourced and ABX-FMT^{JAX} mice over the course of the experiment (Fig. 4.1e, f).

Virgin Mal+ NCI-sourced and ABX-FMT^{JAX} controls exhibit patterns similar to those observed in gravid Mal+ mice (Fig. 4.2). Virgin Mal+ NCI-sourced mice have significantly greater parasite burdens than virgin Mal+ ABX-FMT^{JAX} mice (Fig. 4.2d). However, unlike gravid mice (Fig. 4.1), no significant difference in hematocrit is observed between virgin Mal+ cohorts (Fig. 4.2e). Virgin Mal+ NCI-sourced mice display a significant reduction in weight change over the course of the experiment compared to virgin Mal+ ABX-FMT^{JAX} mice, perhaps reflecting increased morbidity associated with elevated parasite burdens (Fig. 4.2f).

Maternal infection severity does not significantly influence embryo viability at midgestation

Infection was not associated with abortion in gravid Mal+ dams at or prior to GD/ED 10. All successfully mated Mal+ and Mal- mice that exhibited the pregnancy-associated ≥10% increase in body weight by GD/ED 8 were pregnant at sacrifice.

Neither maternal infection status nor maternal treatment group significantly influenced the mean number of total nor the mean number of viable embryos produced by cohorts of Mal+ and Mal- NCI-sourced and ABX-FMT^{JAX} dams (Fig. 4.3a). Similarly, in populations of embryos pooled by dam group, malaria infection severity did not influence embryo viability at GD/ED 10. Gravid Mal+ mice from both cohorts produced a similar proportion of viable embryos: 14 Mal+ NCI-sourced dams produced 157 embryos, 144 of which were viable (92% viability), while a cohort of 8 Mal+ ABX-FMT^{JAX} dams produced 96 embryos, 81 of which were viable (84% viability; P = 0.0973; two-tailed Fisher exact test). Embryo viability did not differ significantly between cohorts in the absence of infection: 11 Mal- NCI-sourced dams produced 132 embryos, 127 of which were viable (96% viability), while a cohort of 5 Mal- ABX-FMT^{JAX} dams produced 64 embryos, 57 of which were viable (89% viability; $P = 0.1505$; two-tailed Fisher exact test).

Infection reduces uterine weight at peak infection in susceptible NCI-sourced dams but not in relatively resistant ABX-FMT^{JAX} dams

Although no significant difference in weight change over the course of the experiment is detected between gravid Mal+ NCI-sourced and ABX-FMT^{JAX} mice (Fig. 4.1f), weight change at GD/ED 10 did differ significantly between groups ($P < 0.0001$; Kruskal-Wallis test). Dunn's pairwise tests were performed for four pairs of groups. Weight change at GD/ED 10 was significantly reduced in Mal+ NCI-sourced dams compared to Mal- NCI-sourced dams ($P = 0.0016$) and Mal+ ABX-FMT^{JAX} dams ($P = 0.0003$; Kruskal-Wallis test with Dunn's multiple comparisons test). No significant difference in weight change at GD/ED 10 was detected between Mal- dams or between Mal+ and Mal- ABX-FMT^{JAX} dams ($P > 0.05$; Kruskal-Wallis test with Dunn's multiple comparisons test).

The extent to which intrauterine growth restriction contributed to this pattern in maternal body weight was explored by measuring uterine weights in gravid Mal- and gravid Mal+ NCI-sourced and ABX-FMT^{JAX} mice sacrificed at GD/ED 10. Uteri collected from susceptible gravid Mal+ NCI-sourced dams weighed significantly less than uteri collected from gravid Mal- NCI-sourced controls (Fig. 4.3b). Infection did not reduce uterine weight in relatively resistant gravid Mal+ ABX-FMT^{JAX} mice compared to gravid Mal- ABX-FMT^{JAX} controls (Fig. 4.3b).

Significant placental sequestration is not observed in either susceptible NCI-sourced dams or resistant ABX-FMT^{JAX} dams at midgestation

The accumulation or sequestration of iRBCs in the maternal blood spaces of the placenta is a hallmark of gestational malaria in humans and is observed in some mouse models for malaria infection in pregnancy [59, 109]. To determine if iRBCs were accumulating in the placentae of Mal+ NCI-sourced or ABX-FMT^{JAX} dams, iRBCs were counted in the maternal blood sinusoids of placentae using Giemsa-stained tissue sections. The placental parasitemias determined using this method are likely to be conservative estimates because not all sectioned iRBCs will have a detectable parasite within the sectioned portion of the iRBC and will not be counted as infected.

Resistant Mal+ ABX-FMT^{JAX} dams tend to have more parasites in the placenta than in the periphery, although statistical significance was not reached (Figure 4.4b). No tendency towards parasite accumulation was observed in the placentae of Mal+ NCI-sourced dams (Figure 4.4a). Taken together, these data indicate that significant accumulation of iRBCs in the placenta is not a feature of placental histopathology in either Mal+ NCI-sourced or Mal+ ABX-FMT^{JAX} dams at GD/ED 10.

However, placental parasite burdens are significantly different in Mal+ NCI-sourced and ABX-FMT^{JAX} dams. Reflecting the difference in peripheral parasitemia between dam cohorts,

placental parasitemia in gravid Mal+ NCI-sourced mice is significantly higher than placental parasitemia in gravid Mal+ ABX-FMT^{JAX} mice at GD/ED 10 (Fig. 4.4c).

Peripheral cytokine titers do not vary significantly as a function of maternal infection severity or pregnancy status

Plasma cytokine concentrations were measured to test the hypothesis that Mal+ ABX-FMT^{JAX} mice mount a more robust proinflammatory immune response around the time of peak *P. chabaudi chabaudi* AS infection, allowing them to control infection more efficiently than susceptible Mal+ NCI-sourced mice. Titers of the proinflammatory cytokines IFN-γ, TNF-α, IL-1β, IL-6, and IL-17A, as well as IL-10, were measured in the peripheral plasma of gravid and virgin Mal+ NCI-sourced and ABX-FMT^{JAX} mice at GD/ED 10 (Fig. 4.5). No significant differences in cytokine titers were observed as a function of gut microbiota-mediated susceptibility to infection or pregnancy status.

The expression levels of the genes encoding IFN-γ, IL-10, and MCP-1 are elevated in *P. chabaudi chabaudi* AS-exposed conceptuses of NCI-sourced and ABX-FMT^{JAX} dams

The transcriptional response of malaria-exposed conceptuses collected from NCI-sourced dams and ABX-FMT^{JAX} dams was interrogated to determine if maternal infection severity influences conceptus cytokine gene expression at peak infection. The expression of the genes encoding the proinflammatory cytokines IFN-γ, TNF-α, and IL-1β, the anti-inflammatory cytokine IL-10, and the chemokine MCP-1/CCL2 was measured via qPCR (Fig. 4.6a).

In the absence of infection, conceptuses from Mal- NCI-sourced and ABX-FMT^{JAX} dams exhibit similar levels of transcription for all cytokine and chemokine genes examined. In conceptuses collected from both groups of Mal+ dams, the expression levels of *Ifng* and *Il10* were markedly elevated compared to expression in conceptuses collected from Mal- dams (Fig.

4.6a). Similarly, the expression of *Ccl2* was modestly elevated in conceptuses collected from Mal+ dams compared to Mal- dams (Fig. 4.6a). In both groups of Mal+ dams, the expression of *Ifng* was increased approximately 3- to 4-fold and the expression of *Ccl2* was increased nearly 2-fold (Fig. 4.6a). A dramatic difference in transcription between Mal+ NCI-sourced and ABX-FMT^{JAX} conceptuses was only observed in the expression of *Il10* (Fig. 4.6a). In conceptuses collected from Mal+ NCI-sourced dams the expression of *Il10* was elevated nearly 7-fold, while in conceptuses collected from Mal+ ABX-FMT^{JAX} dams the expression of *Il10* was elevated approximately 2-fold (Fig. 4.6a).

Transcription of hypoxia and oxidative stress genes is modestly increased in malaria-exposed conceptuses produced by NCI-sourced dams

The expression of genes associated with hypoxia and oxidative stress responses were evaluated by qPCR in conceptuses collected from NCI-sourced and ABX-FMT^{JAX} dams. The transcription of *Hif1a*, the gene encoding hypoxia-inducible factor 1α, was measured to assess the response to placental hypoxia. Transcription of the antioxidant genes *Sod1*, *Sod2*, *Sod3*, and *Cat* were measured to assess the antioxidant response to infection. These genes encode superoxide dismutase (SOD) 1, SOD2, SOD3, and catalase, all of which interact with and neutralize damaging radicals. The transcription of *Nrf2*, the gene encoding nuclear factor erythroid derived 2 like-2, a transcription factor involved in the oxidative stress response, was also measured to assess the transcriptional response to oxidative stress. Finally, the expression of the gene encoding heme oxygenase (HO), the enzyme that catalyzes the degradation of toxic free heme, was measured. HO is especially significant in the context of malaria infection because the destruction of iRBCs releases free heme, a potent oxidant, into circulation.

Conceptuses produced by Mal- ABX-FMT^{JAX} dams and Mal- NCI-sourced dams displayed similar levels of transcription of these genes (Fig. 4.6b). However, the expression of *Sod1* was increased nearly 2-fold in Mal- ABX-FMT^{JAX} dams compared to Mal- NCI-sourced dams (Fig. 4.6b). This may indicate that ABX-FMT^{JAX} dams experience elevated basal transcription of *Sod1* (Fig. 4.6b).

The expression levels of *Hif1a*, *Sod1*, *Sod2*, *Sod3*, *Cat*, and *Nrf2* were modestly elevated in conceptuses collected from Mal+ NCI-sourced dams compared to Mal- NCI-sourced controls (Fig. 4.6b). The expression of *Ho* is increased by greater than 2-fold in Mal+ NCI-sourced dams compared to Mal- NCI-sourced controls (Fig. 4.6b), perhaps reflecting a compensatory mechanism seeking to neutralize free heme released by the rupture of iRBCs. In contrast, the expression of *Ho* is not elevated in conceptuses collected from relatively resistant Mal+ ABX-FMT^{JAX} mice relative to conceptuses collected from Mal- ABX-FMT^{JAX} dams. Notable differences in the transcription of *Hif1a*, *Sod1*, *Sod2*, *Sod3*, *Cat*, and *Nrf2* were not observed as a function of infection in ABX-FMT^{JAX} dams (Fig. 4.6b).

Discussion

Following infection with *P. chabaudi chabaudi* AS, NCI-sourced and ABX-FMT^{JAX} Swiss Webster mice follow dramatically different trajectories. Gravid Mal+ NCI-sourced mice develop high parasite burdens, severe malarial anemia, and experience a deviation in normal gestational weight gain around the time of peak infection [Ch. 2]. In contrast, gravid Mal+ ABX-FMT^{JAX} mice develop lower parasite burdens, a more modest anemia, and display no change in weight gain compared to gravid Mal- controls [Ch. 3]. In addition, fetal weight at gestational term and postnatal viability are improved in gravid Mal+ ABX-FMT^{JAX} mice compared to gravid Mal+ NCI-sourced animals [Ch. 2, Ch. 3]. The reduced infection severity and improved

pregnancy outcomes observed in ABX-FMT^{JAX} mice compared to NCI-sourced mice are attributable to gut microbiota-mediated resistance to malaria infection conferred by fecal microbial communities associated with mice purchased from JAX [Ch. 3]. These studies demonstrate that the Swiss Webster-*P. chabaudi chabaudi* AS model for malaria in pregnancy allows for the exploration of malaria pathogenesis and pregnancy outcome in the context of variable maternal infection severity because susceptibility to malaria can be influenced by manipulating the gut microbiota. However, the immunological and placental milieu in Mal+ NCI-sourced and ABX-FMT^{JAX} mice at the time of peak infection has not previously been explored.

To examine the immunological and placental environments of mice experiencing high and moderate intensity infection in the Swiss Webster-*P. chabaudi chabaudi* AS model for maternal malaria infection, we sacrificed gravid Mal+ NCI-sourced and ABX-FMT^{JAX} mice and gravid Mal- controls at GD/ED 10. The GD/ED 10 experimental endpoint was selected because we felt that GD/ED 10 could represent the timepoint of maximum stress on the health of the pregnancy. Both Mal+ NCI-sourced and ABX-FMT^{JAX} mice achieve peak peripheral parasitemia around this time. Most gravid Mal+ NCI-sourced mice achieve peak infection at GD/ED 9, while most gravid Mal+ ABX-FMT^{JAX} mice achieve peak infection at GD/ED 10 [Ch. 2, Ch. 3]. Furthermore, gravid Mal+ NCI-sourced mice experience a stasis in gestational weight gain between GD/ED 9 and GD/ED 11, which generally reaches its nadir at GD/ED 10 [Ch. 2]. Finally, inbred B6 and A/J mice infected with *P. chabaudi chabaudi* AS on GD 0 spontaneously abort their pregnancies at approximately GD/ED 10 [56, 57, 88, 101, 109-111].

The reduction in gestational weight gain observed in gravid Mal+ NCI-sourced mice at GD/ED 10 can be partially attributed to intrauterine growth restriction of the conceptuses. Uteri

collected from gravid Mal+ NCI-sourced mice at GD/ED 10 weigh significantly less than those collected from gravid Mal- NCI-sourced controls, although embryo number and viability are not reduced by infection. This suggests that high parasite burdens impede embryo growth. Notably, no significant accumulation of iRBCs in the placenta is detected in either cohort of Mal+ mice, although resistant ABX-FMT^{JAX} dams tend to have more iRBCs in the maternal blood sinusoids of the placenta than in the peripheral blood. We speculate that statistical significance is not reached because the accumulation of iRBCs in the placenta relative to the peripheral parasite load is modest, and the relatively small group of Mal+ ABX-FMT^{JAX} dams does not provide sufficient statistical power. In contrast, no tendency towards parasite accumulation was observed in the placentae of Mal+ NCI-sourced dams. We speculate that the extremely high peripheral parasite burdens observed in many of these dams outpaces the accumulation of iRBCs in the placenta.

P. chabaudi chabaudi AS-infected B6 mice display significant increases in peripheral IFN-γ, IL-1β, and IL-10 prior to achieving peak infection [109, 111]. The levels of IFN-γ and IL-1β drop as peak parasitemia is reached, although IL-10 remains significantly elevated through peak infection [109, 111]. Surprisingly, no differences in the peripheral proinflammatory immune response were detected between Mal+ NCI-sourced and ABX-FMT^{JAX} dams at GD/ED 10. However, measurement at GD/ED 10 may fail to capture significant differences in cytokine titers between susceptible and resistant cohorts of mice. Gravid Mal+ NCI-sourced dams generally achieve peak parasitemia on GD/ED 9 and gravid Mal+ ABX-FMT^{JAX} dams generally achieve peak parasitemia around GD/ED 10, so the nonsignificant differences in peripheral cytokines titers between Mal+ cohorts may reflect the contraction of the anti-malarial immune response by GD/ED 10. Significant increases in peripheral cytokine titers as a function of

infection severity may be most evident prior to peak infection. Future experiments that assess plasma cytokine concentrations during the ascending phase of infection in NCI-sourced and ABX-FMT^{JAX} dams will be required to determine if our observations reflect the pattern of cytokine expression observed in *P. chabaudi chabaudi* AS-infected B6 mice.

The transcriptional response of malaria-exposed conceptuses differs subtly between Mal+ NCI-sourced dams and Mal+ ABX-FMT^{JAX} dams at GD/ED 10. The expression of *Ifng* and *Ccl2* is similarly increased in both cohorts of Mal+ dams compared to Mal- controls. Only the expression of *Il10* is definitively greater in the conceptuses of Mal+ NCI-sourced dams compared to Mal+ ABX-FMT^{JAX} dams. Like the systemic proinflammatory immune response, it is possible that transcription within Mal+ NCI-sourced conceptuses is returning to baseline by GD/ED 10, although elevated *Il10* expression persists through peak infection. Earlier sampling may reveal profound differences in the transcriptional responses of conceptuses collected from susceptible NCI-sourced dams and resistant ABX-FMT^{JAX} dams.

The elevation in placental *Il10* expression in gravid Mal+ mice is consistent with the detection of elevated levels of IL-10 in plasma collected from malaria-infected placentae [55, 56, 60]. Maternal immune cells within the infected placenta produce a significant amount of IL-10 [55, 64, 65, 72]; however, the contribution of fetally-derived cells cannot be excluded. The expression of *Il10* is significantly elevated in placental tissues collected from women infected with *P. falciparum* at the time of delivery compared to uninfected placentae [160, 161]. This indicates that the Swiss Webster-*P. chabaudi chabaudi* AS model for gestational malaria recapitulates the upregulation of *Il10* transcription by placental tissues observed in outbred human populations, suggesting that this model reflects the placental environment observed in human gestational malaria.

These results hint at a potential mechanism underpinning the differences in pregnancy outcome observed between susceptible Mal+ NCI-sourced dams and resistant Mal+ ABX-FMT^{JAX} dams. In human gestational malaria, inflammatory signaling associated with intervillositis disrupts placental amino acid and glucose transport, contributing to fetal growth restriction [93, 94, 96, 98]. Maternal inflammatory infiltrate, or intervillositis, was not measured in either group of Mal+ dams. However, the transcription of the anti-inflammatory cytokine *Il10* was elevated in conceptuses of Mal+ NCI-sourced dams compared to conceptuses from Mal+ ABX-FMT^{JAX} dams. This may indicate that a more significant proinflammatory response occurred in the conceptuses of Mal+ NCI-sourced dams prior to sacrifice, necessitating a more significant upregulation of *Il10* expression to counteract damaging inflammation at the maternal-fetal interface. If true, increased inflammation within the local environment of conceptuses produced by Mal+ NCI-sourced dams might have resulted in a more extreme disruption of amino acid and glucose transport, causing reduced embryo growth. However, the potential contribution of maternal anorexia or maternal metabolic disruption due to severe infection in Mal+ NCI-sourced dams cannot be excluded.

Intriguingly, the expression of the antioxidant gene *Sod1* is approximately two-fold higher in Mal- ABX-FMT^{JAX} dams compared to Mal- NCI-sourced dams, suggesting that the transcriptional setpoint of *Sod1* may be slightly higher in Mal- ABX-FMT^{JAX} mice. The mechanism by which this occurs, and its potential significance, is unclear. The expression of *Hif1a*, *Sod1*, *Sod2*, *Sod3*, and *Nrf2* are modestly elevated in Mal+ NCI-sourced dams compared to Mal- NCI-sourced controls. This is inconsistent with data generated in *P. chabaudi chabaudi* AS-infected B6 mice, which display large increases in the expression of *Sod2* and *Sod3* at GD/ED 10 compared to uninfected controls [88]. This discrepancy could reflect an elevated

antioxidant response to more severe oxidative stress in B6 mice. Oxidative damage to the placenta and embryo viability are inversely related in Mal+ B6 mice [88]. Therefore, it is possible that placental oxidative stress, and the compensatory antioxidant response, is less widespread in Mal+ Swiss Webster mice reflected by their ability to carry pregnancies to term.

The expression of *Ho* is modestly increased in conceptuses produced by Mal+ NCI-sourced dams compared to Mal- controls. Infection does not increase the expression of *Ho* in ABX-FMT^{JAX} dams. This may reflect the greater parasite burdens in Mal+ NCI-sourced mice. Compared to Mal+ ABX-FMT^{JAX} dams, Mal+ NCI-sourced mice experience the destruction of more erythrocytes, likely resulting in greater levels of free heme in the plasma. The increase in *Ho* transcription in Mal+ NCI-sourced mice may represent the response to a relatively large amount of free heme. This is consistent with observations made in women with gestational malaria. Significantly higher levels of heme and HO-1 are detected in the plasma of women with malaria at the time of delivery, suggesting that HO-1 is upregulated in response to the malaria-associated increase in plasma free heme [162]. We speculate that the upregulation of *Ho* protects conceptuses from heme-mediated oxidative damage, perhaps helping to preserve pregnancy in heavily infected Swiss Webster dams.

Further studies are required to identify the precise causes and mechanisms underlying the different pregnancy outcomes observed in Mal+ NCI-sourced and ABX-FMT^{JAX} dams. However, the data presented here demonstrate the ability of this model to probe the relationships between maternal parasite burden and pregnancy outcome. We anticipate that the ability to tune maternal infection severity by altering the gut microbiota will be a valuable addition to the toolkit of mouse models available for the study of malaria infection in pregnancy.

Acknowledgments

We thank Julie Nelson at the Flow Cytometry Facility of the Center for Tropical and Emerging Global Diseases for flow cytometry services and technical assistance. Research reported in this manuscript was supported by the National Institute of Allergy and Infectious Diseases and the Eunice Kennedy Shriver National Institute of Child Health and Human Development of the National Institutes of Health under award numbers T32AI060546 (to CDMS), and R01HD46860 and R21AI111242 (to JMM). The content is solely the responsibility of the authors and does not necessarily represent official views of the Eunice Kennedy Shriver National Institute of Child Health and Human Development, the National Institute of Allergy and Infectious Diseases, or the National Institutes of Health.

Table 4.1. Primer sequences targeting cytokine, chemokine, antioxidant, and hypoxia response mRNA transcripts.
Mouse-specific forward (FP) and reverse (RP) primers used in real time PCR for the amplification of gene-of-interest and housekeeping (*Ubc*) transcripts. Amplicon size and total intron size, where applicable, are also listed.

Gene	Forward and Reverse Primers	Amplicon size	Total intron size
Ubc	FP: 5'-CAGTGTTACCACCAAGAAGGT-3'	119	N/A
	RP: 5'-GAAAACTAAGACACCTCCCCCA-3'		
Ifng	FP: 5'-AGCAAGGCGAAAAAGGATGC-3'	132	2358
	RP: 5'-CTTCCTGAGGCTGGATTCCG-3'		
Tnf	FP: 5'-ATCGGTCCCCAAAGGGATGA-3'	159	1036
	RP: 5'-GTCTTTGAGATCCATGCCGT-3'		
Il1b	FP: 5'-TGAAGTTGACGGACCCCAAA-3'	127	1544
	RP: 5'-TGATACTGCCTGCCTGAAGC-3'		
Il10	FP: 5'-CTGAAGACCCTCAGGATGCG-3'	127	2628
	RP: 5'-TGGCCTTGTAGACACCTTGG-3'		
Ccl2	FP: 5'-GATGCAGTTAACGCCCCACT-3'	172	N/A
	RP: 5'-CCCATTCCTTCTTGGGGTCA-3'		
Hif1a	FP: 5'-CTGCAAGGTCGACAACTCCT-3'	132	N/A
	RP: 5'-GTTCCTGGGCTGGACAGTTT-3'		
Sod1	FP: 5'-GGAACCATCCACTTCGAGCA-3'	136	1850
	RP: 5'-CTGCACTGGTACAGCCTTGT-3'		
Sod2	FP: 5'-GGACCCATTGCAAGGAACAAC-3'	180	1413
	RP: 5'-TGAGTGAGGTTTCACTTCTTGC-3'		
Sod3	FP: 5'-GCAACTCAGAGGCTCTTCCTC-3'	175	3890
	RP: 5'-CCCCTGGATTTGACATGGTGA-3'		
Cat	FP: 5'-CACTGACGAGATGGCACACT-3'	175	2308
	RP: 5'-TGTGGAGAATCGAACGGCAA-3'		
Nrf2	FP: 5'-AGCCAGCTGACCTCCTTAGA-3'	131	N/A
	RP: 5'-AGTGACTGACTGATGGCAGC-3'		
Ho	FP: 5'-CATAGCCCGGAGCCTGAATC-3'	147	2083
	RP: 5'-AGCATTCTCGGCTTGGATGT-3'		

Figure 4.1. Parasitemia, hematocrit, and weight change in gravid *P. chabaudi chabaudi* AS-infected NCI-sourced and ABX-FMT^{JAX} Swiss Webster mice.

a. Parasitemia in gravid Mal+ mice was estimated by flow cytometry and is presented as the percentage of iRBCs in the peripheral blood.
b. Percent hematocrit was measured throughout infection in gravid Mal+ NCI-sourced and ABX-FMT^{JAX} mice and gravid Mal- controls.
c. Weight change in gravid Mal+ NCI-sourced and ABX-FMT^{JAX} mice and gravid Mal- controls.
d. Area under the curve (AUC) was calculated for the parasitemia curve of each individual mouse. A statistically significant difference in parasite burdens is detected between gravid Mal+ NCI-sourced and ABX-FMT^{JAX} mice by AUC analysis (Student's *t* test, $P < 0.001$).
e. AUC was calculated for the hematocrit curve of each individual mouse. A statistically significant difference in hematocrit is observed between Mal+ and Mal- NCI-sourced dams ($P = 0.0087$; Kruskal-Wallis with Dunn's post-test for multiple comparisons).
f. AUC was calculated for the weight change curve of each individual mouse. No statistically significant differences in weight change are observed between dams ($P > 0.05$; Kruskal-Wallis with Dunn's post-test for multiple comparisons).

Gravid Mal+ NCI-sourced $n = 14$; Gravid Mal- NCI-sourced $n = 11$; Gravid Mal+ ABX-FMT^{JAX} $n = 8$; Gravid Mal- ABX-FMT^{JAX} $n = 5$; *** $P \leq 0.001$; ** $P \leq 0.01$; ns $P > 0.05$.

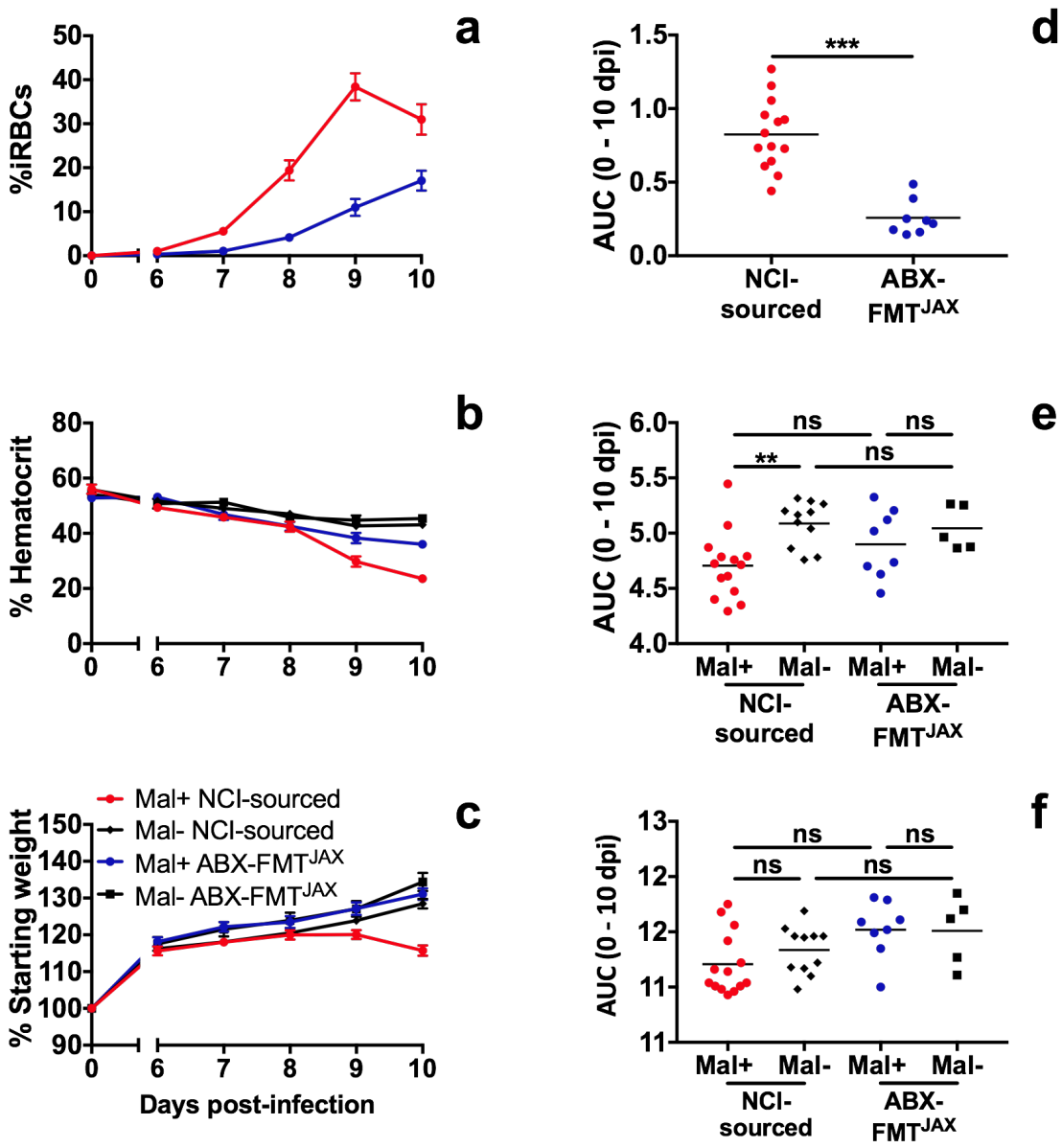
a
%iRBCs
50
40
30
20
10
0
0
6
7
8
9
10
b
% Hematocrit
80
60
40
20
0
c
% Starting weight
150
140
130
120
110
100
90
Mal+ NCI-sourced
Mal- NCI-sourced
Mal+ ABX-FMTJAX
Mal- ABX-FMTJAX
Days post-infection
d
AUC (0 - 10 dpi)
1.5
1.0
0.5
0.0
***
NCI-sourced
ABX-FMTJAX
e
AUC (0 - 10 dpi)
6.0
5.5
5.0
4.5
4.0
ns
ns
**
ns
Mal+
Mal-
Mal+
Mal-
NCI-sourced
ABX-FMTJAX
f
AUC (0 - 10 dpi)
13
12
12
11
11
ns
ns
ns
ns
Mal+
Mal-
Mal+
Mal-
NCI-sourced
ABX-FMTJAX

Figure 4.2. Parasitemia, hematocrit, and weight change in virgin *P. chabaudi chabaudi* AS-infected NCI-sourced and ABX-FMT^{JAX} Swiss Webster mice.

a. Parasitemia in virgin Mal+ mice was estimated by flow cytometry and is presented as the percentage of iRBCs in the peripheral blood.
b. Percent hematocrit was measured throughout infection in virgin Mal+ NCI-sourced and ABX-FMT^{JAX} mice.
c. Weight change in virgin Mal+ NCI-sourced and ABX-FMT^{JAX} mice.
d. AUC was calculated for the parasitemia curve of each individual mouse. A statistically significant difference in parasite burdens is detected between virgin Mal+ NCI-sourced and ABX-FMT^{JAX} mice ($P = 0.0103$; Mann-Whitney test).
e. AUC was calculated for the hematocrit curve of each individual mouse. A statistically significant difference in hematocrit is observed between virgin Mal+ NCI-sourced and ABX-FMT^{JAX} mice ($P > 0.05$; Kruskal-Wallis test).
f. AUC was calculated for the weight change curve of each individual mouse. No statistically significant differences in weight change are observed between virgin Mal+ NCI-sourced and ABX-FMT^{JAX} mice ($P = 0.0094$; Kruskal-Wallis test).

Virgin Mal+ NCI-sourced $n = 14$; Virgin Mal+ ABX-FMT^{JAX} $n = 5$; ** $P \leq 0.01$; * $P \leq 0.05$; ns $P > 0.05$.

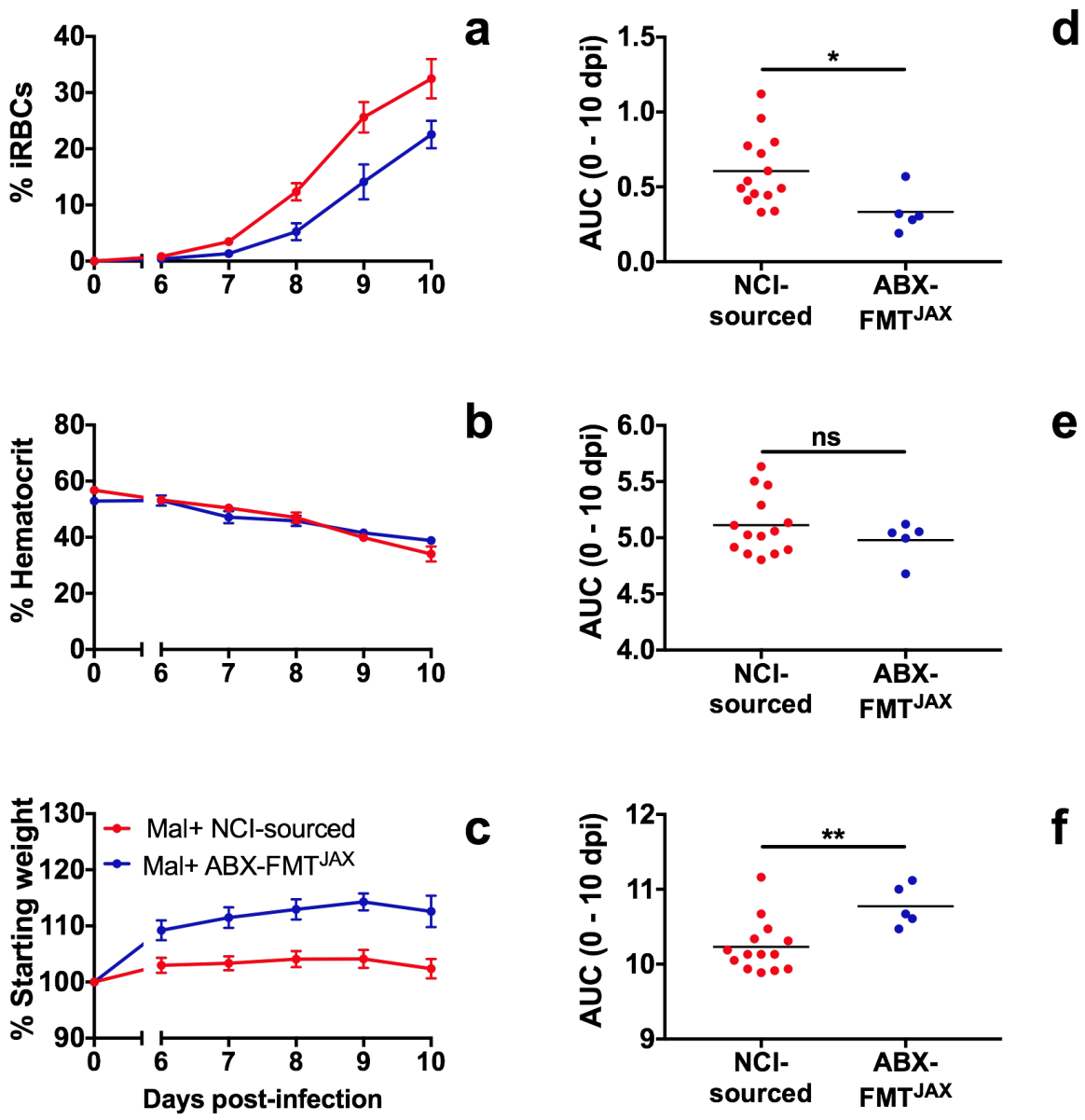
a
% iRBCs
40
30
20
10
0
0
6
7
8
9
10
b
% Hematocrit
80
60
40
20
0
c
% Starting weight
130
120
110
100
90
Mal+ NCI-sourced
Mal+ ABX-FMTJAX
Days post-infection
d
AUC (0 - 10 dpi)
1.5
1.0
0.5
0.0
*
NCI-sourced
ABX-FMTJAX
e
6.0
5.5
5.0
4.5
4.0
ns
f
12
11
10
9
**

Figure 4.3. Embryo number and uterus weights in NCI-sourced and ABX-FMT^{JAX} dams at GD/ED 10.

a. Neither infection status nor maternal treatment group significantly changes the number of total embryos nor the number of viable embryos produced by dams in a cohort ($P > 0.05$; Kruskal-Wallis test with Dunn's post-test for multiple comparisons).
b. Infection is associated with a reduction in uterus weight in NCI-sourced dams ($P = 0.0078$; Kruskal-Wallis test with Dunn's post-test for multiple comparisons).

Gravid Mal+ NCI-sourced $n = 14$; Gravid Mal- NCI-sourced $n = 10$; Gravid Mal+ ABX-FMT^{JAX} $n = 8$; Gravid Mal- ABX-FMT^{JAX} $n = 5$; ** $P \leq 0.01$; ns $P > 0.05$.

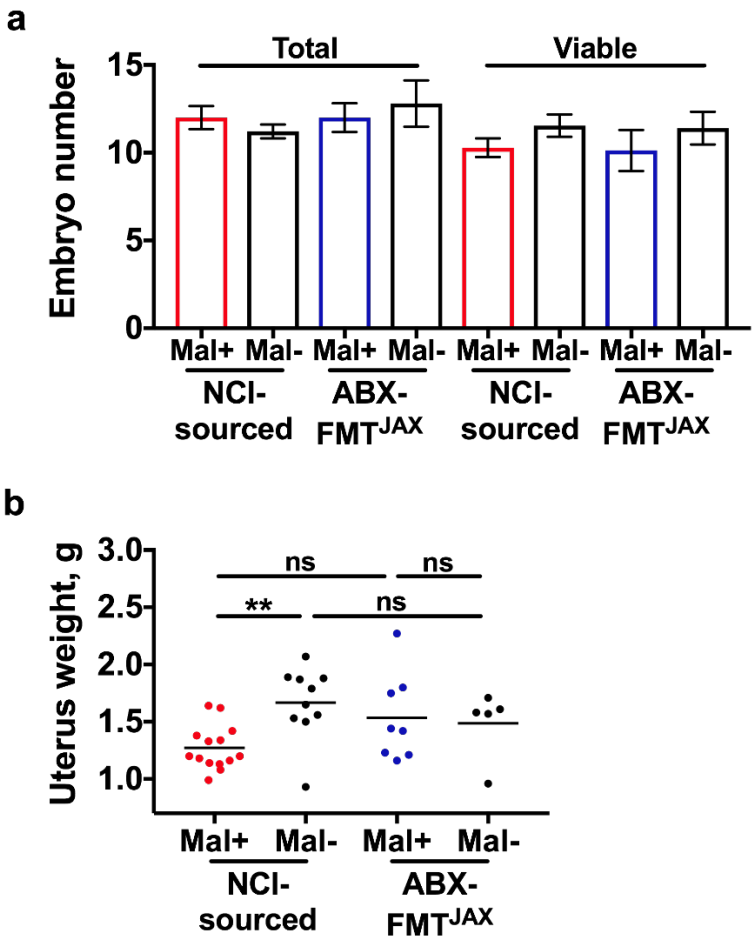
a
Total
Viable
Embryo number
15
10
5
0
Mal+
Mal-
Mal+
Mal-
Mal+
Mal-
Mal+
Mal-
NCI-sourced
ABX-FMTJAX
NCI-sourced
ABX-FMTJAX
b
Uterus weight, g
3.0
2.5
2.0
1.5
1.0
ns
ns
**
ns
Mal+
Mal-
Mal+
Mal-
NCI-sourced
ABX-FMTJAX

Figure 4.4. Peripheral and placental parasite burdens in *P. chabaudi chabaudi* AS-infected NCI-sourced and ABX-FMT^{JAX} dams at GD/ED 10.

a. Paired peripheral and placental parasite burdens in Mal+ NCI-sourced dams. No significant difference between peripheral and placental parasitemia is observed ($P = 0.2402$; Wilcoxon matched-pairs signed rank test).
b. Paired peripheral and placental parasite burdens in Mal+ ABX-FMT^{JAX} dams. Placental parasite burdens tend to be higher than peripheral parasite burdens ($P = 0.0547$; Wilcoxon matched-pairs signed rank test).
c. Placental parasite burdens in Mal+ NCI-sourced and ABX-FMT^{JAX} dams. Placental parasite burdens are significantly higher in Mal+ NCI-sourced dams ($P = 0.0018$; Mann-Whitney test).

Gravid Mal+ NCI-sourced $n = 11$; Gravid Mal+ ABX-FMT^{JAX} $n = 8$; ** $P \leq 0.01$.

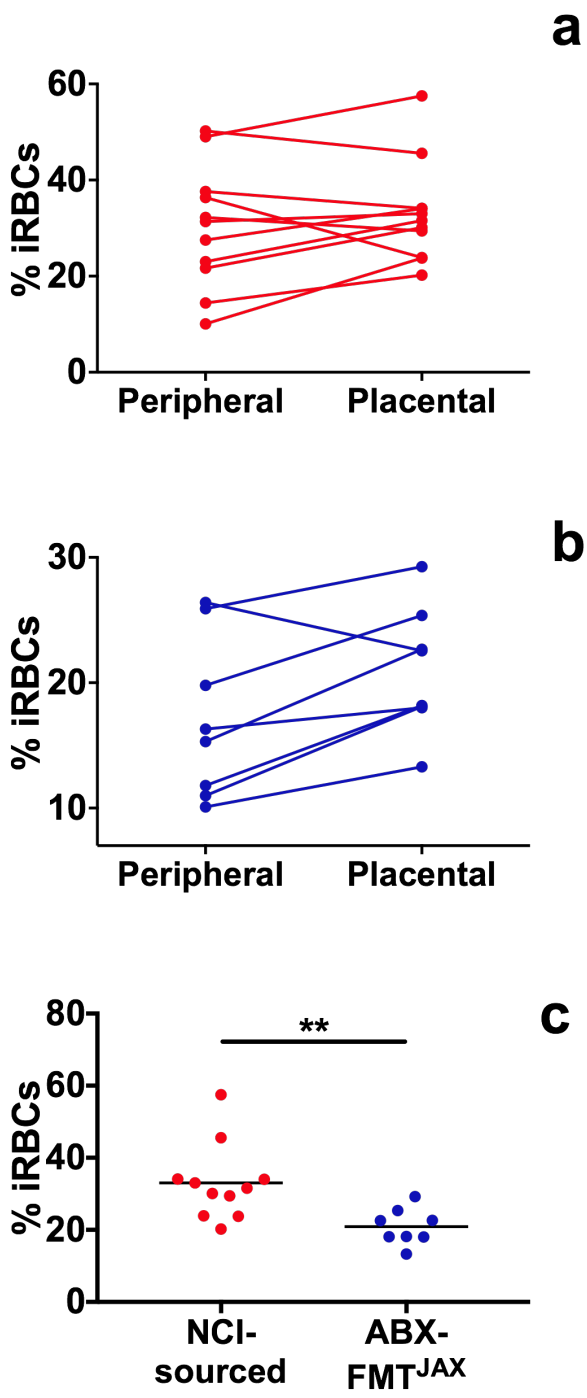
a
60
40
20
0
% iRBCs
Peripheral
Placental
b
30
20
10
% iRBCs
Peripheral
Placental
c
80
60
40
20
0
% iRBCs
**
NCI-
sourced
ABX-
FMTJAX

Figure 4.5. Plasma cytokine titers in virgin and gravid *P. chabaudi chabaudi* AS-infected NCI-sourced and ABX-FMT^{JAX} mice.

No significant differences in cytokine titers were observed as a function of pregnancy status or treatment group ($P > 0.05$; Kruskal-Wallis test with Dunn's post-test for multiple comparisons).

a. IFN-γ in peripheral plasma.
b. IL-1β in peripheral plasma.
c. IL-10 in peripheral plasma.
d. TNF in peripheral plasma.
e. IL-6 in peripheral plasma.
f. IL-17A in peripheral plasma.

Virgin Mal+ ABX-FMT^{JAX} $n = 4$; Gravid Mal+ ABX-FMT^{JAX} $n = 6$; Virgin Mal+ NCI-sourced $n = 5$; Gravid Mal+ NCI-sourced $n = 5$; ns $P > 0.05$.

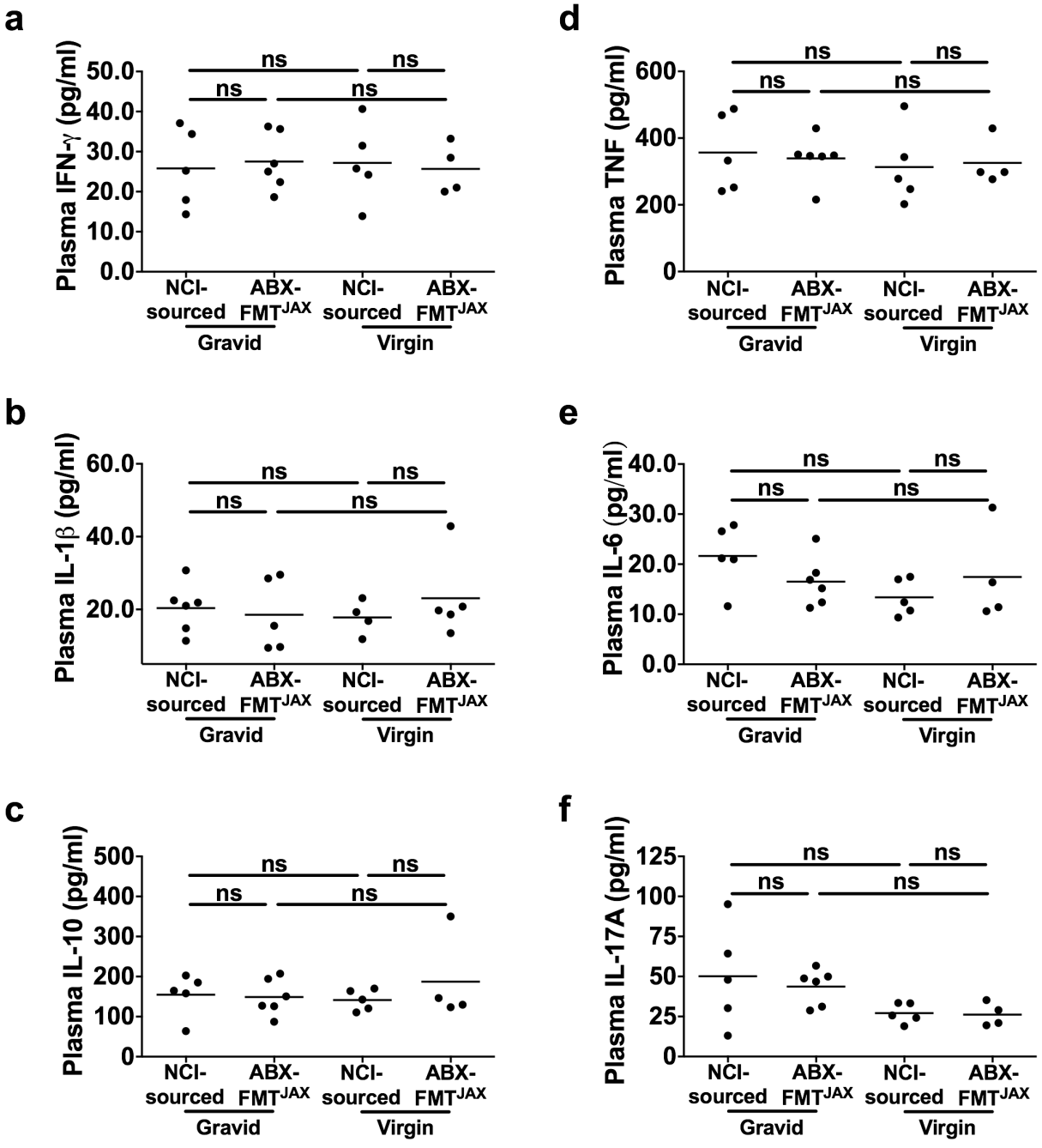
a
Plasma IFN-γ (pg/ml)
50.0
40.0
30.0
20.0
10.0
0.0
ns
ns
ns
ns
NCI-sourced
ABX-FMTJAX
NCI-sourced
ABX-FMTJAX
Gravid
Virgin
b
Plasma IL-1β (pg/ml)
60.0
40.0
20.0
ns
ns
ns
ns
NCI-sourced
ABX-FMTJAX
NCI-sourced
ABX-FMTJAX
Gravid
Virgin
c
Plasma IL-10 (pg/ml)
500
400
300
200
100
0
ns
ns
ns
ns
NCI-sourced
ABX-FMTJAX
NCI-sourced
ABX-FMTJAX
Gravid
Virgin
d
Plasma TNF (pg/ml)
600
400
200
0
ns
ns
ns
ns
NCI-sourced
ABX-FMTJAX
NCI-sourced
ABX-FMTJAX
Gravid
Virgin
e
Plasma IL-6 (pg/ml)
40.0
30.0
20.0
10.0
0.0
ns
ns
ns
ns
NCI-sourced
ABX-FMTJAX
NCI-sourced
ABX-FMTJAX
Gravid
Virgin
f
Plasma IL-17A (pg/ml)
125
100
75
50
25
0
ns
ns
ns
ns
NCI-sourced
ABX-FMTJAX
NCI-sourced
ABX-FMTJAX
Gravid
Virgin

Figure 4.6. Malaria-induced expression of cytokine, chemokine, antioxidant, and hypoxia response genes in *P. chabaudi chabaudi* AS-exposed conceptuses.
a. Transcript levels of mouse *Ifng*, *Tnf*, *Il1b*, *Il10*, and *Ccl2* were quantified by qPCR.
b. Transcript levels of mouse *Hif1a*, *Sod1*, *Sod2*, *Sod3*, *Nrf2*, and *Ho* were quantified by qPCR. Gravid Mal- NCI-sourced $n = 7$; Gravid Mal+ NCI-sourced $n = 9$; Gravid Mal- ABX-FMT^{JAX} $n = 5$; Gravid Mal+ ABX-FMT^{JAX} $n = 8$.

a

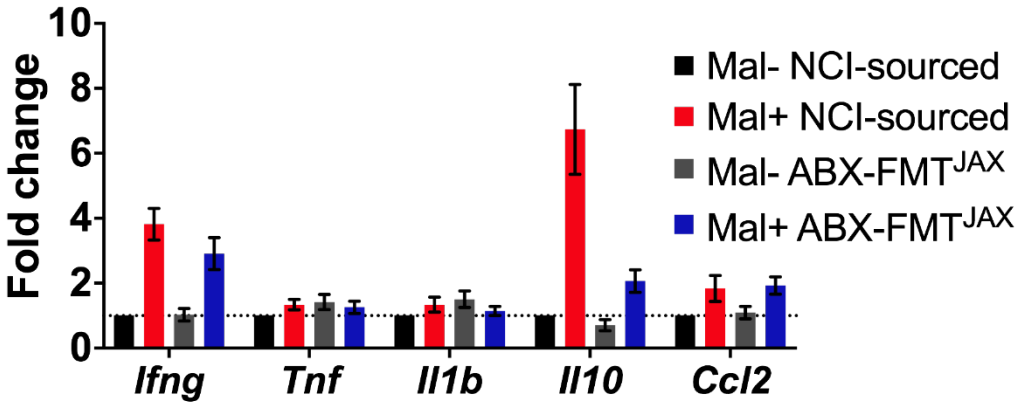
Fold change
10
8
6
4
2
0
Mal- NCI-sourced
Mal+ NCI-sourced
Mal- ABX-FMTJAX
Mal+ ABX-FMTJAX
Ifng
Tnf
Il1b
Il10
Ccl2

b

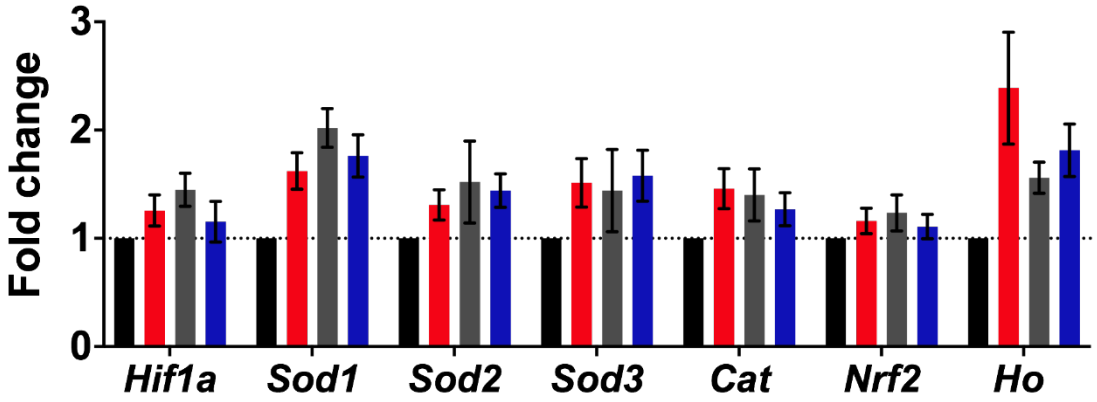
Fold change
3
2
1
0
Hif1a
Sod1
Sod2
Sod3
Cat
Nrf2
Ho

CHAPTER 5

CONCLUSIONS

The toll of *Plasmodium falciparum* infection on pregnant women and their families is profound. Malaria infection in pregnant women causes severe maternal illness and negatively impacts the health of the fetus, resulting in an increased risk of neonatal death [3-12]. In early life, children exposed to gestational malaria are at greater risk of malaria infection [13, 14, 16] and are more likely to develop hyperparasitemia during malaria infection [15]. Furthermore, children exposed to malaria *in utero* may be more likely to display neurodevelopmental defects and develop mental illness [17, 18]. Although *P. falciparum* infection in pregnancy may have a lifelong impact on malaria-exposed children, intermittent preventative treatment in pregnancy (IPTp) with antimalarial drugs does not reach the majority of the pregnant women who should be protected by treatment [1]. In 2016, only 19% of eligible pregnant women received the recommended number of IPTp doses [1]. Furthermore, resistance to sulfadoxine-pyrimethamine, the drug combination historically used for IPTp, is widespread [163]. Artemisinin-based combination therapies were recently determined to be safe for use in pregnant women [164], but artemisinin resistance is also increasing [165]. Therefore, it is extremely important to develop adjunctive therapies to treat malaria in pregnant women.

The development of adjunctive therapies for gestational malaria has been stymied by our incomplete understanding of the pathogenesis of gestational malaria and the mechanisms by which it results in placental dysfunction and poor birth outcomes. Mouse models are important for studying the pathogenesis of malaria infection in pregnancy. My research focuses on the

development and characterization of a novel mouse model for maternal malaria infection in which infection severity can be modulated by the manipulation of the gut microbiota.

In the second chapter of this dissertation, I describe a novel model for transgestational malaria infection utilizing outbred Swiss Webster mice purchased from the National Cancer Institute (NCI) Mouse Repository. Swiss Webster mice infected on gestational day (GD) 0 with *Plasmodium chabaudi chabaudi* AS carry their pregnancies to term and produce live progeny. On average, *P. chabaudi chabaudi* AS-infected Swiss Webster mice do not produce fewer total or viable embryos than uninfected controls, although infection is associated with a significant reduction in fetal weight at term. When dams are allowed to spontaneously deliver, a significant reduction in pup number is observed in the litters of infected dams compared to uninfected controls at weaning. The vast majority of pup loss between GD 18 and weaning occurs within the first 4 days of life. This suggests that maternal infection reduces postnatal viability during the early neonatal period. However, no relationship is detected between maternal infection status and pup weight gain prior to weaning.

The Swiss Webster-*P. chabaudi chabaudi* AS model for malaria infection in pregnancy recapitulates a common outcome observed in women infected with *P. falciparum*. Like human women residing in malaria-endemic regions [4-6, 8], Swiss Webster mice infected with malaria throughout gestation deliver low birthweight progeny that experience an increased risk of neonatal death, although progeny that survive early life develop normally. This model is novel because previously described mouse models entailing the infection of pregnant mice in early gestation uniformly result in pregnancy loss [59, 101, 109-111]. Therefore, we believe that this novel model for transgestational malaria infection is a valuable companion to the mouse models of malaria infection in pregnancy that are currently in use because it models pregnancy

maintenance during maternal malaria infection, as well as malaria-associated neonatal mortality indirectly attributable to low birth weight.

Furthermore, we believe that outbred mice are an experimentally valuable tool because they allow for the exploration of infection in a genetically diverse model population, better reflecting the genetic diversity of humans. We hypothesize that antimalarial responses in outbred Swiss Webster mice are more characteristic of *Mus musculus* as a species than the responses observed in inbred strains. Ultimately, the use of outbred mice may allow for the identification of antimalarial mechanisms relevant in humans because the mechanisms observed are less likely to be artifacts attributable to the innate genetic characteristics of an inbred mouse strain.

The development of this novel model allows for the exploration of two new avenues of research. First, the Swiss Webster-*P. chabaudi chabaudi* AS model enables the exploration of mechanisms that contribute to the antimalarial response while permitting the pregnancy to proceed to term. I am particularly interested in potential future studies comparing gravid *P. chabaudi chabaudi* AS-infected Swiss Webster and C57BL/6 (B6) mice at peak infection (GD 10), when B6 mice abort their pregnancies [57, 101, 109-111]. As the molecular and cellular mechanisms underlying midgestational abortion in infected B6 mice are not fully understood, I anticipate that a comparative approach will allow for the identification of factors driving pregnancy loss in B6 mice, or conversely, pregnancy maintenance in Swiss Webster mice.

In addition to comparative studies, this model may allow for the validation of mechanisms associated with abortion in malaria-infected mice of other strains. The Swiss Webster-*P. chabaudi chabaudi* AS mouse model provides a system in which variables can be altered with the experimental goal of inducing abortion. These studies are an important companion to studies aiming to prolong pregnancy in infected mice by targeting pathogenic host

mechanisms. For example, a simple experiment could be performed to determine if elevated TNF is sufficient to induce pregnancy loss in Swiss Webster dams at peak infection. TNF has previously been identified as a contributor to malaria-associated pregnancy loss in two other mouse models. A small dose of exogenous TNF induces fetal demise in *Plasmodium vinckei*-infected CBA/H mice one day prior to spontaneous fetal loss due to infection [102]. Conversely, the ablation of endogenous TNF in *P. chabaudi chabaudi* AS-infected pregnant B6 mice improves midgestational pregnancy outcomes [101]. If pregnant Swiss Webster mice treated with exogenous TNF at peak infection abort their pregnancies, it could indicate that elevated TNF is sufficient to induce pregnancy loss in malaria-infected Swiss Webster mice and may be sufficient in induce pregnancy loss in malaria-infected women as well. Essentially, this model allows for the experimental induction of abortion in animals that would otherwise remain pregnant, revealing mechanisms that could contribute to pregnancy loss due to gestational malaria.

The second area of research enabled by the development of the Swiss Webster-*P. chabaudi chabaudi* AS mouse model is the study of postnatal outcomes in animals with prolonged *in utero* exposure to maternal malaria infection. The Swiss Webster-*P. chabaudi chabaudi* AS mouse model reliably produces pups that have been exposed to malaria infection for the duration of gestation. These mice can be used to explore the impact of malaria exposure *in utero* on various immunological and developmental parameters. The susceptibility of these progeny to malaria infection could be explored to determine whether maternal infection during pregnancy is associated with exacerbated disease, as observed in human children [13, 14, 16], or relative resistance, as observed in inbred mice [116]. The immunological characteristics of malaria-exposed and unexposed progeny could subsequently be compared. Furthermore,

neurological development could be tracked in the progeny of malaria-infected dams to determine if exposure to *P. chabaudi chabaudi* AS throughout gestation has neurodevelopmental sequelae [18]. The existing studies exploring these questions in mice exposed to malaria infection *in utero* utilize models where the exposure to maternal infection is restricted to the final third of gestation [18, 116]. This model enables the exploration of the impact of prolonged exposure, better modeling the exposure of *P. falciparum*-exposed infants. In addition, this model allows for the exploration of malaria exposure prior to the final week of gestation. We speculate that the duration and timing of infection will significantly influence the developmental impact of maternal malaria infection.

Infection severity in the Swiss Webster-*P. chabaudi chabaudi* AS mouse model for transgestational malaria can be modulated by manipulating the gut microbiota, as described in the third chapter of this dissertation. Surprisingly, we found that the composition of the gut microbiota exerts a more significant influence on susceptibility to malaria infection than the genetic variability within the Swiss Webster mouse population. Following the disruption of the native gut microbiota by antibiotic treatment (ABX), the administration of a fecal microbiota transplant (FMT) consisting of feces collected from NCI-sourced mice (FMT^{NCI}) or the administration of an FMT consisting of feces collected from Jackson Laboratory-sourced mice (FMT^{JAX}) results in recipient mice with distinct microbial communities. We find that ABX-FMT^{JAX} mice develop lower parasite burdens, reduced clinical illness, and exhibit improved fetal and postnatal outcomes compared to ABX-FMT^{NCI} mice. As expected, ABX-FMT^{NCI} mice, which are treated with an autologous FMT, exhibit parasite burdens and pregnancy outcomes consistent with those observed in unmanipulated NCI-sourced Swiss Webster mice, described in Ch. 2.

The mechanisms by which the gut bacteria modulate susceptibility to malaria infection are unknown. In inbred mice, gut microbiota-dependent differences in susceptibility to malaria infection are attributed to differences in the adaptive immune response [125]. Significant differences in the cellular and humoral immune responses are observed as early as 10 and 14 days post-infection (dpi), respectively [125]. However, we observe differences in parasite burden between resistant ABX-FMT^{JAX} and susceptible ABX-FMT^{NCI} mice as early as 7 dpi. We speculate that differences in the innate immune response contribute to this early divergence in parasite burden. Specifically, we hypothesize that gut resident microbes present in resistant ABX-FMT^{JAX} animals enhance the innate immune response in early infection. We are particularly interested in the impact of the gut microbiota on the function of monocytes, the innate immune cells responsible for clearing malaria parasites in early infection [166, 167]. In addition to their critical role in the early control of blood-stage malaria, monocytes can develop an activated phenotype following exposure to either systemic or enteric pathogens that is maintained by epigenetic regulation [168-170]. To test this hypothesis, we could harvest monocytes from the peripheral blood, bone marrow, and lymph nodes of ABX-FMT^{NCI} and ABX-FMT^{JAX} mice prior to and throughout malaria infection. Immunophenotyping assays could be performed by flow cytometry to compare population characteristics and monocyte activation status between resistant and susceptible mice. Epigenetic analysis could be performed to determine if monocytes isolated from mice possessing resistance- or susceptibility-associated gut microbes display the epigenetic signature associated with monocyte activation [170].

Alternatively, the elevated abundance of specific bacterial metabolites, not the bacteria themselves, may alter the immune response to infection or promote enhanced parasite growth. The metabolite pool within the cecum differs significantly between inbred mice displaying gut

microbiota-dependent susceptibility or resistance to *Plasmodium yoelii* infection [126], and it is likely that the microbial metabolites within the plasma differ as well. To explore the potential contribution of bacterial metabolites in this system, we could evaluate the metabolite pools in the cecal lumen and peripheral plasma of susceptible and resistant mice prior to infection. Following the identification of metabolites present at significantly different levels in susceptible and resistant mice, metabolites of interest could initially be selected based on previously published research (reviewed in ref. [127]). Immunological studies could be performed in resistant and susceptible mice to determine if the presence or abundance of specific plasma metabolites is correlated with specific immunological phenotypes. Alternatively, the ability of specific plasma metabolites to promote blood-stage *P. chabaudi chabaudi* AS replication could be confirmed using *in vitro* parasite growth assays.

We believe that gut microbiota-mediated modulation of infection severity expands the Swiss Webster-*P. chabaudi chabaudi* AS model for transgestational malaria infection. By modulating infection severity, we can explore severe and moderate maternal malaria infection using the same mouse-parasite combination. To demonstrate the utility of this technique, I explore the immunological and placental environment in *P. chabaudi chabaudi* AS-infected pregnant mice possessing resistance- or susceptibility- associated gut microbes in Ch. 4. Due to the similar parasite burdens observed in NCI-sourced and ABX-FMT^{NCI} Swiss Webster mice, unmanipulated NCI-sourced animals were used as the malaria susceptible cohort for these experiments.

To assess the impact of maternal infection severity on embryos at peak infection, mice were sacrificed at GD/ED 10. The average number of total and viable embryos produced by NCI-sourced and ABX-FMT^{JAX} dams was not reduced by infection, indicating that neither high

nor moderate intensity infection was associated with embryo demise at GD/ED 10. However, the uteri of infected susceptible NCI-sourced dams weighed significantly less at GD/ED 10 than uteri collected from uninfected controls. No significant reduction in uterine weight was observed as a function of infection in resistant ABX-FMT^{JAX} dams, suggesting that greater maternal parasite burdens impair embryo growth. Significant parasite sequestration in the maternal blood spaces of the placenta was not observed in either cohort of dams. Surprisingly, differences in peripheral cytokine titers were not detected between infected susceptible and infected resistant mice at GD/ED 10. However, most susceptible NCI-sourced mice achieved peak infection on GD/ED 9, so it is possible that the inflammatory response in these mice had receded by GD/ED 10. This pattern would be consistent with the patterns in peripheral cytokine titers observed in *P. chabaudi chabaudi* AS-infected B6 mice around the time of peak infection [111].

The expression of genes associated with inflammation, hypoxia, and oxidative stress were explored in conceptuses collected from susceptible NCI-sourced dams and resistant ABX-FMT^{JAX} dams. As expected, the transcription of genes associated with the proinflammatory response to infection, including *Ifng* and *Ccl2*, were upregulated in conceptuses collected from both infected susceptible NCI-sourced and infected resistant ABX-FMT^{JAX} dams. Notable differences in gene expression between infected cohorts of dams were only observed for *Ho*, the gene encoding heme oxygenase, and *Il10*, the gene encoding the anti-inflammatory cytokine IL-10. The expression of both of these genes was greater in infected susceptible NCI-sourced dams. The upregulation of *Ho*, which degrades heme, may reflect the higher parasite burdens observed in NCI-sourced dams. The greater parasite burdens observed in these mice is likely correlated with larger quantities of free plasma heme as a result of the extensive destruction of infected erythrocytes. *Ho* may protect conceptuses produced by infected dams from oxidative damage

caused by free heme in the uterine blood supply. Similarly, the elevated transcription of *Il10* in infected susceptible NCI-sourced mice compared to infected resistant ABX-FMT^{JAX} mice may indicate a greater compensatory response to inflammation. I speculate that *Il10* transcription in infected NCI-sourced mice reflects a more significant inflammatory response in these conceptuses compared to ABX-FMT^{JAX} conceptuses. I hypothesize that this inflammatory response is diminished at the time of sacrifice (GD 10), although *Il10* remains elevated. Similarly, differences in oxidative stress and hypoxia responses between resistant and susceptible mice may be pronounced earlier in infection. A serial sacrifice study would be required to explore the transcriptional response within conceptuses prior to GD 10.

Regardless of the mechanism explored, future studies are likely to include multiple sampling timepoints. Only minor differences between infected NCI-sourced and ABX-FMT^{JAX} dams were detected at GD 10, but this timepoint may fail to capture differences evident earlier or later in infection. Therefore, future studies may be designed to incorporate serial sacrifices or serial bleeds, so that infection responses can be tracked over the several days spanning peak infection.

The contribution of a wide range of mechanisms to the pathogenesis of gestational malaria could be explored using this model. As hypercoagulation within the placenta is associated with both human and murine gestational malaria [56, 84], the exploration of coagulation in the placentae of infected susceptible NCI-sourced and infected resistant ABX-FMT^{JAX} mice is a logical next step. The expression of coagulation-related genes could be measured in conceptuses around the time of peak infection [56]. Alternatively, western blotting could be performed to measure the expression of proteins associated with coagulation, or histological staining could be performed assess the expression and localization of coagulation-

related proteins. I hypothesize that markers of coagulation would be elevated in both infected cohorts of mice, but that high density infection in susceptible NCI-sourced Swiss Webster mice would be associated with the development of a more robust procoagulant environment.

Mechanisms of pregnancy compromise identified in *P. falciparum*-infected human women could also be explored in mice with high and moderate intensity parasite burdens. In human women, the disruption of uteroplacental blood flow [92], placental amino acid transport [93, 94], and placental autophagy [95] have been associated with low birth weight. Uteroplacental blood flow in both cohorts of infected mice, as well as uninfected controls, could be evaluated by ultrasound [171]. In addition, placental autophagy could be studied via the microscopic identification and quantification of autophagosomes and lysosomes or via the quantification of autophagy-related proteins by western blotting [95]. Finally, placental amino acid transport could be determined by measuring System A and System β amino acid transporter activity in murine placental vesicles [172]. I hypothesize that the disruption of placental blood flow, placental autophagy, and placental amino acid transport would be would be more pronounced in infected susceptible NCI-sourced dams than in infected resistant ABX-FMT^{JAX} dams or uninfected dams, consistent with the reduction in uterine weight observed in susceptible animals as a function of infection. Although these mechanisms have already been identified as significant in human gestational malaria, the use of a mouse model allows for the study of these mechanisms throughout gestation in a tractable system that enables invasive sampling of placental and fetal tissues. In contrast, the studies describing abnormal autophagy and amino acid transport in malaria-infected human placentae rely heavily on human placentae collected following delivery at gestational term [93-95]. Furthermore, if these mechanisms contribute to

poor birth outcomes in *P. chabaudi chabaudi* AS-infected Swiss Webster mice, their potential as therapeutic targets could initially be explored using this model.

Gestational malaria remains a devasting public health challenge, despite ongoing efforts to prevent and treat infections in pregnant women. The development and use of mouse models for gestational malaria are vital for enhancing our understanding of malaria infection in a pregnant host. In the first chapter of this dissertation, I introduce gestational malaria, the mechanisms driving pregnancy compromise in gestational malaria, and discuss mouse models for gestational malaria. In the second chapter of this dissertation, I describe the development of a novel mouse model for transgestational malaria infection. In the third chapter of this dissertation, I demonstrate that infection severity and pregnancy outcomes in this novel model can be modulated by manipulating the composition of the gut microbiota. In the fourth chapter of this dissertation, I demonstrate that gut microbiota-mediated tuning of infection severity can be used to explore the immunological and placental environment in the context of variable maternal infection burdens. I anticipate that the Swiss Webster-*P. chabaudi chabaudi* AS model for transgestational malaria infection, and the ability to modulate susceptibility to infection in this model by altering the gut microbiota, will be valuable tools for the study of malaria infection in pregnancy and the impact of maternal infection on children exposed to malaria *in utero*.

1. WHO, *World Malaria Report 2017*. 2017, World Health Organization: Geneva.

2. Barragan, A., et al., *Age-related buildup of humoral immunity against epitopes for rosette formation and agglutination in African areas of malaria endemicity.* Infect Immun, 1998. **66**(10): p. 4783-7.

3. van Geertruyden, J.P., et al., *The contribution of malaria in pregnancy to perinatal mortality.* Am J Trop Med Hyg, 2004. **71**(2 Suppl): p. 35-40.

4. Steketee, R.W., et al., *The effect of malaria and malaria prevention in pregnancy on offspring birthweight, prematurity, and intrauterine growth retardation in rural Malawi.* Am J Trop Med Hyg, 1996. **55**(1 Suppl): p. 33-41.

5. Steketee, R.W., et al., *The burden of malaria in pregnancy in malaria-endemic areas.* Am J Trop Med Hyg, 2001. **64**(1-2 Suppl): p. 28-35.

6. Luxemburger, C., et al., *Effects of malaria during pregnancy on infant mortality in an area of low malaria transmission.* Am J Epidemiol, 2001. **154**(5): p. 459-65.

7. Cot, M., et al., *Increase of birth weight following chloroquine chemoprophylaxis during the first pregnancy: results of a randomized trial in Cameroon.* Am J Trop Med Hyg, 1995. **53**(6): p. 581-5.

8. Guyatt, H.L. and R.W. Snow, *Malaria in pregnancy as an indirect cause of infant mortality in sub-Saharan Africa.* Trans R Soc Trop Med Hyg, 2001. **95**(6): p. 569-76.

9. Dellicour, S., et al., *Quantifying the number of pregnancies at risk of malaria in 2007: a demographic study.* PLoS Med, 2010. **7**(1): p. e1000221.

10. Murphy, S.C. and J.G. Breman, *Gaps in the childhood malaria burden in Africa: cerebral malaria, neurological sequelae, anemia, respiratory distress, hypoglycemia, and complications of pregnancy.* Am J Trop Med Hyg, 2001. **64**(1-2 Suppl): p. 57-67.

11. Walker, P.G., et al., *Estimated risk of placental infection and low birthweight attributable to Plasmodium falciparum malaria in Africa in 2010: a modelling study.* Lancet Glob Health, 2014. **2**(8): p. e460-7.

12. Rogerson, S.J., et al., *Burden, pathology, and costs of malaria in pregnancy: new developments for an old problem.* Lancet Infect Dis, 2018. **18**(4): p. e107-e118.

13. Boudova, S., et al., *Placental but Not Peripheral Plasmodium falciparum Infection During Pregnancy Is Associated With Increased Risk of Malaria in Infancy.* J Infect Dis, 2017. **216**(6): p. 732-735.

14. Le Port, A., et al., *Infections in infants during the first 12 months of life: role of placental malaria and environmental factors.* PLoS One, 2011. **6**(11): p. e27516.

15. Sylvester, B., et al., *Hyperparasitaemia during clinical malaria episodes in infants aged 0-24 months and its association with in utero exposure to Plasmodium falciparum.* BMC Res Notes, 2018. **11**(1): p. 232.

16. Tassi Yunga, S., et al., *Increased Susceptibility to Plasmodium falciparum in Infants is associated with Low, not High, Placental Malaria Parasitemia.* Sci Rep, 2018. **8**(1): p. 169.

17. McDonald, C.R., R.E. Elphinstone, and K.C. Kain, *The impact of placental malaria on neurodevelopment of exposed infants: a role for the complement system?* Trends Parasitol, 2013. **29**(5): p. 213-9.

18. McDonald, C.R., et al., *Experimental Malaria in Pregnancy Induces Neurocognitive Injury in Uninfected Offspring via a C5a-C5a Receptor Dependent Pathway.* PLoS Pathog, 2015. **11**(9): p. e1005140.

19. Jin, Y., C. Kebaier, and J. Vanderberg, *Direct microscopic quantification of dynamics of Plasmodium berghei sporozoite transmission from mosquitoes to mice.* Infect Immun, 2007. **75**(11): p. 5532-9.

20. Kitchen, S.F., *Malariology; a comprehensive survey of all aspects of this group of diseases from a global standpoint*. Vol. 2. 1949, Philadelphia,: Saunders.

21. Blanford, J.I., et al., *Implications of temperature variation for malaria parasite development across Africa.* Sci Rep, 2013. **3**: p. 1300.

22. Smith, J.D., et al., *Switches in expression of Plasmodium falciparum var genes correlate with changes in antigenic and cytoadherent phenotypes of infected erythrocytes.* Cell, 1995. **82**(1): p. 101-10.

23. Baruch, D.I., et al., *Cloning the P. falciparum gene encoding PfEMP1, a malarial variant antigen and adherence receptor on the surface of parasitized human erythrocytes.* Cell, 1995. **82**(1): p. 77-87.

24. Barry, A.E., et al., *Population genomics of the immune evasion (var) genes of Plasmodium falciparum.* PLoS Pathog, 2007. **3**(3): p. e34.

25. Chookajorn, T., et al., *Epigenetic memory at malaria virulence genes.* Proc Natl Acad Sci U S A, 2007. **104**(3): p. 899-902.

26. Chen, Q., et al., *Developmental selection of var gene expression in Plasmodium falciparum.* Nature, 1998. **394**(6691): p. 392-5.

27. Ukaegbu, U.E., et al., *A Unique Virulence Gene Occupies a Principal Position in Immune Evasion by the Malaria Parasite Plasmodium falciparum.* PLoS Genet, 2015. **11**(5): p. e1005234.

28. Giha, H.A., et al., *Antibodies to variable Plasmodium falciparum-infected erythrocyte surface antigens are associated with protection from novel malaria infections.* Immunol Lett, 2000. **71**(2): p. 117-26.

29. Moll, K., et al., *Generation of cross-protective antibodies against Plasmodium falciparum sequestration by immunization with an erythrocyte membrane protein 1-duffy binding-like 1 alpha domain.* Infect Immun, 2007. **75**(1): p. 211-9.

30. Zhou, J., et al., *Opsonization of malaria-infected erythrocytes activates the inflammasome and enhances inflammatory cytokine secretion by human macrophages.* Malar J, 2012. **11**: p. 343.

31. Fried, M., et al., *Malaria elicits type 1 cytokines in the human placenta: IFN-gamma and TNF-alpha associated with pregnancy outcomes.* J Immunol, 1998. **160**(5): p. 2523-30.

32. Ricke, C.H., et al., *Plasma antibodies from malaria-exposed pregnant women recognize variant surface antigens on Plasmodium falciparum-infected erythrocytes in a parity-dependent manner and block parasite adhesion to chondroitin sulfate A*. J Immunol, 2000. **165**(6): p. 3309-16.

33. Staalsoe, T., et al., *Variant surface antigen-specific IgG and protection against clinical consequences of pregnancy-associated Plasmodium falciparum malaria.* Lancet, 2004. **363**(9405): p. 283-9.

34. David, P.H., et al., *Parasite sequestration in Plasmodium falciparum malaria: spleen and antibody modulation of cytoadherence of infected erythrocytes.* Proc Natl Acad Sci U S A, 1983. **80**(16): p. 5075-9.

35. Crocker, I.P., et al., *Syncytiotrophoblast degradation and the pathophysiology of the malaria-infected placenta.* Placenta, 2004. **25**(4): p. 273-82.

36. Ismail, M.R., et al., *Placental pathology in malaria: a histological, immunohistochemical, and quantitative study.* Hum Pathol, 2000. **31**(1): p. 85-93.

37. Salanti, A., et al., *Selective upregulation of a single distinctly structured var gene in chondroitin sulphate A-adhering Plasmodium falciparum involved in pregnancy-associated malaria.* Mol Microbiol, 2003. **49**(1): p. 179-91.

38. Reeder, J.C., et al., *The adhesion of Plasmodium falciparum-infected erythrocytes to chondroitin sulfate A is mediated by P. falciparum erythrocyte membrane protein 1.* Proc Natl Acad Sci U S A, 1999. **96**(9): p. 5198-202.

39. Muthusamy, A., et al., *Plasmodium falciparum-infected erythrocytes adhere both in the intervillous space and on the villous surface of human placenta by binding to the low-sulfated chondroitin sulfate proteoglycan receptor.* Am J Pathol, 2004. **164**(6): p. 2013-25.

40. Beeson, J.G., et al., *Plasmodium falciparum isolates from infected pregnant women and children are associated with distinct adhesive and antigenic properties.* J Infect Dis, 1999. **180**(2): p. 464-72.

41. Fried, M. and P.E. Duffy, *Adherence of Plasmodium falciparum to chondroitin sulfate A in the human placenta.* Science, 1996. **272**(5267): p. 1502-4.

42. Khattab, A., et al., *Variants of Plasmodium falciparum erythrocyte membrane protein 1 expressed by different placental parasites are closely related and adhere to chondroitin sulfate A.* J Infect Dis, 2001. **183**(7): p. 1165-9.

43. Sartelet, H., et al., *Hyperexpression of ICAM-1 and CD36 in placentas infected with Plasmodium falciparum: a possible role of these molecules in sequestration of infected red blood cells in placentas.* Histopathology, 2000. **36**(1): p. 62-8.

44. Beeson, J.G. and G.V. Brown, *Plasmodium falciparum-infected erythrocytes demonstrate dual specificity for adhesion to hyaluronic acid and chondroitin sulfate A and have distinct adhesive properties.* J Infect Dis, 2004. **189**(2): p. 169-79.

45. Beeson, J.G., et al., *Adhesion of Plasmodium falciparum-infected erythrocytes to hyaluronic acid in placental malaria.* Nat Med, 2000. **6**(1): p. 86-90.

46. Maubert, B., L.J. Guilbert, and P. Deloron, *Cytoadherence of Plasmodium falciparum to intercellular adhesion molecule 1 and chondroitin-4-sulfate expressed by the syncytiotrophoblast in the human placenta.* Infect Immun, 1997. **65**(4): p. 1251-7.

47. Rogerson, S.J., et al., *Chondroitin sulfate A is a cell surface receptor for Plasmodium falciparum-infected erythrocytes.* J Exp Med, 1995. **182**(1): p. 15-20.

48. Maubert, B., et al., *Development of antibodies against chondroitin sulfate A-adherent Plasmodium falciparum in pregnant women.* Infect Immun, 1999. **67**(10): p. 5367-71.

49. Fried, M., et al., *Maternal antibodies block malaria.* Nature, 1998. **395**(6705): p. 851-2.

50. Walter, P.R., Y. Garin, and P. Blot, *Placental pathologic changes in malaria. A histologic and ultrastructural study.* Am J Pathol, 1982. **109**(3): p. 330-42.

51. Bulmer, J.N., et al., *Placental malaria. I. Pathological classification.* Histopathology, 1993. **22**(3): p. 211-8.

52. Muehlenbachs, A., et al., *A novel histological grading scheme for placental malaria applied in areas of high and low malaria transmission.* J Infect Dis, 2010. **202**(10): p. 1608-16.

53. Ordi, J., et al., *Massive chronic intervillositis of the placenta associated with malaria infection.* Am J Surg Pathol, 1998. **22**(8): p. 1006-11.

54. Rogerson, S.J., et al., *Placental monocyte infiltrates in response to Plasmodium falciparum malaria infection and their association with adverse pregnancy outcomes.* Am J Trop Med Hyg, 2003. **68**(1): p. 115-9.

55. Suguitan, A.L., Jr., et al., *Changes in the levels of chemokines and cytokines in the placentas of women with Plasmodium falciparum malaria.* J Infect Dis, 2003. **188**(7): p. 1074-82.

56. Avery, J.W., et al., *Maternal malaria induces a procoagulant and antifibrinolytic state that is embryotoxic but responsive to anticoagulant therapy.* PLoS One, 2012. **7**(2): p. e31090.

57. Sarr, D., et al., *Differential roles of inflammation and apoptosis in initiation of mid-gestational abortion in malaria-infected C57BL/6 and A/J mice.* Placenta, 2015.

58. Bulmer, J.N., et al., *Placental malaria. II. A semi-quantitative investigation of the pathological features.* Histopathology, 1993. **22**(3): p. 219-25.

59. Neres, R., et al., *Pregnancy outcome and placenta pathology in Plasmodium berghei ANKA infected mice reproduce the pathogenesis of severe malaria in pregnant women.* PLoS One, 2008. **3**(2): p. e1608.

60. Fried, M., et al., *Systemic Inflammatory Response to Malaria During Pregnancy Is Associated With Pregnancy Loss and Preterm Delivery.* Clin Infect Dis, 2017. **65**(10): p. 1729-1735.

61. Chaisavaneeyakorn, S., et al., *Immunity to placental malaria. IV. Placental malaria is associated with up-regulation of macrophage migration inhibitory factor in intervillous blood.* J Infect Dis, 2002. **186**(9): p. 1371-5.

62. Abrams, E.T., et al., *Host response to malaria during pregnancy: placental monocyte recruitment is associated with elevated beta chemokine expression.* J Immunol, 2003. **170**(5): p. 2759-64.

63. Chaisavaneeyakorn, S., et al., *Levels of macrophage inflammatory protein 1 alpha (MIP-1 alpha) and MIP-1 beta in intervillous blood plasma samples from women with placental malaria and human immunodeficiency virus infection.* Clin Diagn Lab Immunol, 2003. **10**(4): p. 631-6.

64. Moore, J.M., et al., *Immunity to placental malaria. I. Elevated production of interferon-gamma by placental blood mononuclear cells is associated with protection in an area with high transmission of malaria.* J Infect Dis, 1999. **179**(5): p. 1218-25.

65. Moore, J.M., et al., *Hemozoin differentially regulates proinflammatory cytokine production in human immunodeficiency virus-seropositive and -seronegative women with placental malaria.* Infect Immun, 2004. **72**(12): p. 7022-9.

66. Barrera, V., et al., *Host fibrinogen stably bound to hemozoin rapidly activates monocytes via TLR-4 and CD11b/CD18-integrin: a new paradigm of hemozoin action.* Blood, 2011. **117**(21): p. 5674-82.

67. Keller, C.C., et al., *Acquisition of hemozoin by monocytes down-regulates interleukin-12 p40 (IL-12p40) transcripts and circulating IL-12p70 through an IL-10-dependent mechanism: in vivo and in vitro findings in severe malarial anemia.* Infect Immun, 2006. **74**(9): p. 5249-60.

68. Dostert, C., et al., *Malarial hemozoin is a Nalp3 inflammasome activating danger signal.* PLoS One, 2009. **4**(8): p. e6510.

69. Keller, C.C., et al., *Reduced peripheral PGE2 biosynthesis in Plasmodium falciparum malaria occurs through hemozoin-induced suppression of blood mononuclear cell cyclooxygenase-2 gene expression via an interleukin-10-independent mechanism.* Mol Med, 2004. **10**(1-6): p. 45-54.

70. Skorokhod, O.A., et al., *Hemozoin (malarial pigment) inhibits differentiation and maturation of human monocyte-derived dendritic cells: a peroxisome proliferator-activated receptor-gamma-mediated effect.* J Immunol, 2004. **173**(6): p. 4066-74.

71. Green, M.D., L. Xiao, and A.A. Lal, *Formation of hydroxyeicosatetraenoic acids from hemozoin-catalyzed oxidation of arachidonic acid.* Mol Biochem Parasitol, 1996. **83**(2): p. 183-8.

72. Perkins, D.J., et al., *In vivo acquisition of hemozoin by placental blood mononuclear cells suppresses PGE2, TNF-alpha, and IL-10.* Biochem Biophys Res Commun, 2003. **311**(4): p. 839-46.

73. Arese, P., F. Turrini, and H. Ginsburg, *Erythrophagocytosis in malaria: Host defence or menace to the macrophage?* Parasitol Today, 1991. **7**(1): p. 25-8.

74. Schwarzer, E., et al., *Impairment of macrophage functions after ingestion of Plasmodium falciparum-infected erythrocytes or isolated malarial pigment.* J Exp Med, 1992. **176**(4): p. 1033-41.

75. Schwarzer, E., et al., *Malaria-parasitized erythrocytes and hemozoin nonenzymatically generate large amounts of hydroxy fatty acids that inhibit monocyte functions.* Blood, 2003. **101**(2): p. 722-8.

76. Serghides, L. and K.C. Kain, *Peroxisome proliferator-activated receptor gamma-retinoid X receptor agonists increase CD36-dependent phagocytosis of Plasmodium falciparum-parasitized erythrocytes and decrease malaria-induced TNF-alpha secretion by monocytes/macrophages.* J Immunol, 2001. **166**(11): p. 6742-8.

77. McGilvray, I.D., et al., *Nonopsonic monocyte/macrophage phagocytosis of Plasmodium falciparum-parasitized erythrocytes: a role for CD36 in malarial clearance.* Blood, 2000. **96**(9): p. 3231-40.

78. Turrini, F., et al., *Phagocytosis of Plasmodium falciparum-infected human red blood cells by human monocytes: involvement of immune and nonimmune determinants and dependence on parasite developmental stage.* Blood, 1992. **80**(3): p. 801-8.

79. Sampaio, N.G., E.M. Eriksson, and L. Schofield, *Plasmodium falciparum PfEMP1 Modulates Monocyte/Macrophage Transcription Factor Activation and Cytokine and Chemokine Responses.* Infect Immun, 2018. **86**(1).

80. Lucchi, N.W., et al., *Plasmodium falciparum-infected red blood cells selected for binding to cultured syncytiotrophoblast bind to chondroitin sulfate A and induce tyrosine phosphorylation in the syncytiotrophoblast.* Placenta, 2006. **27**(4-5): p. 384-94.

81. Lucchi, N.W., D.S. Peterson, and J.M. Moore, *Immunologic activation of human syncytiotrophoblast by Plasmodium falciparum.* Malar J, 2008. **7**: p. 42.

82. Chaisavaneeyakorn, S., et al., *Immunohistological characterization of macrophage migration inhibitory factor expression in Plasmodium falciparum-infected placentas.* Infect Immun, 2005. **73**(6): p. 3287-93.

83. Lucchi, N.W., et al., *Natural hemozoin stimulates syncytiotrophoblast to secrete chemokines and recruit peripheral blood mononuclear cells.* Placenta, 2011. **32**(8): p. 579-85.

84. Imamura, T., et al., *Expression of tissue factor, the clotting initiator, on macrophages in Plasmodium falciparum-infected placentas.* J Infect Dis, 2002. **186**(3): p. 436-40.

85. Greer, I.A. and C. Nelson-Piercy, *Low-molecular-weight heparins for thromboprophylaxis and treatment of venous thromboembolism in pregnancy: a systematic review of safety and efficacy.* Blood, 2005. **106**(2): p. 401-7.

86. Megnekou, R., et al., *Impact of placental Plasmodium falciparum malaria on the profile of some oxidative stress biomarkers in women living in Yaounde, Cameroon.* PLoS One, 2015. **10**(8): p. e0134633.

87. Sharma, L., J. Kaur, and G. Shukla, *Role of oxidative stress and apoptosis in the placental pathology of Plasmodium berghei infected mice.* PLoS One, 2012. **7**(3): p. e32694.

88. Sarr, D., et al., *Oxidative Stress: A Potential Therapeutic Target in Placental Malaria.* Immunohorizons, 2017. **1**(4): p. 29-41.

89. Jaramillo, M., et al., *Hemozoin increases IFN-gamma-inducible macrophage nitric oxide generation through extracellular signal-regulated kinase- and NF-kappa B-dependent pathways.* J Immunol, 2003. **171**(8): p. 4243-53.

90. Keller, C.C., et al., *Elevated nitric oxide production in children with malarial anemia: hemozoin-induced nitric oxide synthase type 2 transcripts and nitric oxide in blood mononuclear cells.* Infect Immun, 2004. **72**(8): p. 4868-73.

91. Zhang, B., et al., *Placenta-specific drug delivery by trophoblast-targeted nanoparticles in mice.* Theranostics, 2018. **8**(10): p. 2765-2781.

92. Dorman, E.K., et al., *Impaired uteroplacental blood flow in pregnancies complicated by falciparum malaria.* Ultrasound Obstet Gynecol, 2002. **19**(2): p. 165-70.

93. Boeuf, P., et al., *Plasmodium falciparum malaria elicits inflammatory responses that dysregulate placental amino acid transport.* PLoS Pathog, 2013. **9**(2): p. e1003153.

94. Dimasuay, K.G., et al., *Inhibition of placental mTOR signaling provides a link between placental malaria and reduced birthweight.* BMC Med, 2017. **15**(1): p. 1.

95. Dimasuay, K.G., et al., *Impaired placental autophagy in placental malaria.* PLoS One, 2017. **12**(11): p. e0187291.

96. Baumann, M.U., et al., *Regulation of human trophoblast GLUT1 glucose transporter by insulin-like growth factor I (IGF-I).* PLoS One, 2014. **9**(8): p. e106037.

97. Chandrasiri, U.P., et al., *Insight into the pathogenesis of fetal growth restriction in placental malaria: decreased placental glucose transporter isoform 1 expression.* J Infect Dis, 2014. **209**(10): p. 1663-7.

98. Umbers, A.J., et al., *Placental malaria-associated inflammation disturbs the insulin-like growth factor axis of fetal growth regulation.* J Infect Dis, 2011. **203**(4): p. 561-9.

99. Cindrova-Davis, T.F., N. M. E.; Jones, C. J. P.; Kingdom, J.; Burton, G. J, *Evidence of oxidative stress-induced senescence in mature, post-mature and pathological human placentas.* Placenta, 2018. **68**: p. 15-22.

100. Brabin, B.J. and P.M. Johnson, *Placental malaria and pre-eclampsia through the looking glass backwards?* J Reprod Immunol, 2005. **65**(1): p. 1-15.

101. Poovassery, J.S., et al., *Malaria-induced murine pregnancy failure: distinct roles for IFN-gamma and TNF.* J Immunol, 2009. **183**(8): p. 5342-9.

102. Clark, I.A. and G. Chaudhri, *Tumor necrosis factor in malaria-induced abortion.* Am J Trop Med Hyg, 1988. **39**(3): p. 246-9.

103. Georgiades, P., A.C. Ferguson-Smith, and G.J. Burton, *Comparative developmental anatomy of the murine and human definitive placentae.* Placenta, 2002. **23**(1): p. 3-19.

104. Oduola, A.M., et al., *Effects of malaria (Plasmodium berghei) on the maternal-fetal relationship in mice.* J Protozool, 1982. **29**(1): p. 77-81.

105. Vinayak, V.K., et al., *Influence of malarial infection on the maternal-foetal relationship in pregnant mice.* Aust J Exp Biol Med Sci, 1986. **64 (Pt 3)**: p. 223-7.

106. Hioki, A., Y. Hioki, and H. Ohtomo, *Influence of pregnancy on the course of malaria in mice infected with Plasmodium berghei.* J Protozool, 1990. **37**(3): p. 163-7.

107. Cross, C.E. and J. Langhorne, *Plasmodium chabaudi chabaudi (AS): inflammatory cytokines and pathology in an erythrocytic-stage infection in mice.* Exp Parasitol, 1998. **90**(3): p. 220-9.

108. Stevenson, M.M., J.J. Lyanga, and E. Skamene, *Murine malaria: genetic control of resistance to Plasmodium chabaudi.* Infect Immun, 1982. **38**(1): p. 80-8.

109. Poovassery, J. and J.M. Moore, *Murine malaria infection induces fetal loss associated with accumulation of Plasmodium chabaudi AS-infected erythrocytes in the placenta.* Infect Immun, 2006. **74**(5): p. 2839-48.

110. Sarr, D., et al., *Plasmodium chabaudi AS induces pregnancy loss in association with systemic pro-inflammatory immune responses in A/J and C57BL/6 mice.* Parasite Immunol, 2012. **34**(4): p. 224-35.

111. Poovassery, J. and J.M. Moore, *Association of malaria-induced murine pregnancy failure with robust peripheral and placental cytokine responses.* Infect Immun, 2009. **77**(11): p. 4998-5006.

112. Desai, M., et al., *Epidemiology and burden of malaria in pregnancy.* Lancet Infect Dis, 2007. **7**(2): p. 93-104.

113. Barboza, R., et al., *TLR4-Mediated Placental Pathology and Pregnancy Outcome in Experimental Malaria.* Sci Rep, 2017. **7**(1): p. 8623.

114. Eling, W., *Survival of parasites in mice immunized against Plasmodium berghei.* Tropenmed Parasitol, 1978. **29**(2): p. 204-9.

115. van Zon, A.A. and W.M. Eling, *Depressed malarial immunity in pregnant mice.* Infect Immun, 1980. **28**(2): p. 630-2.

116. Sharma, A., et al., *Heterologous Infection of Pregnant Mice Induces Low Birth Weight and Modifies Offspring Susceptibility to Malaria.* PLoS One, 2016. **11**(7): p. e0160120.

117. Tuikue Ndam, N., et al., *Persistent Plasmodium falciparum infection in women with an intent to become pregnant is a risk factor for pregnancy-associated malaria.* Clin Infect Dis, 2018.

118. van Zon, A.A. and W.M. Eling, *Pregnancy associated recrudescence in murine malaria (Plasmodium berghei).* Tropenmed Parasitol, 1980. **31**(4): p. 402-8.

119. Laroque, A., et al., *Genetic control of susceptibility to infection with Plasmodium chabaudi chabaudi AS in inbred mouse strains.* Genes Immun, 2012. **13**(2): p. 155-63.

120. Chia, R., et al., *The origins and uses of mouse outbred stocks.* Nat Genet, 2005. **37**(11): p. 1181-6.

121. Martins, Y.C., et al., *Characterization of cerebral malaria in the outbred Swiss Webster mouse infected by Plasmodium berghei ANKA.* Int J Exp Pathol, 2009. **90**(2): p. 119-30.

122. Sam-Yellowe, T.Y. and R.C. Judd, *Passive immunization against Plasmodium chabaudi malaria with Pch 21 merozoite monoclonal antibody.* Parasitol Res, 1990. **76**(5): p. 457-60.

123. Yilmaz, B., et al., *Gut microbiota elicits a protective immune response against malaria transmission.* Cell, 2014. **159**(6): p. 1277-89.

124. Ravindran, B., A.K. Satapathy, and M.K. Das, *Naturally-occurring anti-alpha-galactosyl antibodies in human Plasmodium falciparum infections--a possible role for autoantibodies in malaria.* Immunol Lett, 1988. **19**(2): p. 137-41.

125. Villarino, N.F., et al., *Composition of the gut microbiota modulates the severity of malaria.* Proc Natl Acad Sci U S A, 2016. **113**(8): p. 2235-40.

126. Stough, J.M., et al., *Functional Characteristics of the Gut Microbiome in C57BL/6 Mice Differentially Susceptible to Plasmodium yoelii.* Front Microbiol, 2016. **7**: p. 1520.

127. Shibata, N., J. Kunisawa, and H. Kiyono, *Dietary and Microbial Metabolites in the Regulation of Host Immunity.* Front Microbiol, 2017. **8**: p. 2171.

128. Yooseph, S., et al., *Stool microbiota composition is associated with the prospective risk of Plasmodium falciparum infection.* BMC Genomics, 2015. **16**: p. 631.

129. Taniguchi, T., et al., *Plasmodium berghei ANKA causes intestinal malaria associated with dysbiosis.* Sci Rep, 2015. **5**: p. 15699.

130. Mooney, J.P., et al., *Inflammation-associated alterations to the intestinal microbiota reduce colonization resistance against non-typhoidal Salmonella during concurrent malaria parasite infection.* Sci Rep, 2015. **5**: p. 14603.

131. Koren, O., et al., *Host remodeling of the gut microbiome and metabolic changes during pregnancy.* Cell, 2012. **150**(3): p. 470-80.

132. Gohir, W., et al., *Pregnancy-related changes in the maternal gut microbiota are dependent upon the mother's periconceptional diet.* Gut Microbes, 2015. **6**(5): p. 310-20.

133. Coleman, S.J., et al., *Syncytial nuclear aggregates in normal placenta show increased nuclear condensation, but apoptosis and cytoskeletal redistribution are uncommon.* Placenta, 2013. **34**(5): p. 449-55.

134. Jimenez-Diaz, M.B., et al., *Quantitative measurement of Plasmodium-infected erythrocytes in murine models of malaria by flow cytometry using bidimensional assessment of SYTO-16 fluorescence.* Cytometry A, 2009. **75**(3): p. 225-35.

135. Abatan, O.I., K.B. Welch, and J.A. Nemzek, *Evaluation of saphenous venipuncture and modified tail-clip blood collection in mice.* J Am Assoc Lab Anim Sci, 2008. **47**(3): p. 8-15.

136. Kulandavelu, S., et al., *Embryonic and neonatal phenotyping of genetically engineered mice.* ILAR J, 2006. **47**(2): p. 103-17.

137. Iwaki, S., A. Matsuo, and A. Kast, *Identification of newborn rats by tattooing.* Lab Anim, 1989. **23**(4): p. 361-4.

138. Lawn, J.E., et al., *4 million neonatal deaths: when? Where? Why?* Lancet, 2005. **365**(9462): p. 891-900.

139. Natama, H.M., et al., *Additional Screening and Treatment of Malaria During Pregnancy Provides Further Protection Against Malaria and Nonmalarial Fevers During the First Year of Life.* J Infect Dis, 2018.

140. Rakoff-Nahoum, S., et al., *Recognition of commensal microflora by toll-like receptors is required for intestinal homeostasis.* Cell, 2004. **118**(2): p. 229-41.

141. Reikvam, D.H., et al., *Depletion of murine intestinal microbiota: effects on gut mucosa and epithelial gene expression.* PLoS One, 2011. **6**(3): p. e17996.

142. Fransen, F., et al., *BALB/c and C57BL/6 Mice Differ in Polyreactive IgA Abundance, which Impacts the Generation of Antigen-Specific IgA and Microbiota Diversity.* Immunity, 2015. **43**(3): p. 527-40.

143. Rodriguez-Palacios, A., et al., *'Cyclical Bias' in Microbiome Research Revealed by A Portable Germ-Free Housing System Using Nested Isolation.* Sci Rep, 2018. **8**(1): p. 3801.

144. Lightfoot, Y.L., et al., *Colonic immune suppression, barrier dysfunction, and dysbiosis by gastrointestinal bacillus anthracis Infection.* PLoS One, 2014. **9**(6): p. e100532.

145. Yang, T., et al., *Gut dysbiosis is linked to hypertension.* Hypertension, 2015. **65**(6): p. 1331-40.

146. Bokulich, N.A., et al., *Quality-filtering vastly improves diversity estimates from Illumina amplicon sequencing.* Nat Methods, 2013. **10**(1): p. 57-9.

147. Rideout, J.R., et al., *Subsampled open-reference clustering creates consistent, comprehensive OTU definitions and scales to billions of sequences.* PeerJ, 2014. **2**: p. e545.

148. McDonald, D., et al., *An improved Greengenes taxonomy with explicit ranks for ecological and evolutionary analyses of bacteria and archaea.* ISME J, 2012. **6**(3): p. 610-8.

149. Antharam, V.C., et al., *Intestinal dysbiosis and depletion of butyrogenic bacteria in Clostridium difficile infection and nosocomial diarrhea.* J Clin Microbiol, 2013. **51**(9): p. 2884-92.

150. Lozupone, C., et al., *UniFrac: an effective distance metric for microbial community comparison.* ISME J, 2011. **5**(2): p. 169-72.

151. Cho, I., et al., *Antibiotics in early life alter the murine colonic microbiome and adiposity.* Nature, 2012. **488**(7413): p. 621-6.

152. Cox, L.M., et al., *Altering the intestinal microbiota during a critical developmental window has lasting metabolic consequences.* Cell, 2014. **158**(4): p. 705-721.

153. Ji, S.K., et al., *Preparing the Gut with Antibiotics Enhances Gut Microbiota Reprogramming Efficiency by Promoting Xenomicrobiota Colonization.* Front Microbiol, 2017. **8**: p. 1208.

154. Chudnovskiy, A., et al., *Host-Protozoan Interactions Protect from Mucosal Infections through Activation of the Inflammasome.* Cell, 2016. **167**(2): p. 444-456 e14.

155. Adeghe, A.J. and J. Cohen, *A better method for terminal bleeding of mice.* Lab Anim, 1986. **20**(1): p. 70-2.

156. Canobbio, I., et al., *Platelet amyloid precursor protein is a modulator of venous thromboembolism in mice.* Blood, 2017. **130**(4): p. 527-536.

157. Schmittgen, T.D. and K.J. Livak, *Analyzing real-time PCR data by the comparative C(T) method.* Nat Protoc, 2008. **3**(6): p. 1101-8.

158. Mamo, S., et al., *Quantitative evaluation and selection of reference genes in mouse oocytes and embryos cultured in vivo and in vitro.* BMC Dev Biol, 2007. **7**: p. 14.

159. Solano, M.E., et al., *Identification of suitable reference genes in the mouse placenta.* Placenta, 2016. **39**: p. 7-15.

160. Agudelo, O.M., et al., *Submicroscopic infection of placenta by Plasmodium produces Th1/Th2 cytokine imbalance, inflammation and hypoxia in women from north-west Colombia.* Malar J, 2014. **13**: p. 122.

161. Sarr, D., et al., *Chronic infection during placental malaria is associated with up-regulation of cycloxygenase-2.* Malar J, 2010. **9**: p. 45.

162. Salifu, H., et al., *Iron Supplementation Alters Heme and Heme Oxygenase 1 (HO-1) Levels In Pregnant Women in Ghana.* SOJ Microbiol Infect Dis, 2016. **4**(3).

163. Okell, L.C., J.T. Griffin, and C. Roper, *Mapping sulphadoxine-pyrimethamine-resistant Plasmodium falciparum malaria in infected humans and in parasite populations in Africa.* Sci Rep, 2017. **7**(1): p. 7389.

164. Kakuru, A., et al., *Dihydroartemisinin-Piperaquine for the Prevention of Malaria in Pregnancy.* N Engl J Med, 2016. **374**(10): p. 928-39.

165. Dondorp, A.M., et al., *Artemisinin resistance in Plasmodium falciparum malaria.* N Engl J Med, 2009. **361**(5): p. 455-67.

166. Lagasse, H.A., et al., *Recruited monocytes modulate malaria-induced lung injury through CD36-mediated clearance of sequestered infected erythrocytes.* J Leukoc Biol, 2016. **99**(5): p. 659-71.

167. Sponaas, A.M., et al., *Migrating monocytes recruited to the spleen play an important role in control of blood stage malaria.* Blood, 2009. **114**(27): p. 5522-31.

168. Askenase, M.H., et al., *Bone-Marrow-Resident NK Cells Prime Monocytes for Regulatory Function during Infection.* Immunity, 2015. **42**(6): p. 1130-42.

169. Kleinnijenhuis, J., et al., *Bacille Calmette-Guerin induces NOD2-dependent nonspecific protection from reinfection via epigenetic reprogramming of monocytes.* Proc Natl Acad Sci U S A, 2012. **109**(43): p. 17537-42.

170. Quintin, J., et al., *Candida albicans infection affords protection against reinfection via functional reprogramming of monocytes.* Cell Host Microbe, 2012. **12**(2): p. 223-32.

171. Phoon, C.K., O. Aristizabal, and D.H. Turnbull, *40 MHz Doppler characterization of umbilical and dorsal aortic blood flow in the early mouse embryo.* Ultrasound Med Biol, 2000. **26**(8): p. 1275-83.

172. Kusinski, L.C., et al., *Isolation of plasma membrane vesicles from mouse placenta at term and measurement of system A and system beta amino acid transporter activity.* Placenta, 2010. **31**(1): p. 53-9.